2010

Molecular Basis of the Role of Kindlin 2 in Cell Adhesion

Hettiarachchige Dhanuja Deepamalee Perera
Cleveland State University

MOLECULAR BASIS OF THE ROLE OF KINDLIN 2 IN CELL ADHESION

HETTIARACHCHIGE DHANUJA DEEPAMALEE PERERA

Bachelor of Science in General Chemistry

University of Colombo, SRI LANKA

January, 2002

Master of Science in Analytical Chemistry

University of Colombo, SRI LANKA

January, 2005

Submitted in partial fulfillment of the requirements for the degree

DOCTOR OF PHILOSOPHY IN BIOANALYTICAL CHEMISTRY

at the

CLEVELAND STATE UNIVERSITY

Dec, 2010

This thesis/dissertation has been approved for the Department of Chemistry and College of Graduate Studies of Cleveland State University by

_____ Date:_____
Jun Qin, PhD, CCF-LRI
Primary Research Advisor

_____ Date:_____
Yan Xu, PhD, CSU-Chemistry, Cleveland State University
Academic Advisor

_____ Date:_____
Edward Plow, PhD, CCF-LRI
Advisory Committee Member

_____ Date:_____
Alan Riga, PhD, CSU-Chemistry, Cleveland State University
Advisory Committee Member

_____ Date:_____
Saurav Misra, PhD, CCF-LRI
External Examiner

DEDICATION

To my family…….

ACKNOWLEDGEMENTS

There are many that I sincerely thank who helped me to make this thesis happen and unfortunately I would not be able to express gratitude to all due space limitation. First I would like to sincerely thank my advisor Dr. Jun Qin for his support in many ways. His guidance, understanding and patience during these five years made me through hard times of the projects to success. I always admire his very unique managerial skills and his thrive in scientific research.

I would like to thank to my thesis research committee Dr. Yan Xu, Dr. Edward Plow, Dr. Alan Riga, Dr. Saurav Misra and Dr. Robert Wei for their valuable suggestions, useful and knowledgeable discussions.

This thesis would not happen without the support of the following individuals: Dr. Yang-Qing Ma for providing figures 3.1, 4.9 and 4.10; Dr. Koichi Fukuda for providing Kindlin 2 PH domain protein; Dr. Jun Yang for providing lipid vesicles (LUVs); Dr. Jianmin Liu for providing integrin β3 cytoplasmic tail mutant peptide.

I also like to thank Dr. Jun Yang for teaching me tools of NMR; Dr. Koichi Fukuda and Dr. Saurav Misra for guiding me through X-ray crystallography; Dr. Sujay Ithychanda for valuable hints and suggestions in molecular biology; Dr. Richard Page for assistance in model structure generation and Mr. Xiaolun Zhang for assisting in protein purification. I am thankful to all my colleagues in Dr. Qin Lab and Dr. Misra Lab for providing a good lab environment.

I specially would like to thank the Department of Chemistry of the Cleveland State University and the Department of Molecular Cardiology of the Lerner Research

Institute (Cleveland Clinic Foundation) for giving me an opportunity to carry out my research projects.

My parents and sisters have been of immense support in many ways and there love helped me always throughout my life. Especially, I am indebted to my husband, for his love and immense support. I admire the price-less support of my mother-in-law and friends who helped me throughout these years.

MOLECULAR BASIS OF THE ROLE OF KINDLIN 2 IN CELL ADHESION

H. DHANUJA D. PERERA

ABSTRACT

Kindlins are a novel family of cytoskeleton proteins that plays an important role in the activation of heterodimeric integrin transmembrane receptors. These receptors play a vital role in cell adhesion, cell migration and other cellular processes. The Kindlin protein family consists of three homologous proteins, Kindlin 1, 2 and 3 with differential tissue distribution and varying expression levels in human. Mutations of Kindlin 1 protein are clinically linked to Kindler Syndrome. Kindlin 2 knockdown studies have shown embryonic lethality in mouse, but no diseases have been clinically testified. Kindlin 3 mutations are associated with bleeding disorders, e.g. LADIII.

Talin is a cytoskeleton protein, which is a well known and widely studied activator of integrin receptors. Talin and Kindlin bind to non-overlapping binding sites on integrin β3 cytoplasmic tail. Their cooperation significantly enhances integrin activation compared to integrin activation by Talin activity itself. Kindlin and Talin share similar structural homology. A unique feature in the Kindlin FERM domain compared to the FERM domain of Talin is that the FERM domain of Kindlin is split by a PH domain.

The main focus of the study was to understand the role of Kindlin 2 in the complex process of integrin activation. To gain structural insight, we have determined the 3D structure of Kindlin 2 N-terminal F0 domain by using Nuclear Magnetic Resonance Spectroscopy. More than 90% of the backbone and side chain NMR resonances have been assigned. Kindlin 1 and 2 F0 domains share 62% sequence homology and have a similar ubiquitin-like beta grasp fold. However, there are distinct differences between Kindlin 1 and 2 F0 domain structures, which may contribute to functional differences. An *in vivo* assay has shown that deletion of the F0 domain from the Kindlin 2 full length protein abolishes integrin activation. Thus, Kindlin 2 F0 domain plays a significant role in integrin activation. Our *in vitro* data have shown a very weak interaction between Kindlin 2 F0 domain and integrin β3 cytoplasmic tail /membrane/PIP. In addition, we measured a 1μM affinity for Kindlin 2 PH domain and PIP3 interaction. Altogether these data suggest that both the F0 and PH domains of Kindlin 2 interact with the membrane surface and facilitate the effect of Kindlin 2 in integrin activation.

Besides Talin and Kindlin, the focal adhesion protein Migfilin, also promotes integrin activation. It has been reported that the C terminally located LIM domains of Migfilin, bind predominantly to Kindlin N-terminal region. We have tested the interaction between Kindlin 2 N-terminus and Migfilin LIM domain proteins. Our data show a weak interaction between 11-143 fragment and Migfilin LIM23 domain of Migfilin. Though Kindlin, Talin and Migfilin are likely to be spatially close during integrin activation, here we have eliminated the interaction between Migfilin-Talin H and Kindlin F0-Talin H domains.

In summary, the N-terminally located F0 domain of Kindlin 2 is crucial for integrin activation. The interactions of the F0 and PH domains of Kindlin 2 with the membrane suggest a role in anchoring to the membrane surface. The N-terminal 11-143 residues of Kindlin 2 are necessary for the interaction with Migfilin LIM domain. Overall, the N-term region of Kindlin 2 plays a key role in the complex process of integrin activation.

TABLE OF CONTENTS

ABBREVIATIONS

cDNA, complementary DNA

CHO cells, Chinese Hamster Ovary cells

CT, cytoplasmic tail

C-ter, The C- terminal region of the protein

ECM, Extra Cellular Matrix

EGFP, Enhanced Green Fluorescent Protein

FERM domain, 4.1 protein, Ezrin, Radixin, Moesin domain

HSQC, Heteronuclear Single Quantum Coherence

ITC, isothermal Titration Calorimetry

MES, 4-morpholineethanesulfonic acid

NMR, Nuclear Magnetic Resonance

N-ter, The N- terminal region of the protein

PIP2, Phosphatidylinositol 4,5-bisphosphate

PIP3, Phosphatidylinositol 3,4,5-triphosphate

PTB domain, Phosphotyrosine Binding Domain

SPR, Surface Plasmon Resonance

LIST OF TABLES

LIST OF FIGURES

Chapter 1

Chapter 3

Chapter 5

Chapter 7

Appendices.

CHAPTER I

INTRODUCTION

1.1 Integrins

Integrins are transmembrane cell adhesion receptors mediating cell-cell adhesion, cell migration and other cellular processes. They are present in all metazoans but not found in the kingdom plantae and fungi (Hynes et al., 2002). Integrins are heterodimeric receptors formed by an α subunit and a β subunit which are non-covalently linked to each other. Each subunit has 3 distinctive structural regions: The ectodomain, a short transmembrane helix and the cytoplasmic peptide tail (Barczyk et al., 2000). The Integrin ectodomain exists in two conformations: the bent conformation and the extended conformation. In the bent conformation the subdomains of the integrin ectodomain are more compact and the ligand binding site is faced towards the plasma membrane. This conformation holds integrin in a low affinity state for ligand binding. In the extended conformation the subdomains of the ectodomain of integrin are less compact and the ligand binding site is faced towards the extra cellular matrix of the cell. This conformation has a high affinity for ligand binding and is also termed activated integrins.

In vertebrates the integrin receptor family consists of 24 members that are formed by 18 α and 8 β subunits (Takada et al., 2007). These are grouped into four categories based on ligand binding receptors: RGD receptors, Collagen receptors, Laminin receptors and Leukocyte specific receptors (Figure 1.1).

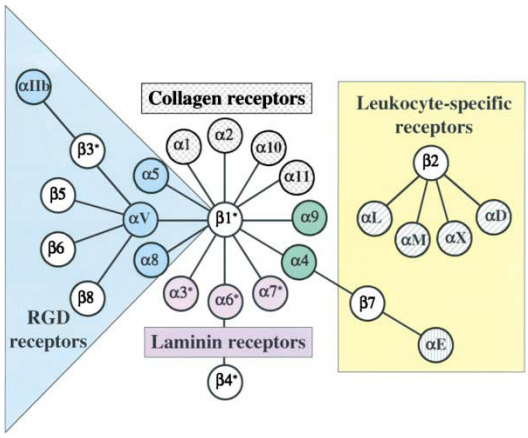

Figure 1.1. Types of Integrin Receptors. Adopted from (Hynes et al., 2002). In mammals, 18 alpha and 8 beta subunits are assembled in to 24 different heterodimers. Integrins are the main receptors for ECM proteins, they can also bind to other components like receptors (ICAMs, VCAM), molecules like fibrinogen and pathogens (e.g. viruses and bacteria).There are different integrin subfamilies based on sequences, binding properties / expression patterns: RGD-binding integrins in blue, the laminin-binding integrins in purple, the leukocyte integrins in yellow, collagen binding receptors in grey.

The 24 different types of integrin receptors have varying degrees of expression and some have tissue specificity. For example, Integrin αIIbβ3 is present on platelet membrane surface and recognizes fibronectins and fibrinogen. Its interaction is linked to platelet aggregation and wound healing. α6β4 integrins are present on epithelial cell surface and specifically binds to laminin.

Integrin cytoplasmic tail (CT) is crucial for integrin signaling (Vinogradava, O. et al., 2002 and others). The CT tails of the α and β subunits of integrin receptors have conserved amino acid sequences among different members within the group (Calderwood, 2004). Two NPxY motifs are present in almost all cytoplasmic tail sequences of the β subunit, except in integrin β2, which has two NPxF motifs. The first $NPxY^{747}$ motif of integrin β3 is important for Talin interaction and the second $NPxY^{759}$ motif interacts with Kindlin. This interaction is the hallmark for subsequent activation of integrins.

Integrins are the largest group of cell adhesion receptor. In addition to cell signaling, integrins also play a central role in many cellular processes. Dysfunction of integrins has reported to cause severe embryonic malformation (Keller et al., 2001; Martin-Bermudo et al., 1998). The function of integrin is crucial for proper homeostasis and its regulation has been linked to many diseases such as cancer and atherosclerosis. A large effort has been made to develop therapeutic drugs that directly target integrins (Cox, et. al., 2010).

1.2. Integrin Activation and Signaling

During the process of integrin activation, integrins undergo a conformational transition from a bent conformation to the extended conformation. Integrin associated signaling is bi-directional, inside-out and outside-in signaling. A large number of proteins are associated with the integrin in-side out signaling mechanism. As mentioned earlier, Kindlin and Talin directly regulate integrin activation. In addition, other proteins like

Filamin, ILK, CIB and Migfilin are also involved in tight regulation of the integrin inside-out signaling mechanism.

At the resting state or inactive state of integrins, the interaction between the CT of the αIIb and β3 subunits form a clasp that holds integrin at its inactive conformation. Structural studies revealed that the PTB domain of Talin binds to the $NPxY^{474}$ motif near the membrane-proximal region of the integrin β3 CT (Vinogradova et al., 2002; Garcia-Alvarez et al., 2003; Wegener et al., 2007; Yang et al., 2009). This binding eventually disrupts the membrane-proximal clasp that holds the αIIb and β3 subunits together. This process transforms the ectodomain of integrin from a bent to an extended conformation which has a high affinity for ligand binding (Calderwood et al., 2002; Garcia-Alvarez et al., 2003; Qin et al., 2004). Interestingly, most recent studies have revealed that the

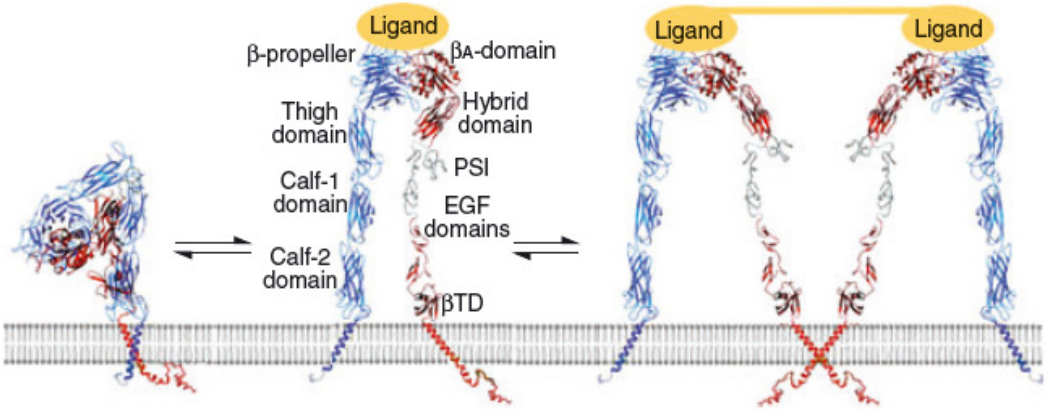

Figure 1.2. Integrin activation. Adopted from Y-Q. Ma, J. Qin and E. F. Plow, 2007.

interaction between integrin β CT and Talin is not sufficient to activate integrins at its full activation potential. Other proteins like Kindlin act as co-activators in Talin induced integrin activation resulting in a significant increase in integrin activation (Shi et al.,

2007). The PTB domain in Kindlin 2 F3 subdomain interacts with the distal $NxxY^{759}$ motif of the integrin β3 CT and the coordinated interaction of both Kindlin and Talin with the integrin CT has shown to lead to an increased activation of integrins (Ma et al., 2008; Montanez et al., 2008).

Once activated, integrins bind to extracellular matrix (ECM) ligands and transmit signals from the extracellular matrix (ECM) to the cell interior. This pathway is the outside-in signaling. Despite decades of studies on integrin signaling, the mechanism of integrin activation is still not clearly understood. Not much is known about the detailed mechanism of inside-out signaling and specifically how Kindlin and Talin cooperate to induce potent integrin activation. We are interested in understanding the role of Kindlin in the process of Talin induced integrin activation.

1.3. Focal adhesion

Focal adhesions are multimeric and dynamic protein complexes assembled around activated integrins/integrin clusters which link the ECM and the cytoskeleton of the cell. There are four levels of grouping based on factors like composition, localization and size: focal complexes, focal adhesions, fibrillar adhesions and matrix adhesions. Each has a distinct role in cells such as cell migration, cell-cell adhesion, cell proliferation, cell differentiation etc. (Wozniak et al., 2004). This thesis investigates the role of key focal adhesion proteins, integrin β3 CT, Kindlin, Migflin and Talin with particular focus on Kindlin.

1.4. Kindlins

Kindlins are a relatively novel group of cytoplasmic proteins. They have gained much attention for their roles in disease development. More recently, accumulating data for their role in integrin activation has become an area of interest (Goult et al., 2009; Harburger et al., 2009; Larjava et al., 2008; Ma et al., 2008; Montanez et al., 2008; Moser et al., 2008; Ussar et al., 2006). However, not much is known about the structural details of Kindlins or its role in integrin activation.

1.4.1. Kindlin protein family

The Kindlin protein family in human consists of three homologous proteins, Kindlin 1, 2 and 3. Kindlin 1 was the first to be identified by Siegel et al. This group further identified two additional Kindlin 1 like proteins, MIG-2 and MGC10966, which they renamed as Kindlin 2 and Kindlin 3 respectively (Siegel et al., 2003). The first Kindlin ortholog to be identified was UNC-112 in *C. elegans*. All Kindlin proteins and UNC-112 share common features in their domain structure and amino acid sequences.

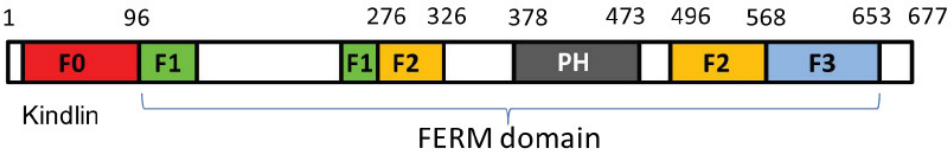

Figure 1.3. Kindlin-1 protein structural domains.(Goult et al., 2009). Kindlin 1 and 3 proteins have similar structural domains. The F2 subdomain is split by a PH domain, the F0 domain is located at the very N-terminus and the F3 subdomain at the C-terminus.

All Kindlin proteins have a FERM domain and a N-terminally located F0 domain. A unique feature of Kindlin FERM domain compared to other FERM domains of all other proteins is that the F2 subdomain of the FERM is split by the PH domain (Fig 1.3). To date the structure of F0 subdomain of Kindlin 1 has been elucidated by Goult et al. (Goult et al., 2009).

PH domains (Plekstrin Homolgy domain) are present in many proteins. They are known to bind to phosphoinositides with specificities to the inositol ring, helping in localizing proteins to the membrane surface and involving in regulatory mechanisms. PH domains that bind to G proteins and protein kinase C are part of signal transduction pathways (Shaw, G., 1996). The role of the PH domain of Kindlin is not yet known.

FERM domains are evolutionary conserved structural domains which serve in various cellular signaling mechanisms. They consist of 3 subdomains, F1, F2 and F3. FERM domains are found in many proteins and bind with specificities to phosphoinositides. Both Talin and Kindlin have FERM domains. The F3 subdomain of Kindlin and Talin show similar homologies and are known to bind to non-overlapping sites of integrin β3 cytoplasmic tails. Talin F3 subdomain binds to phosphoinositides and its interaction activates Talin for subsequent interaction with integrin CT (Goksoy et al., 2009). The interaction between Kindlin F3 subdomain and phophoinositides remains for potential investigation.

Kindlin proteins are encoded from 3 different chromosomes. Kindlin 1 from chromosome 20, Kindlin 2 from chromosome 14 and Kindlin 3 from chromosome 11 (Weinstein et el., 2003).

Kindlin 1 or FERMT1 is 677 residues in length and has a molecular mass of 77.3 KDa. Siegel et al. group have first demonstrated that Kindlin co localizes with vinculin in focal contacts. Kindlin 1 is a phosphoprotein where the serine residues at position 170 and 179 are phosphorylated (Dephoure N., et al., 2008). There are four isoforms described in Kindlin 1 protein but their individual functions are not known (http://www.uniprot.org/uniprot/Q9BQL6).

Kindlin 2 is a 68KDa protein and is 680 amino acids in length. It displays 60% sequence identity to Kindllin 1 and 49% sequence identity to Kindlin 3. Human Kindlin 2 two exist in two isoforms produced by alternative splicing (http://www.uniprot.org/uniprot/Q96AC1). Isoform 1 is considered as the canonical sequence. Kindlin 2 isoform has certain differences at the C terminus: residues 627-680 are missing, residues 625-626 are TV→NS and residue 534 is an insertion of Q→QPGYIRDL. Phosphorylation of serine residues at position 159, 181 and 666 of the sequence have been identified in Kindlin 2 (Ussar et al., 2006). A unique feature of Kindlin 2 sequence among other Kindlin proteins is the nuclear localization signal (NLS), which spans between 152-172 amino acid region.

Kindlin 3 is 677 residues in length and is widely known as FERMT3. Kindlin 3 is expressed in the hematopoitic tissues and plays a fundamental role in cell adhesion, integrin activation, wound healing etc. Kindlin 3 is also found as two isoforms in human, (http://www.uniprot.org/uniprot/Q86UX7) residues 360-363 in isoform 2 are missing from isoform 1 sequence. Post-translational phosphorylations are identified at positions 8, 11 and 504 of the sequence.

1.4.2. Diseases associated with Kindlins.

Kindler syndrome is a rare but severe skin condition, which is caused by autosomal recessive genes of KIND1 mutation/s. It is the first skin disorder, which has been identified to occur due to a non-systematic connection of the cell between the extra cellular matrix and actin cytoskeleton (Siegel et al., 2003). Major symptoms appear to be skin blistering due to skin fragility, sensitivity to the exposure of the sun, unusual melanin distribution and wrinkling of the skin. Altogether the individual shows a prematurely aged appearance at early childhood (Theresa Kindler in 1954).

To date there are no diseases related to Kindlin 2 mutations. Kindlin 2 knock down mice are embryonicaly lethal heightening the significance of Kindlin 2 during embryogenesis. In fact Kindlin 2, among other Kindlin proteins plays a central role in early cardiogenesis (Mackinnon et al., 2002; Williams and Waterston, 1994; Xu et al., 2006). Its crucial role might not be completed with impaired functions of the protein.

LAD-III is a leukocyte adhesion deficiency syndrome and is linked to Kindlin 3 mutations. Patients with LAD-III have an extended bleeding time and show a lack of ability of leukocytes to bind to the ECM.

Despite a lot of studies have focused on diseases associated with Kindlins, not much is known about the disease pathologies. Even less is known about the particular functions and structure of Kindlin proteins.

1.4.3. Tissue Distribution and Biological Roles of Kindlins.

Kindlins are widely expressed in the human body. Ussar et al. have shown the distribution of Kindlin proteins in adult and embryonic mouse. Kindlin 3 expression is

found in all hematopoetic tissues: spleen, thymus, lymph node, and lungs (Fig 1.4.). Mouse Kindlin 2 RNA expression was observed in all tissue types with a high level of expression in heart, lung, skeletal muscle, bladder, stomach and kidney. Kindlin 1 showed a higher expression of RNA levels in the colon, and bladder compared to a weaker expression in the skin, intestine and kidney. The expression of Kindlin 1 protein in the dermis of the skin is much weaker than in the expression of the epidermis, whereas the reverse is true for Kindlin 2 expression. Interestingly, malfunction of Kindlin 1 in the epidermis cannot be compensated by epidermal Kindlin 2 or with dermal Kindlin 1. This implies different functions of Kindlin 1 and 2 in the epidermis, and is the underlying cause for the Kindler Syndrome (Ussar et al., 2003). Another study has shown that Kindlin proteins have different sub cellular localization (Bailkowska et al., 2010).

In addition to differential tissue expression, cancer cells also report an increased expression of Kindlin 2 protein. Kindlin 2 was up regulated in the nucleus of cancer cells suggesting that Kindlin 2 plays a major role in tumor growth (An et al., 2010b; Wu, 2005).

A recent study by Has, C. et al. revealed a role in Kindlin2 in adult skin tissue. Kindlin 2 is strongly up-regulated during wound healing of the human skin. It has shown to initiate integrin clustering and activation in fibroblasts cells, subsequently regulating the formation and maturation of focal adhesions and reorganization of the actin cytoskeleton (He et al., 2010). In myocytes, Kindlin 2 localizes to Z-discs of cardiomyocytes (Ussar et al., 2006).

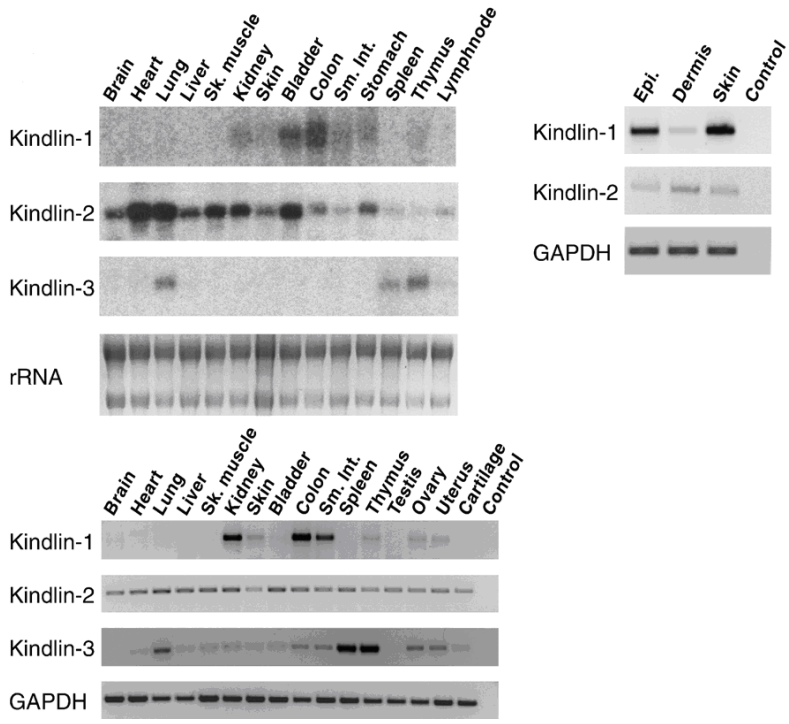

Figure 1.4. Tissue distribution of Kindlin proteins. Adopted from (Ussar et al., 2006).

1.4.4. Binding partners of Kindlin.

There are three groups of proteins been identified in literature that interacts with Kindlin (An et al., 2010a). They are integrin β1, β2, β3 cytoplasmic tails, ILK and Migfilin.

Integrin β1, β2 and β3

Using keratinocytes from normal and Kindler Syndrome patients, Siegel et al. have first demonstrated that there is a direct correlation between Kindlin 1 and integrin β1 activation (Siegel et al., 2003). Kindlin 1 protein has shown to bind directly to β1 and β3 integrins (Harburger et al., 2009)(Ussar et al., 2008). The FERM domain of Kindlin 1 and 2 is sufficient for the interaction with integrin β CT (Harburger et al., 2009; Shi and Wu, 2008). Within the FERM domain, the F3 subdomain is important for the interaction

with integrin. Mutations of residue $K^{610,}$ W^{612} and L^{651} to Alanine in Kindlin 1 completely suppress the interaction to integrin β1 tail. In Kindlin 2, the mutation of W^{615} showed a dramatic effect on β3 interaction and subsequent integrin activation (Ma et al., 2008). Recent studies have shown that tyr^{795} phophorylation has a low affinity for Kindlin 2 binding. These data suggest a regulatory mechanism of Kindlin 2 in integrin activation (Bledzka, K. et al., 2010). In addition, Kindlin 3 has shown to bind to β2 integrin on neutrophils and promotes integrin activation (Moser et al., 2009).

Kindlin and Talin bind to different regions of the integrin CT and promote integrin activation. But how exactly these two binding events promote integrin activation remains elusive.

Migfilin.

Migfilin protein was first identified as a Kindlin binding protein (Tu et al., 2003). Migfilin, also known as Cal (Akazawa et al., 2004) or FBLP-1A (Takafuta et al., 2003), is a 367 amino acid protein. It has central proline rich region, an unstructured N-terminal region and three C-terminal LIM domains. There are three homologous Migfilin proteins in human (Figure 1.5). The Migfilin(s) homolog lacks the proline rich region in its structure, whereas the FBLP-1 lacks the LIM 3 domain. Migfilin has multiple binding partners; the LIM domains of Migfilin mediate the interaction between Migfilin and Kindlin 2. This interaction is required for the recruitment of Migfilin to the focal adhesions. The N-terminal region of Migfilin binds to Filamin and inhibits the negative regulatory effect of Filamin in integrin activation (Kiema et al., 2006; Ithychanda et al., 2009a; Wu, 2005). Src is a protein kinase, which also interacts with Migfilin, which has shown to protect the process of anoikis (Zhao et al., 2009).

Migfilin has multiple roles and different co-localizations in the cell. In the nucleus it serves as a transcription co-factor. And in the cell cytoplasm, it interacts with cadherin β catenin complex for cell-cell adhesion. And recruitment to focal adhesion is accomplished by interacting with Kindlin.

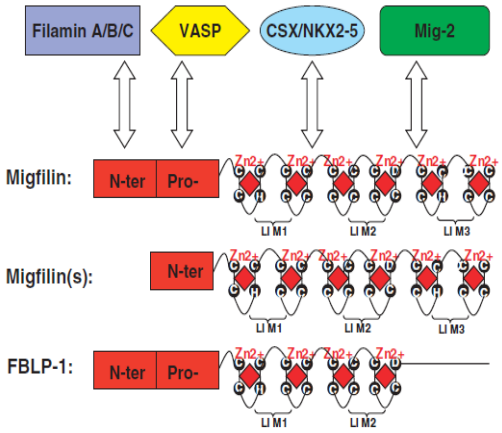

Figure 1.5. Migfilin interacting domains. (Wu, 2005). There are 3 isoforms of Migfilin in human. Migfilin, Migfilin(s) which lacks the proline rich region and FBLP-1 which lacks LIM 3 domain. Four binding partners of Migfilin have been identified so far. Mig-2 or Kindlin 2 interacts to LIM23 domain.

ILK.

Integrin linked Kinase shortened as ILK was first identified as an integrin β1 binding protein in 1996 (Hannigan et al., 1996). ILK is a 59kDa, comprises of a pseudokinase domain, a PH domain and (Fukuda et al., 2009) four ankyrin like repeats. Kindlin 2 is required for the localization of ILK to focal adhesions (Montanez et al., 2006). Interestingly, both ILK and Kindlin 2 were overexpressed at the growing front of malignant mesothelioma tumor and weakly expressed at the middle of the tumor. This shows that both ILK and Kindlin 2 are important for cell migration (An et al., 2010b).

The interaction between ILK and Kindlin has not been investigated at the molecular level.

1.5. Aim of the project

Despite the detailed information on the clinical significance and biological role of Kindlin proteins, much is not known about the mechanism of cooperate regulation of Talin and Kindlin in integrin activation. Moreover, even less is known about the structural aspects of Kindlin proteins and their functions. This thesis focuses on investigating the molecular mechanism of Kindlin, predominantly Kindlin 2, and its binding partners in regulating Talin induced integrin activation.

Based on facts from literature, we have proposed a model for integrin activation, which is shown in a schematic diagram in figure 1.6. The model suggests that Filamin is bound to integrin at the resting or inactive states of integrins. Migfilin is able to bind to Filamin and displace Filamin from the integrin β CT. This interaction makes the integrin β CT available for potent activation by Talin and Kindlin, a key process of all cell adhesive processes. Data from our laboratory have shown that Migfilin displaces Filamin from integrin and promote integrin activation (Ithychanda et al., 2009b; Ithychanda et al., 2009c). However, some of the key aspects of the model are yet to be proved.

In vivo studies by Tu and co-workers have shown that Migfilin is recruited to focal adhesion sites via Kindlin 2. More specifically, the LIM domains of Migfilin have shown to be responsible for this interaction with Kindlin 2 (Tu et al., 2003). The interaction between Kindlin C-ter and integrin has been established through several

studies (Ma et al., 2008; Malinin et al., 2010). The binding interface between Kindlin and Migfilin is assumed to be between the LIM domains of Migfilin and Kindlin N-ter region. But how exactly this binding interaction occurs is not clear. In addition how significant this binding interaction is for integrin activation and subsequent cellular processes needs to be evaluated and will be addressed in this thesis.

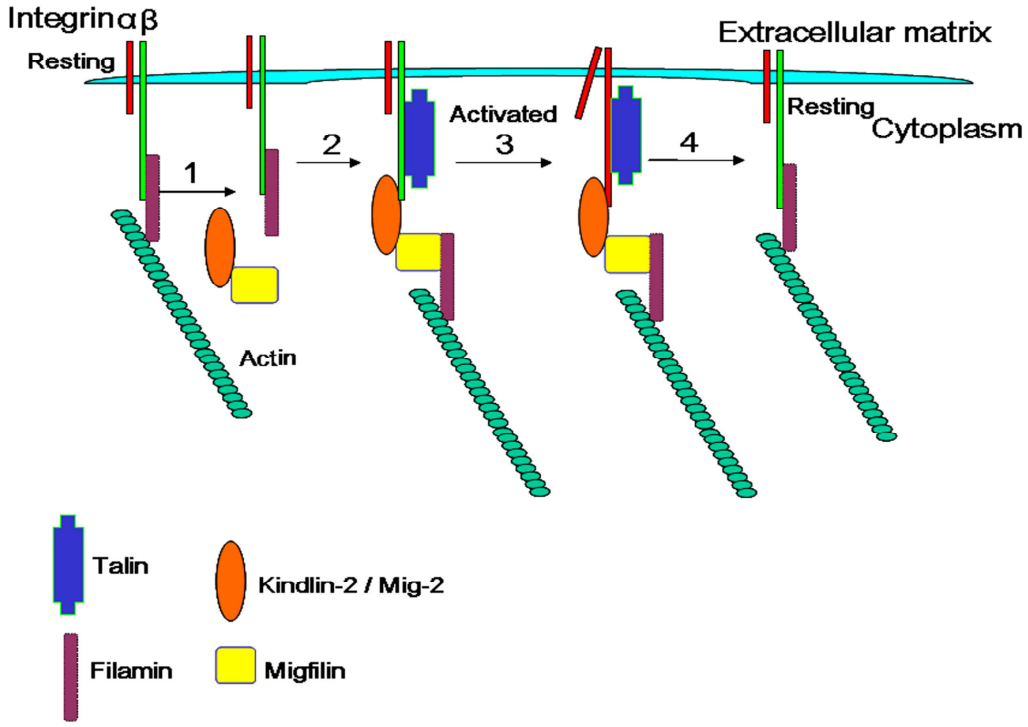

Figure 1.6. A model for the Migfilin/filamin interaction in regulating integrin activation and cytoskeleton reassembly. Migfilin is recruited by Kindlin-2 (Mig-2) to integrin adhesion sites (Tu et al., 2003). The recruited Migfilin promotes the dissociation of inhibitory filamin from integrins and facilitates the talin/integrin interaction as well as the anchoring of kindlins to integrin beta CTs and strengthens the talin effect in integrin activation. Since filamin is a major actin crosslinking protein critical for maintaining the actin network, the Migfilin-induced disconnection between integrin and filamin may also cause temporal rearrangement of the integrin-actin linkage to facilitate the cytoskeleton remodeling.

Another interesting aspect of the model is how Kindlin interacts with the integrin CT and other proteins to facilitate directly or indirectly in Talin induced integrin activation. Talin is a known activator of integrin activation and the mechanism of integrin activation and the auto inhibitory mechanisms are well established (Goksoy et al., 2008) (Shattil et al., 2010) (Vinogradova et al., 2002; Vinogradova et al., 2004). However, the contributory mechanism of Kindlin in Talin induced integrin activation is unclear. It has been shown through various functional assays from our collaborators', that the interaction between Kindlin 2 PTB domain and integrin β3 CT has a pronounced effect on integrin activation. More specifically phosphorylation of Y^{759} of integrin CT has a negative effect on Kindlin 2 binding (Shi et al., 2007; Ma et al., 2008; Bledzka et al., 2010). Up to date there is no structural information on the interaction between Kindlin 2 C-terminal F3 domain and integrin. We aim to understand the interaction between Kindlin 2 C-ter and integrin through structure based analysis and understand its role in the mechanism of integrin activation.

Lack of descriptive information about the structural details of Kindlin 2 in literature makes it difficult to evaluate our hypothesis to understand its function. To have a better understanding of the protein in a structural point of view, we have obtained a model structure of the full length Kindlin 2 protein.

To evaluate our hypothesis's we undertook a vigorous structure based investigation approach using NMR as our major tool. A structural analysis allowed us to understand the molecular mechanism of interaction and pin down the exact binding interfaces.

Our aims are as follow:

1. To solve the structure of Kindlin 2 N-ter.

2. To understand the functional significance of Kindlin 2 N-ter.

3. To resolve the structural determinants of Kindlin 2, Talin and Migfilin.

4. To understand and evaluate the interactions of Kindlin 2 C-ter.

Overall, both *in vivo* and *in vitro* experiments should help us to elucidate the mechanism of cooperate regulation of integrin. This work broadens our understanding of how Kindlin 2, Talin and Migfilin interactions mediate integrin activation. To date, there is a lack of information about the structural details of Kindlin and its interactions in particular. These aims will give us a molecular level understanding about the subdomain structure and function of Kindlin 2 and will help us to understand the pathogenesis of related human diseases.

CHAPTER II

TECHNIQUES IN STRUCTURAL BIOLOGY

2.1. Nuclear Magnetic Resonance Spectroscopy

2.1.1. Overview

NMR is a branch of spectroscopy where the inherent property of magnetization splitting of nuclei is observed by the interaction of radio frequency wave. This phenomenon was observed in 1946. Since then a large number of discoveries in the field of NMR have led to applications like macromolecular structure determination, Magnetic Resonance Imaging, interaction studies such as molecular dynamics and kinetics. NMR is the only technique available which allows performing experiments in all three states of matter, solid, gas and liquid. Liquid NMR is the most common of all for small molecules like organic compounds, pharmaceuticals and macromolecules such as protein, DNA etc. Solid state NMR is becoming popular, to overcome certain drawbacks in liquid NMR. NMR on gaseous samples is the least common in the field.

NMR is one of the two techniques available to determine three dimensional structures at atomic resolution. Macromolecular X-ray crystallography is the other. Despite the occurrence of a huge percentage of protein crystal structures in the protein databank, NMR has been the method of choice in understanding the dynamic function of a binding interaction (Wuthrich, 1991). The significance of the NMR technique was appreciated by winning the Nobel prizes in 2002 - Kurt Wurthrich, 2001- Richard. R. Ernst, 1952 – Felix Bloch for their contributions. The discovery of Fourier transformation and the development of multi dimensional NMR spectroscopy in the late 1960 were the most important turning points in the field of NMR. Advancement from fully-manual to semi-automated with the improvement/development of various computer software packages and the discovery of recombinant protein technology improved the area of 3D biological structure determination. Nowadays, NMR is playing an important role in 3D structure determination, structural genomics and protein-protein interaction studies.

The goal of this thesis is to understand the molecular role of Kindlin 2 in integrin activation. The structure of Kindlin 2 protein helps us to elucidate the binding interactions at an atomic level. Here we have used NMR as the method of choice for structure determination of Kindlin 2 F0 subdomain. In addition, we used NMR as our primary tool to understand protein-protein interactions.

2.1.2. Protein structure determination

Protein structure determination is a multiple step process (Wuthrich, 1989a; Wuthrich, 1989b). In brief, the first step in the process of protein structure determination

is sample preparation, which is followed by data collection, data processing, assignment and structure calculation. A very short outline of each step is described below.

Sample preparation

A typical NMR sample for structure determination must have an average concentration of 1mM protein. With the development of Shigemi NMR tubes the volume requirement has significantly reduced from 0.4ml to 0.2ml. Isotope labeling is another requirement for protein NMR, which reduces spectrum complexities and eases the process of structure determination.

Proteins comprise of naturally occurring isotopes of ^{12}C, ^{1}H, ^{14}N etc. ^{1}H is a magnetically active atom that plays a key role in NMR. Although ^{12}C nuclei is magnetically inactive and ^{14}N is less sensitive for detection, their corresponding isotopes, ^{13}C and ^{15}N, are magnetically active and sensitive for detection (spin half) and can be easily incorporated into proteins using isotope labeling methods (Sambrook et al., 1989). Isotopic labeling is an essential step in a wide range of applications in NMR (Montelione et al., 2000; Shuker et al., 1996). Currently, the most widely used method for labeling proteins is recombinant protein expression. A ^{1}H, ^{13}C and ^{15}N triple labeled protein sample increases NMR spectral resolution and simplifies subsequent structure determination steps.

NMR spectra - data collection

For small proteins with less than 50 amino acids (<10KDa), homonuclear 2D experiments such as COSY, TOCSY and NOESY are sufficient for structure determination (Wuthrich et al., 1982). However, for larger proteins (>100 amino acids)

homonuclear spectra become crowded and heteronuclear multidimensional experiments are necessary for better signal resolution and less spectral complexities.

The most widely used heteronuclear 2D NMR technique is HSQC (heteronuclear single quantum coherence). The magnetization is transferred from ^{1}H backbone proton to the attached ^{15}N of backbone NH_2 group via scalar couplings. Thus each amino acid in the protein with N-H group gives a signal in an HSQC spectrum.

To further simplify and improve resolution of protein spectra for the determination of structure, 3D NMR experiments are crucial. A number of triple resonance NMR experiments were developed for ^{15}N, ^{13}C and $^{1}H/^{2}H$ isotope labeled proteins.

Assignment

The process of cross-connecting resonance signals of NMR spectra to atomic nuclei of proteins is termed assignment. The assignment process has two steps. First, the backbone assignment of the protein and second the side chain assignment of each amino acid of the protein. There are different sets of multidimensional through-bond experiments, which transfers magnetization through the peptide bonds and are used for the resonance assignment of protein.

For small proteins the most simple and straightforward method for protein backbone assignment is to analyze CBCANH and CBCACONH spectra. An alternative method for large proteins with >100 amino acid residues is to find backbone linkages through HNCO, HNCACO, HNCA and HNCACO NMR spectra (Muhandiram and Kay). Nowadays, computer programs are used for the semi-automatic backbone assignment of proteins. MARS, PASA, GANA are well-known among them. The side chain resonances

are commonly assigned through HCCH-TOCSY. This experiment couples aliphatic side chain protons and ^{13}C resonances through J-coupling constants. Once the resonance assignment is complete the next step is restraint generation.

Restraints

There are several types of restraints that are used for structure determination: (1) Distance restraints are the distance between two atoms; these are obtained from NOESY spectra (Jeener et al., 1979; Williamson et al., 1985; Williamson et al., 1985). (2) Dihedral angle constraints from J coupling constants and chemical shifts; obtained automatically through TALOS program. (3) Residual dipolar couplings. (4) H-bonds and disulfide bond restrains.

In NOESY experiments, the magnetization is transferred through-space between nuclei close in proximity via nuclear Ovenhausen effect. The intensity of a peak in a NOESY spectrum is related to the distance between the two proton nuclei (Wiliamson et al., 1985). Ideally, the intensity of a NOESY cross-peak is directly proportional to 1/r-6 of the distance between the two atoms. But experimentally this is not always true. Various factors affect the NOE signal intensity such as indirect magnetization transfers due to spin diffusion.

TALOS is a program (Cornilescu et al., 1999) that searches a database of high resolution protein structures. It relates experimentally measured backbone chemical shifts to chemical shifts in already known secondary structures, and correlates that to backbone torsion angles.

Structure calculation

The next step is structure calculation. Various software packages are used for structure calculation: XPLOR-NIH, CYANA etc. All restraints that were determined experimentally are used as an input for calculating an ensemble of 3D structures.

The quality of NMR structures

There are several parameters to access the quality of NMR structures. One measure is the convergence. A high convergence of the calculated ensemble of superimposed structures reflects by the low standard deviation of the coordinates of the structures. However, a good convergence does not necessarily represent the accuracy of a structure. The Ramachandran plot is another parameter which evaluates validity of the backbone torsion angles (Ramachandran et al., 1963). The backbone of a protein should have a RMSD (measures the position of each atom coordinate on average throughout all the structures) of 0.4º and side chain atoms a RMSD of 1.0º for a structure with high precision. A high resolution NMR structure has on average 15-20 NOE distance restraints per residue and 3.5 long range distance restraints per residue in the structured regions.

2.1.3. Methods and materials

We acquired all NMR experiments at 298K under 600, 800 and 900 MHz BRUKER AVANCE spectrometers equipped with a cryoprobe. We used NMR-PIPE (Delaglio et al., 1995), PIPP (Garrett et al., 1991), NMRDraw and NMR View (Johnson and Blevins, 1994) to process out NMR data.

NMR sample preparation and data collection for structure calculation

I prepared a 1mM of ^{15}N and ^{13}C labeled Kindlin 2 1-105 sample for NMR data collection and dialyzed the protein against a buffer solution containing 50mM Sodium phosphate, 100mM sodium Chloride, 1mM DTT, 0.05% of sodium azide at pH 6.8, with a final of 10% (v/v) D_2O. HNCA (Kuboniwa et al., 1994), HNCO, HNCACB (Muhandiram and Kay), HNCACO, HSQC and CBCACONH spectra were acquired on a cryoprobe equipped 600 MHz spectrometer.

I prepared a 100% D_2O sample for 2D-TOCSY experiment, and an isotopically unlabeled 1mM Kindlin 2 1-105 sample for the collection of NOESY spectra.

Protein backbone assignment

We used PASA protocol for the initial semi-automatic sequential backbone assignment (Xu et al., 2006). We analyzed the ambiguous connections manually using HNCO - HNCACO and HNCA - HNCACB for the sequential assignment of backbone amides.

Protein side chain assignments

We used HCC(CO)NH and CC(CO)NH triple resonance spectra for assigning hydrogen nuclei and carbon nuclei respectively. In addition, we used HCCH-TOCSY experiment and NOSEY experiments to assist in the protein side chain assignment.

Interaction studies

For 2D ^{15}N-^{1}H-HSQC (Kay et al., 1992) experiments, 0.05-0.2mM protein samples were dialyzed against 50mM Sodium phosphate buffer containing 100mM Sodium Chloride at pH 6.8 buffer. I removed DTT from the buffers during interaction studies with Migfilin LIM domains but was present for all other experiments. We used

the pulse sequences dk-hsqc and fhsqc3gpph for almost all HSQC experiments. We collected spectra on a BRUKER AVANCE ICE spectrometer equipped with a cryoprobe.

2.2. Recombinant protein expression and purification

The requirement of a high concentration of protein is one requirement for NMR. A typical NMR sample for structural studies needs around sub molar concentration of protein. Such high amount of protein is difficult to purify from native cells i.e. it's time consuming and non economical. Recombinant Protein Expression technologies are commonly used to obtain a high concentration of pure protein.

Fusion proteins are used for the ease of purification. Histidine tag, Glutathione transferase Tag and Maltose binding protein Tag are commonly used fusion proteins which ease the isolation of target protein from crude lysate.

2.2.1. Protein expression optimization

Theoretically, recombinant protein expression techniques have a potential to express high levels of proteins. However, this is not observed *in vivo*. There are a limitless number of factors that suppress, limit, and prevent the expression of recombinant proteins in *E. coli* bacteria. In addition, the expressed protein can encounter endless factors which prevent it from being able to isolate. The stability of the protein is one important factor which reduces the yield of the protein. The instability could be due to many reasons such as prone for proteolytic cleavages, inherent instability of the protein etc. Precipitation of the protein is another factor which reduces the final yield of the protein. Protein aggregation is a common incident in recombinant protein expression

systems. Aggregation can be explained as a process of oligomerization of protein. This could be lower oligomer formation such as dimers, trimer, tetramer or higher oligomers. Lower oligomers are manageable for functional analysis. Oligomerization can be nonspecific by forming aggregates. Most often unfolded proteins and very hydrophobic proteins have a tendency to form massive aggregates. In fact, there are many other reasons which abolish the expression of a protein which will not be discussed in detail here.

2.2.2. Materials and methods

Kindlin 2 constructs.

We used the cDNA of full length human Kindlin 2 as a template for subcloning. I chose the boundaries for each protein according to secondary structure prediction of the full length Kindlin 2 obtained from the PSIPRED web server. In later subclonings, I used the 3D model structure of full length Kindlin 2 to assist in choosing the boundaries of the protein. For Kindlin 2 N terminal sequences, I used EcoRI and XhoI or XbaI restriction enzyme sites to clone the insert into the cloning vector. For C terminal sequences, I used either BamHI and NotI, or BamHI and XbaI restriction enzyme sites for cloning purposes. The cDNA of the C-terminal FERM regions have multiple restriction enzyme sites within their sequences. I cloned the cDNA of each insert in to cloning vectors shown in Table 2.1: PGEX-4T-1 (Pharmacia) or pGEX-4T-1 derived parallel GST 1 (pGST-1) for GST fusion proteins, pHis-1 or pET30a or pET15b for His-tagged fusion proteins and pMAL-c2x or pMBP-1 for MBP fusion proteins. I cloned some sequences into pMAL-c2x-His tag engineered cloning vector which was kindly provided from Dr. Jun Yang. I

transformed the cloned protein expression vectors into DH5α bacterial host strains and plated on appropriate antibiotic resistant plates. The bacterial colonies were subjected to colony PCR (Sambrook) to screen for positive colonies bearing our cloned insert. We used a Miniprep or Midiprep preparation (Promega) to isolate DNA plasmids from bacterial cells of our cloned protein expression vectors. Finally, I used the support of the CCF sequencing core to verify the accuracy of the cloned sequences. I transformed

KINDLIN-2 BOUNDARIES	FUSION TAG	BACTERIAL HOST STRAIN
1-134	HIS	Rosetta 2
	GST	Rosetta 2
1-154	HIS	Rosetta 2
1-158	HIS	Rosetta 2
1-218	GST	Rosetta 2
11-177	GST	Rosetta 2
11-143	HIS	Rosetta 2
	GST	Rosetta 2
	GST	BL21(DE3) gold
	MBP	Rosetta 2
	MBP	BL21 (DE3) RIP
	MBP-HIS	Rosetta 2
1-105	GST	BL21 (DE3) pLys
	HIS	BL21 (DE3) pLys
	GST	Rosetta 2
	GST	Rosetta 2
	GST	Rosetta 2
95-276	GST	Rosetta 2
95-168	GST	Rosetta 2
95-268	GST	Rosetta 2
95-154	GST	Rosetta 2
155-268	GST	Rosetta 2

Table 2.1. Kindlin-2 N' term recombinant proteins.

KINDLIN-2 BOUNDARIES	FUSION TAG	BACTERIAL HOST STRAIN
565-658	GST	BL21 (DE3)
		MBP-HIS BL21 (DE3)
		BL21 (DE3)
		Rosetta (DE3)
		Rosetta 2 (DE3)
567-662	HIS	Rosetta 2
	GST	Rosetta 2
567-665	HIS	Rosetta 2
	GST	BL21 (DE3) pLys
		Rosetta 2
567-680	GST	BL21 (DE3) pLys
		Rosetta 2
485-665	GST	BL21 (DE3) pLys
		Rosetta 2
395-567	GST	Rosetta 2
459-567	GST	Rosetta 2
477-567	GST	Rosetta 2

Table 2.2. Mig-2 C' term recombinant proteins.

sequence verified protein expression vectors into one or more protein expression *E.coli* bacterial strains, BL21 (DE3), BL21 (DE3) pLys, BL21 (DE3) pLys Gold, BL21 (DE3) RIP (Stratagene) and Rosetta 2.

Migflin constructs.

cDNA of human Migfilin(s) was kindly provided from our collaborators. I used PCR to amplify the cDNA of the C terminal LIM domains, LIM123 (residues 172-367 and 172-373), LIM23 (residues 241-367 and 241-373), LIM2 (residues 241-304) and LIM3 (residues 298-367) of human Migfilin. We used a high fidelity DNA polymerase,

Pfu Ultra DNA polymerase (Invitrogen), for PCR reactions. I used parallel GST-1 and parallel His-1 vectors for most of the cloning work. All parallel vectors were kindly provided by Dr. Saurav Misra. I transformed sequence verified protein expression vectors into Rosetta 2 (DE3) for subsequent protein expression.

Talin constructs.

Full length human Talin 1 encoding cDNA sequence was provided from Dr. Ma Yang-Qing. I cloned Talin head domain and its subdomains into parallel His-1 vectors. I ordered all primers from Integrated DNA technologies, and used PCR with primers consisting EcoRI and XhoI restriction sites to amplify cDNA of Talin F0 domain residues 1-86, Talin F0F1 residues 1-206, Talin F1 residues 86-206, Talin F2F3 residues 206-429 and Talin H (F0F1F2F3 residues 1-429). I transformed the sequence verified constructs into BL21 (DE3) for protein expression.

Optimization.

All constructs were optimized for their expression and protein solubility at varying temperatures. I used induction temperatures ranging from 15ºC, 20ºC, 25ºC and 37ºC for a temperature dependant optimization, IPTG concentrations between 0.2mM and 1mM for optimization for protein expression, and time of induction from 4hrs, 16hrs, 18hrs and 24hrs. I employed this approach for almost all constructs individually.

We implemented an intense optimization approach for Kindlin 2 11-143 construct. For this construct besides the aforementioned optimization strategy I performed the following strategies to increase the final yield of the protein: protein re-folding using decreasing percentage of urea and Foldt Screen (Hampton Research), auto-induction medium for protein expression, chaperone assisted folding (Takara) by co-

expression of chaperones, applying a cold shock and heat shock for bacterial cells, codon optimization for bacterial expression, varying of vector i.e. fusion tags (GST, HIS, MBP, MBP-HIS, NUS-HIS), surface cysteine mutation, and use of a variety of detergents.

Protein expression and purification.

After optimization, we expressed the fusion proteins in LB (Lennox L Broth) culture media or TB (Terrific Broth) culture media (RPI co-operation) and harvested at 3500rpm for 15min (Sorvall). We suspended the cell pellets in the lysis buffer which was incorporated with 10mg of lysozyme per 50ml lysis buffer, EDTA free protease inhibitor cocktail (Biocompare), deoxyribonuclease and Magnesium ions. We froze the mixture in liquid nitrogen and incubated the frozen cell pellets at 4ºC with slow rotation overnight for cell lysis. The cell lysis procedure for proteins that tend to be unstable (Kindlin 2 168-268) was different. Those cells were immediately ruptured after harvesting by mechanical methods using a French-press or short pulses of sonication. I used phosphate buffered saline (PBS) as the lysis buffer for GST fusion proteins, a 20mM Tris buffer with 0.2mM NaCl, 1mM EDTA, 10µM beta mercapthoethanol buffer solution as the lysis buffer for MBP tagged protein and 300 mM phosphate buffer with 500 mM NaCl, pH 8.0 containing 10mM imidazole for His fusion proteins.

We purified the fusion protein using affinity chromatography with Nickel-NTA resin (Qiagen), Glutathione sepharose 4b resin (GE healthcare), and amylose resin (NEB) for each HIS, GST and MBP fusion protein purifications respectively. We cleaved the fusion tag with a suitable protease which is TEV protease for proteins derived from parallel cloning vectors, Thrombin protease (Sigma) for pGEX derived cloning vectors and pET15b and Faxtor Xa protease (Novagen) for pET30a cloning vectors in

appropriate buffers and cleavage conditions. We further purified the protein using size exclusion chromatography, either Superdex 75 or Superdex 200 matrix (Amersham Bioscience) depending on the size of the protein.

Isotope labeling

Isotopically labeled proteins are required for 3D NMR experiments for structure determination. We used $^{15}NH_4Cl$ as the ^{15}N source and ^{13}C glucose as the ^{13}C source in culture medium to obtain ^{15}N and / or ^{13}C enriched proteins.

During isotopic labeling of Zinc finger proteins, I added 1ml of 0.1M $ZnCl_2$ per 1L to the media just before induction of protein. We routinely performed overnight induction either at room temperature or at 20ºC. For Migfilin LIM domains, the best optimization condition in LB is induction overnight at 15ºC, and for isotope labeled LIM domains the best induction temperature was 25ºC.

Mutagenesis

Kindlin 2 11-143 protein has two Cysteines. I introduced a point mutation at C12S of Kindlin2 11-143 construct using the Quick Change Site Directed Mutagenesis Kit (Stratagene).

I prepared a sequence deletion mutation for the integrin activation assay performed by Dr. Ma. I deleted residues ranging from 11-143 from the full length Kindlin 2 sequence using Quick Change Site Directed Mutagenesis Kit (Stratagene).

2.3. Macromolecular X-ray crystallography

Besides NMR, macromolecular X-ray crystallography is the widely used technique for 3D protein structure determination. More than 80% of the protein structures deposited in the protein data bank (PDB) are derived from X-ray crystallography. The basic principle in X-ray crystallography relies on the diffraction of the X-ray wave by the electron cloud of the protein. Structure determination by X-ray crystallography involves multiple steps. The major requirement for X-ray structure determination is the requirement of a 'solid' protein crystal. The crystal should be >10A° in length in all 3 dimensions, with uniform composition and lack of physical imperfections. The crystal is placed in an X-ray beam and its diffraction patterns or reflections at continual angles throughout the crystals z axis are recorded. All recorded reflections are processed via mathematical formulations computationally and subsequent refinement produces a 3 dimensional protein structure.

Structure determination by X-ray Crystallography takes less time and is automatic compared to NMR that takes a longer time with more manual involvement. NMR protein structure determination is limited to 30-40 kDa protein whereas in X-ray Crystallography there is no size limitation. However, X-ray crystallographic approaches always require a crystal or multi crystal complex of the protein, which limits its usage as some proteins are difficult to crystallize or not able to crystallize at all. Most importantly, X-ray crystallography will not show the dynamic effects of an interaction process, rather it gives a snapshot of an end result of an interaction. Therefore, besides structure determination, NMR plays a crucial role in the understanding of the dynamic function of

a binding interaction process. (Wuthrich, 1991). Besides NMR, we used X-ray crystallography as an alternative step for protein structure determination.

2.3.1. Materials and methods

Kindlin 2 11-143 and 1-105

We expressed Kindlin 2 11-143 and 1-105 protein expression constructs as a GST fusion proteins in E. coli BL21 (DE3) pLys cell line. A cold shock was applied to cell cultures by incubating the cultures in an ice-water bath for 30 min, followed by induction with 0.5mM IPTG at room temperature 298K for 16hrs. The purified protein was concentrated to 1mM (15mg/ml) and dialyzed overnight into crystallization buffer containing 20mM Tris-HCl, 50mM NaCl, pH 7.0, and 1mM DTT. We transformed Kindlin 2 11-143 construct into B834, a Methionine auxotroph bacterial strain of *E. coli*, to obtain Selenomethionine labeled protein.

Crystallization

We used the hanging drop vapor diffusion method for growing crystals (McPherson et al., 1995). We used Commercially available crystal screening kits for screening around >600 different crystal conditions, Crystal Screen I & II, Salt Rx, Index, Wizard I & II, Nextal Classic L suite, Protein Complex, Additive screen (Hampton Research screening kits, Qiagen screening kits). Each crystal drop had a total volume of 2µl comprising of 1 µl of 15mg/ml protein and 1µl of crystallization condition. The well volume was 150µl. I optimized crystallization buffer for its pH, buffer concentration, additive/precipitant concentration and salt concentration.

X-Ray data collection and analysis

We flash froze crystals after soaking in a gradient of cryoprotectant solutions. The gradient soaking follows as: the crystal was first transferred from the crystallization buffer to a 10% Ethylene glycol containing crystallization buffer, from there to a 5% glycerol and 15% Ethylene glycol mixture containing crystallization buffer and finally into a 5% glycerol and 20% Ethylene glycol containing crystallization buffer solution. We acquired diffraction data using Case Pharmacology X-ray facility and at the Advance Photon Source at Argonne National Laboratory IL. At Case X-ray facility, the crystal to detector distance was 80mm. We collected diffraction data at 0.5º oscillation angle throughout 180º and exposed each frame for 30 sec. Finally, we analyzed our acquired diffraction data using HKL2000 software.

2.4. Isothermal Titration Calorimetry (ITC)

2.4.1. Overview

ITC has become an invaluable tool in biological sciences and pharmaceutical industry. We used ITC to understand the energetics of our binding interactions. ITC measures the associated heat change of an interaction process at constant pressure and is able to obtain all thermodynamic parameters such as ΔG, ΔH, ΔS, Ka / Kd and stoicheometry, in one single experiment giving a complete thermodynamic profile of the binding interaction. ITC can be used with any buffer, at any pH, any solution whether clear or turbid. Despites its significant advantages, ITC has several drawbacks. One main consideration is the amount of sample material required for one single experiment. In

addition, ITC can only measure a heat energy difference of a particular reaction. But there are reactions which are entropically driven and are not able to detect by ITC.

2.4.2. Design of an ITC experiment

Strong binding < 0.1nM and weak binding > 10nM interactions cannot be evaluated for its precision and accuracy by ITC. The value of c (c= Ka[M]n) should be between 1-1000 to perform an accurate experiment with a sigmoidal curve.

When designing an experiment, the ligand and macromolecule, should be in the exactly same buffer. Control experiments should be performed to evaluate the heat of dilution of the macromolecule-protein, heat of dilution of the ligand and heat of mixing. The concentrations of the protein and ligands have to be accurately measured as it directly correlates with the final results. The choice of buffer is important as certain buffers containing large molecules (Tris buffer) have a large heat of dilution signal in which the actual binding signal can be masked. To achieve better sensitivity the choice of buffer should always be a small ion buffer such as phosphate. Reducing agents like DTT may cause unstable and noisy baselines which may affect the end-results. Furthermore, degassing buffers is a very important step as the entrapment of tiny air-bubbles in the system can contribute to a noisy base-line. Data analysis is performed using ORIGIN 7.0 software which was provided by Microcal Corporation.

2.4.3. Materials and methods

Talin and lipid interaction

We performed a series of ITC titrations between Talin subdomains and PIP2 lipids. I dialyzed Talin proteins of 50μM concentrations overnight into buffer containing

50mM Sodium phosphate, 150mM NaCl, pH 6.8. The buffers were filtered using a 0.2µ filter and degassed thoroughly. I suspended the lipids of PIP2 C4 and PIP2 C6 (Echelon) in the buffer being prepared to a final of 1mM. All experiments were carried out at 298K with a stirring speed of 300rpm. I performed titrations of a total of 30 injections with an injection volume of 7.5µl and 4 min spacing time between each injection. Finally, I collected data on a VP-ITC instrument from Microcal Inc. and analyzed results using Origin 7.0 software.

Talin and Migfilin interaction

I used a 50µM concentration of Talin F0 for the initial ITC titration experiment. I dialyzed all protein samples, ligand and macromolecule, overnight into the same buffer of 50mM Sodium phosphate, 100mM NaCl, pH 6.8. The titration was performed on a ITC_{200} ultrasensitive micro-calorimeter instrument (Microcal). I performed the titration between Talin F0 and Migfilin LIM23 in 2µl aliquots of 30 injections. I used a 2mM of LIM23 as the syringe protein concentration, and analyzed the results using Origin 7.0 software from Microcal.

2.5. Surface Plasmon Resonance Spectroscopy (SPR)

Surface Plasmon Resonance Spectroscopy (SPR) is the most widely used technique to study and characterize an interaction between two molecules. We used SPR to understand the binding affinity of a particular interaction, the need of a small sample size and versatility of the instrumentation and usage. However, the error associated of a weak interaction and using small molecules is high.

The basic principle underlying SPR was discovered in 1950s. The phenomenon of the emission of surface Plasmon radiation at the total internal reflection angle of a light beam at two density mediums (with one coated with a metal layer) is the basic principle in SPR. However, the first instrument was developed in the late 1980's. The intensity of the emitted surface Plasmon wave is proportional to many factors such as the type of metal, the thickness of the metal layer and the density of the medium. The mass density of the medium is utilized in biosensor chip development by immobilizing a wide variety of ligands.

2.5.1. Materials and methods

We performed all experiments on a BIACORE 3000 (Amersham Pharmacia) instrument at CCF-LRI Biotechnology core. We used CM5 sensor chips (Biacore) for most SPR experiments. EDC, NHS and ethanolamine were prepared from the amine coupling kit (Biacore). I filtered and degassed all buffers though a 0.2μ filter and also used research grade buffers from Biacore.

Kindlin 2 and Migfilin interaction

We immobilized Kindlin 2 11-143, full length Kindlin 2 and Kindlin 2 1-105 on CM5 sensor chip flow cells using amine coupling chemistry. Densities reached to 1000 RU during immobilization. We exchanged all ligands to exact buffer as the running buffer. Ligands used for interaction studies are: Migfilin LIM23, LIM1, LIM2, LIM3, LIM123 and LIM12. Data collecting was achieved using Biacore control 3000 software and data analysis was done using BIAevaluation software version 4.0. All experiments

were done at 25ºC unless otherwise noted. The running buffer used was 50mM Sodium phosphate, 100mM NaCl, pH 7.0.

Talin and Migfilin interaction

We immobilized Talin F0 and Talin F0F1 proteins on CM5 sensor chip the same way described above. HBS buffer from Biacore was used as the running buffer. Migfilin LIM23 and LIM1 proteins were the interacting partners for the experiment.

Kindlin 2 PH domain and PIP3 interaction

I immobilized PIP3 lipids on a L1 sensor chip the same way as described above. HBS buffer from Biacore was used as the running buffer. Kindlin 2 PH domain (provided by Dr. K. Fukuda) was used as the interacting partners for the experiment.

CHAPTER III

KINDLIN 2 N TERMINAL STRUCTURE

3.1. Introduction

Kindlin family proteins play an important role in the human body. The health related importance of Kindlin 2 was described earlier in chapter 1. Its role in cardiogenesis as well as in maintaining the homeostasis of adult heart function makes Kindlin 2 unique among the Kindlin family proteins (Dowling et al., 2008; Hatcher and Basson, 2008; Orlic et al., 2001). Lack of adequate structural information of Kindlin family proteins makes us difficult to understand the molecular mechanism of its function. Kindlin 2 is a relatively novel protein and structural details about Kindlin 2 are hardly known. However, the F0 domain of Kindlin 1 protein was recently resolved (Goult, B.T. et al., 2009). This chapter specifically discusses the structural details of Kindlin 2 N-terminal F0 domain.

3.2. Expression of Kindlin-2 N terminal domains

The requirement of a sub-molar concentration of protein is one of the crucial factors in protein structure determination. In addition, the stability of the protein at room temperature for two weeks is another major requirement. Proteins that fall into both categories are not abundant *in vivo*. Kindlin 2 is such a cumbersome protein which required a trial-and-error approach and a subsequent optimization strategy for expression, yield, solubility and stability of the expressed domains. Lack of information in literature about the expression conditions of Kindlin variants made us to put an extra effort and time on getting the protein for structural studies. Our approach was as follows:

1. Choosing boundaries and cloning according to secondary structure prediction and tertiary model structure prediction of the protein.
2. Checking the instability index, occurrence of rare codons etc of the protein.
3. Optimization for expression
4. Optimization for yield
5. Optimization for protein solubility

    Aggregated proteins

    Precipitation of the protein

    Stability of the protein
6. Back to 1 if none of the approaches succeeded.

Selection of proper boundaries for a protein is the most important step that affects the final yield and stability of the protein. I selected the boundaries according to the predicted secondary structure of the protein of interest. In here I chose the boundary so that it falls into a coiled region of high probability (see Appendix 1).

Multiple constructs engineered for Kindlin 2 N-terminal and their expression conditions are shown in table 3.1. Most constructs were challenging in terms of obtaining the encoded protein in soluble and stable conformation. I carried out an extensive optimization approach for each construct. Kindlin 2 11-143 was the initial construct which resulted a soluble protein but yielded less than 1mg per Liter of LB culture. I have described multiple optimization strategies below which I used to improve the yield of Kindlin 2 11-143 protein.

A major fraction of the protein accumulated in inclusion bodies. I performed a protein refolding approach from inclusion bodies for Kindlin 2 11-143 protein. Among the available methods, we chose refolding via a decreasing percentage of urea concentrations. I compared the ^{1}H-^{15}N HSQC spectra of the native and refolded ^{15}N labeled protein. The spectra were completely different implying that refolding failed for Kindlin 2 11-143 construct.

There will be always a controversy arisen when a human protein is expressed in a bacterial expression system. Compared to the easiness of handling, low turn-around time and recombinant protein expression, bacterial expression systems are always preferred against eukaryotic expression systems. To avoid or reduce the conflict of proper folding of the protein we used a chaperone co-expression to assist protein folding. I transformed different types of chaperone encoding plasmids into the bacterial strains containing our expression constructs (Takara). A significant increase in the yield of soluble protein could not be observed for Kindlin 2 11-143 protein.

The codon usage in bacteria is somewhat different from that of Eukaryotic cells. The relative frequency that certain human codons are used in bacteria is different as well.

For example a human CCC codon for proline has a 0.4% average frequency been used per 100 codons compared to other proline encoding codons CCU – O.7%, CCA – 0.8%, CCG – 2.4%. As a result there will be a pause during translation as the ribosome has to 'wait' until it gets the CCC tRNA. If the occurrence of rare codons is high moreover consecutive, the ribosome may stop translating the protein resulting in a truncated protein or may allocate a wrong codon. To prevent such incidents there are bacterial expression systems being introduced which increase the pool of rare codon tRNAs within the bacteria. E.g. Rosetta, Rosetta2, RIPL etc. Kindlin 2 11-143 has several rare codons. The expression of the construct in Rosetta 2 bacterial cells did not increase the solubility of the protein (Burgress-Brown et al., 2008, Pro. Exp. Purifi.).

Another addition for this approach was to synthesize the DNA sequence after codon optimization. In here the whole DNA sequence of Kindlin 2 11-143 was synthesized selecting or changing rare codons for more abundant codons in bacteria. I cloned the cDNA or minigene (IDT, Integrated DNA Technology) into a suitable vector and analyzed its expression. Results did not show a significant improvement of soluble protein.

MIG-2 BOUNDARIES	FUSION TAG	BACTERIAL HOST STRAIN	PROTEIN EXPRESSION	PROTEIN SOLUBILTY	GEL FILTRATION
1-134	HIS	Rosetta 2 (DE3)	+	insoluble	
	GST		+	insoluble	
1-154	HIS	Rosetta 2 (DE3)	+	partly soluble	Aggregate
1-158	HIS	Rosetta 2 (DE3)	+	insoluble	
1-218	GST	Rosetta 2 (DE3)	+	insoluble	
11-177	GST	Rosetta 2 (DE3)	+	partly soluble	
11-143	HIS	Rosetta 2 (DE3)	+	insoluble	
	GST	Rosetta 2 (DE3)	++	soluble	monomer
	GST	BL21(DE3) pLys	++	soluble	monomer
	MBP	Rosetta 2 (DE3)	+	soluble	monomer
	MBP	BL21 (DE3) RIP	+	soluble	monomer
1-105	GST	BL21(DE3) pLys	+++	soluble	monomer

Table 3.1. Summary of Kindlin 2 N-terminal constructs.

There are endless possibilities to argue to what may be the cause for poor expression and insolubility and what can be done next. However, two major approaches were selected and used in this study. First is to subclone a certain region of interest of the protein cDNA and optimize extensively for its expression, solubility etc. for a soluble monomeric /oligomeric stable protein. Second is to subclone a large number of constructs simultaneously varying the boundaries of the protein and check their expression and solubility. Having attempted both strategies, it is quite evident, that the time spent for optimizing a protein of a particular construct for endless possibilities is way more time consuming and not cost-effective than varying the boundaries of the protein.

3.3. The structure of Kindlin 2 N-terminal

To understand the role of Kindlin-2 N-terminal in integrin activation, it is essential to know the molecular level details about the protein. In order to obtain the structure in an atomic level resolution of Kindlin 2 N-terminal, we used a two part approach, NMR and X-ray crystallography for potential structure determination of the protein. The techniques were described in Chapter II.

3.3.1. Crystallographic approach for Kindlin 2 11-143

We performed crystallization trials for both Kindlin 2 1-105 and 11-143 proteins. Despite the vast yield difference between the two constructs, <1mg/L of LB culture media for K2 11-143 and >10mg/L of LB culture media for K2 1-105, we were able to obtain sufficient protein for initial crystallization setup. A single crystal was obtained for

Kindlin 2 11-143 protein but Kindlin 2 1-105 protein showed no signs of crystallization hits so far. Several images of the crystals in different crystallization conditions are shown in figure 3.1. The Kindlin 2 full length model structure (Fig 3.10.) shows that there is long floppy overhang at the C-terminus from residues 95 to 105 which might have prevented tight crystal packing i.e. crystallization. According to the NMR structure of Kindlin 2 1-105 (next sub-chapter) the N-terminal 1-12 residues show a very dynamic behavior. This may be another reason to prevent crystallization of Kindlin 1-105 protein. In contrast, in Kindlin 2 11-143 construct, residues 95 to 143 forms an anti parallel beta sheet and a small helix at the C- ter which might have helped in better crystal packing and promoted protein crystallization. The model structure was not present at the time of choosing domain boundaries for cloning. Having the model structure currently, a much better construct would be residues 12-95 or 20-95, which reflects the core region of the Kindlin 2 F0 domain.

We obtained multiple crystallization conditions for Kindlin 2 11-143 protein from the initial trial. These are:

1. 1.4M sodium potassium phosphate, pH 8.2.
2. 0.1M Tris, pH 8.5, 1.2M sodium potassium tartrate tetrahydrate.
3. 0.1M Tris , pH 8.5, 0.7M tri-sodium citrate dehydrate

All conditions where crystallization has occurred had a pH higher than 8.0. Thus Kindlin 2 11-143 protein crystallization is pH sensitive. We performed optimization around the crystallization condition for pH, salt concentration, temperature and buffer concentration. The best crystallization condition was 1.6M sodium potassium phosphate at pH 8.2.

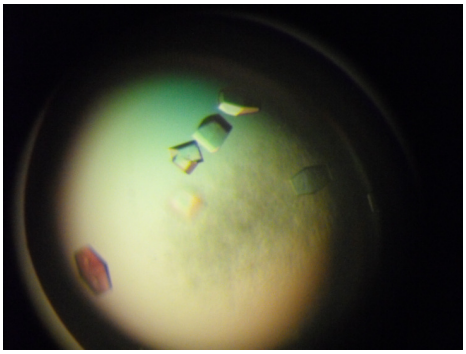

(a)

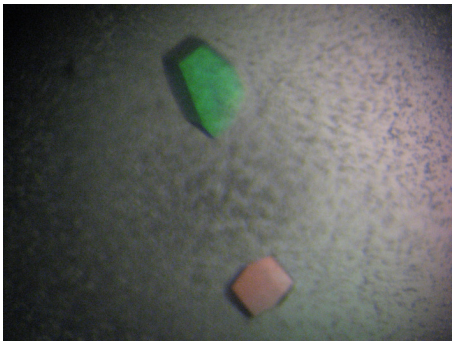

(c)

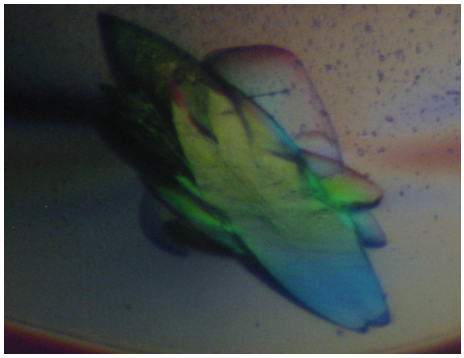

(b)

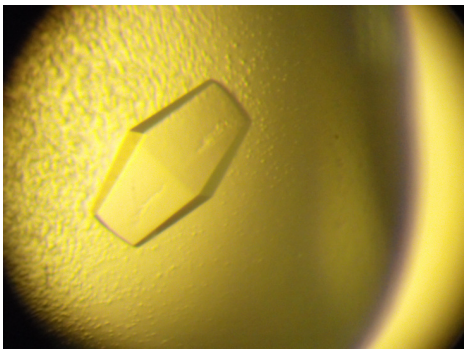

(d)

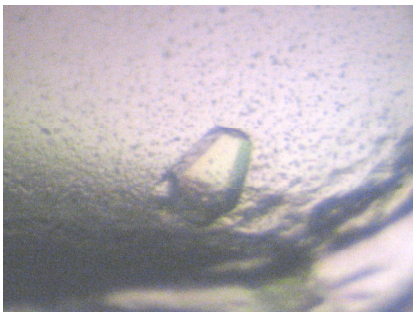

(e)

Figure 3.1. Protein crystal images of Kindlin 2 11-143. (a), (b) and (d) grown in 1.4 M sodium potassium phosphates, pH 8.2. (c) protein crystal was grown from 0.1M Tris, pH 8.5, 1.2M sodium potassium tartrate tetrahydrate. And crystal (e) in 0.1M Tris, pH 8.5, 0.7M tri-sodium citrate dehydrate.

Further optimization using the additive screen kit for the optimized condition revealed a 0.1mM of spermidine as the additive constituent. Crystal cryoprotection was achieved through a sequential gradient of quick soaks explained in the experimental section of chapter 2.3.

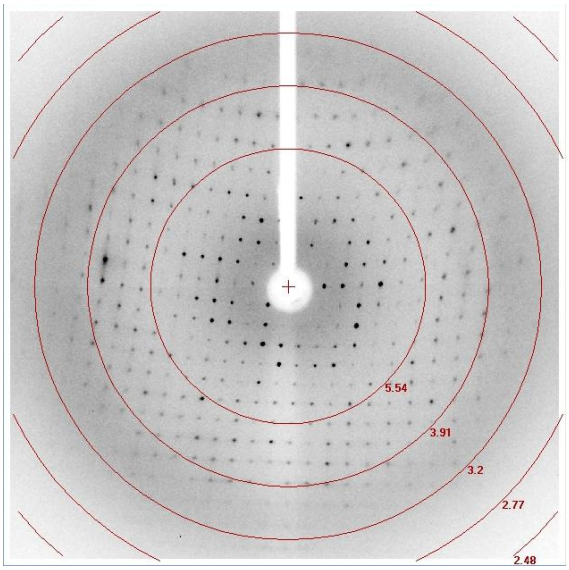

Figure 3.2. Diffraction pattern of Kindlin 2 11-143 protein crystal. The diffraction patterns on other oscillation angles show severe overlap. The crystal is diffracting to 3.0 angstrom resolution, but the 3D structure could not be resolved due to severe spectral overlap.

An image of the diffraction pattern of Kindlin 2 11-143 protein crystal is shown in figure 3.2. We collected images at 0.5º oscillation angles. A severe overlap was seen among most consecutive images. We analyzed the data by HKL2000 software and the initial analysis revealed that the crystals diffracted to 2.9 Å resolutions with a space group of p21212. We were not successful in the structure determination process due to severe overlap of data points. Data analysis from both in-house x-rays and synchrotron light source failed due to severe peak overlap of reflections.

A future approach would be 0.25º oscillation angle image collection with an increase in detector distance. This may expand the peak positioning on the film and may prevent the peak overlap. However, due to the very low yield of the protein and difficulties in reproducibility, crystallization setup for Kindlin 2 11-143 was not convenient.

3.3.2. NMR structure of Kindlin2 N-terminal 1-105

Kindlin 2 1-105 protein is stable even for weeks at room temperature. I was able to concentrate the protein up to 2mM without any signs of precipitation. We used a one milli-molar of ^{15}N and ^{13}C doubly labeled sample for structure determination. The ^{15}N-^{1}H HSQC spectrum shows excellent chemical shift dispersion with uniform signal intensities suitable for detailed NMR studies.

We selected peaks prior resonance assignment, using NMRview software. We first selected peaks of the HSQC spectrum, followed by selecting peaks in triple resonance spectra HNCACB and HNCACO. Residues 8 and 68 are overlapping in the HSQC spectrum. Another cluster of overlapping residues in HSQC spectrum was observed for residues 25, 42 and 66. HNCACB, HNCA and CBCACONH were comparatively analyzed for confirmative peak picking in HNCACB spectrum. Similarly HNCACO and HNCO spectra were comparatively analyzed for peak picking in HNCACO spectrum. There were difficulties in 100% resonance assignment of HNCACB and HNCACO spectra due to overlap of resonances but more than 95% residues were assigned.

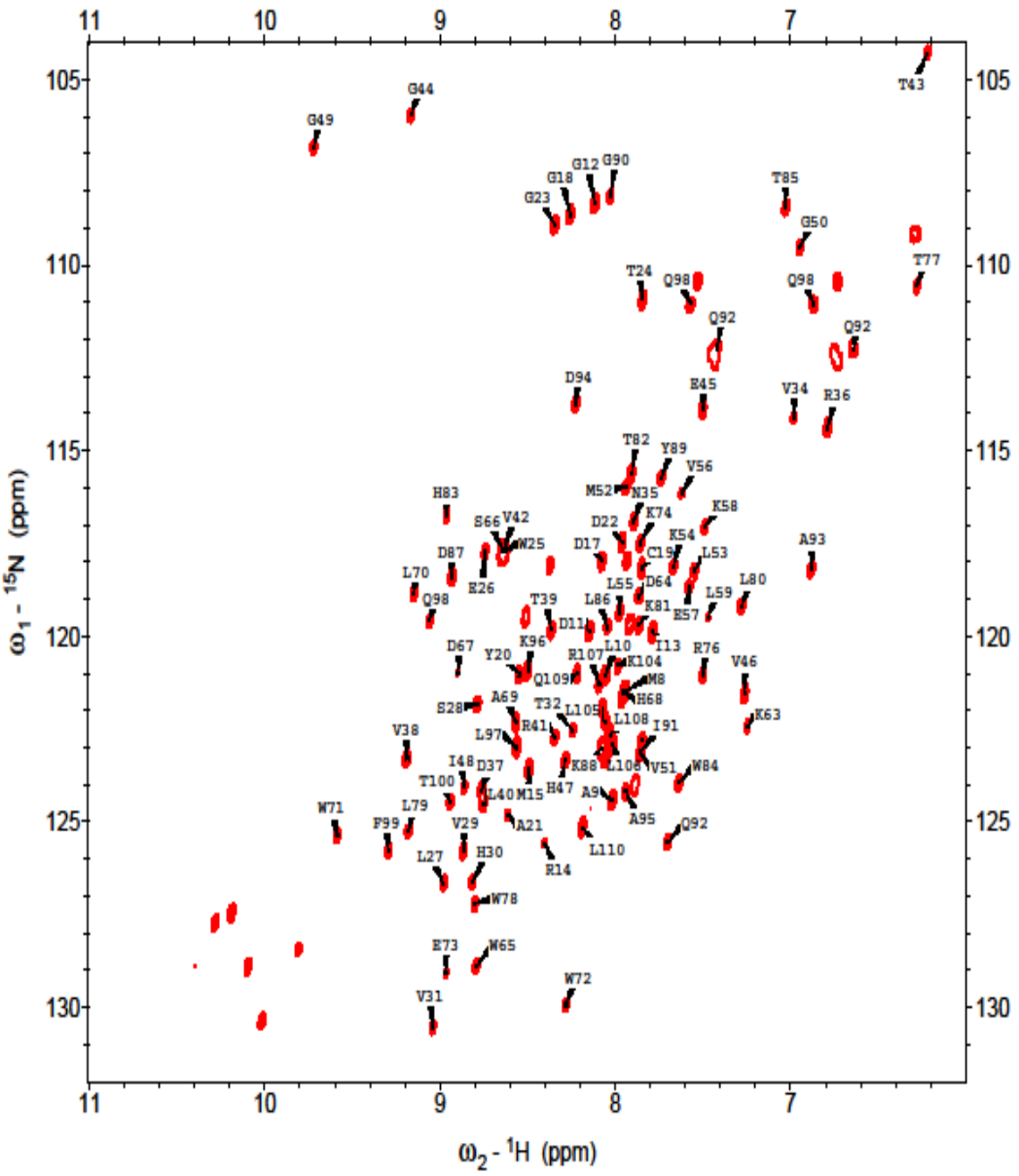

Figure 3.3. ^{1}H-^{15}N HSQC spectrum of Kindlin 2 1-105. The peaks are labeled with the corresponding assignment of Kindlin 2 1-105 residues

Backbone assignment We used PASA, a software for automatic backbone assignment, for backbone assignment (Xu et al., 2006). The chemical shift tables of HSQC, HNCACB and HNCACO spectra were used as the input for PASA. We completed all ambiguous assignments manually. 88% of the backbone assignment was completed (99/112 residues). There are 9 missing peaks: 4 proline residues and residues 33, 60, 61, 62, 75 which were unable to assign. The assigned HSQC spectrum is shown in figure 3.3.

We calculated the secondary structure of the protein from the C α and C β chemical shifts obtained from assigned spectra listed above. The secondary structure prediction shows that the protein comprises of a combination of helices and beta sheets. The prediction is shown in figure 3.4. An extended helix is observed between residues 46-58 and a short helix is predicted from the chemical shift indices between residues 85-89. Beta strands are predicted between residues 24-30, 36-43, 67-73 and 96-100.

Side chain assignment was not 100% complete. We were able to assign approximately 85% of the peaks from both HC(CO)NH and C(CO)NH spectra. Most of the peaks were missing and some show severe overlap. A stretch of alternative long side chain amino acids leucines and arginines showed missing and overlapping spin systems.

HCCH-TOCSY spectra were helpful in assisting in side chain assignment of the protein.

The 3D structure We calculated the 3D structure as described in section 2.1.3. The N-ter Kindlin 2 1-105 structure has an ubiquitin-like beta-grasp fold, similar to Kindlin 1 structure. A 12 residues long alpha helix (residues 48-59) is partly surrounded by 5 beta sheets of variable lengths. The solution structure is shown in Figure 3.5 and was calculated from a total of 1304 restraints. The table of structural statistics for the solution

structure is shown in table 3.2. The structured core represents residues 16-93 (corresponding to residues 23-100 in our structure) has a convergence of 0.4Å.

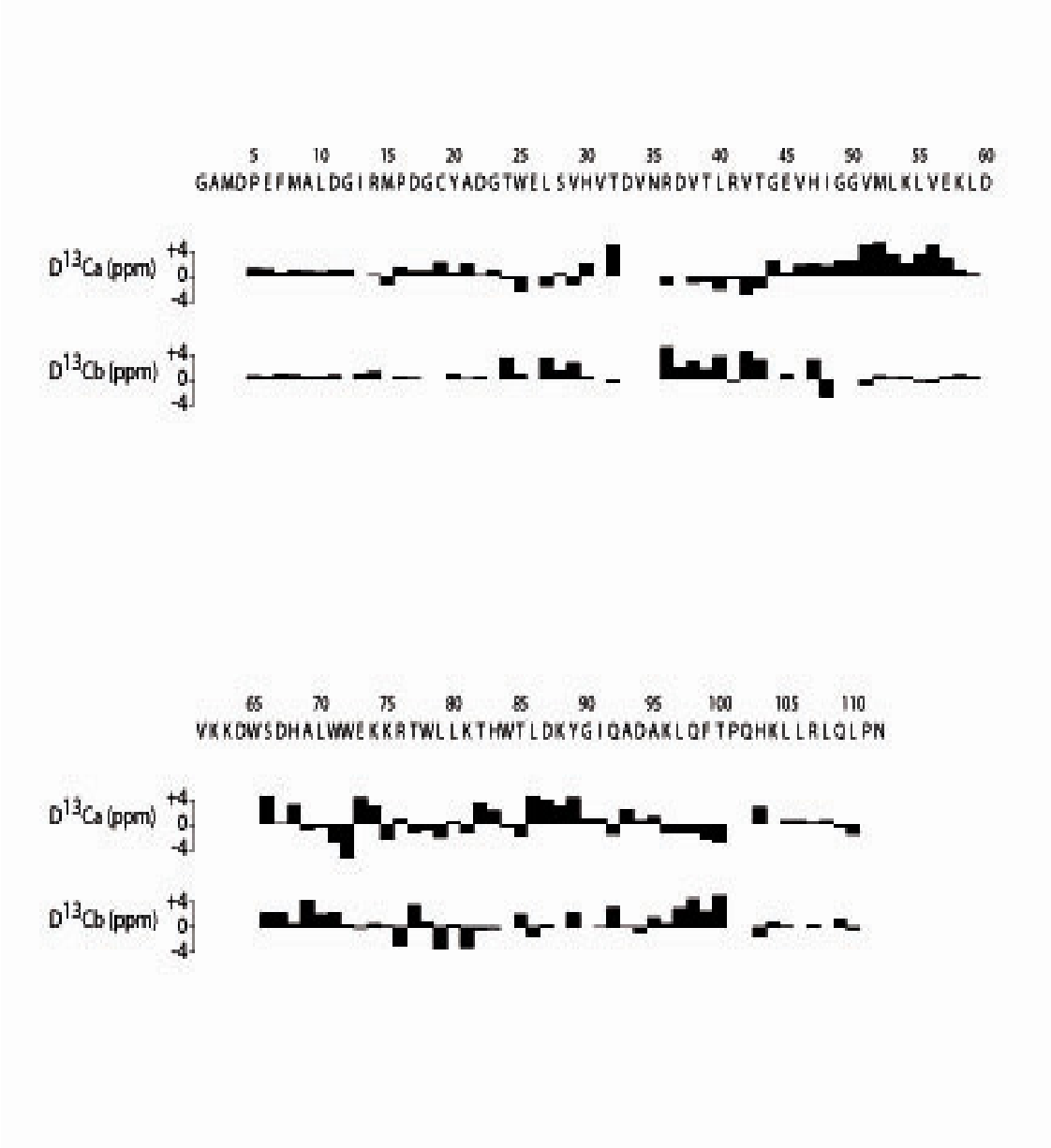

Figure 3.4. Secondary structure predictions of Kindlin 2 1-105. Chemical shift indices correspond to 13Cα and 13Cβ spin resonances of each residue.

The N-terminal 1-18 residues of Kindlin 2 1-105 structure shows a helical feature spanning residues 6-12 (13-19res in our construct) which we defined by a distinct set of NOEs. A beta hairpin is seen within residues 25-42, with β1 from residue 25-31 and β2 from residues 36-42. Hydrogen bonds were observed between 25-42, 27-40, 29-38 and 31-36 residues. The turn is defined by 4 residues in which residue Asp 33 is a missing spin system. The first helix, α1 is 12 residues in length (res 48-59). Residues 60-62 are missing spin systems. The loop from residue 59 to 69 is less defined due to the missing stretch of spin systems. Residues 69 to 71 and 77-79 form short beta strands β3 and β4 respectively. The fifth beta strand β5, defined by residues 98-100, runs in-between β1 and β3 with hydrogen bond contacts to both β1 and β3 strands. These strands form a beta sheet which covers the hydrophobic side chains of the α1 helix.

The Ramachandran plot is shown in figure 3.6, which is a sum of 20 low energy structures out of 100 structures. 96.4% of residues between 8-101 residues of Kindlin 2 F0 domain structure belong into the category of allowed region in the Ramachandran plot. The missing spin systems, residues 33 and 60 on the plot are violated among all 20 calculated low energy structures in the Ramachandran plot. Structural statistics for the low energy 20 structures are shown in table 3.2. The overlay of the 100 lowest energy structures is shown in figure 3.7. This figure show high convergence of the structures between residues 23-100. However the N-terminal tail residues 8-23 display a dynamic behavior.

Overall, Kindlin 2 F0 domain structure is in excellent agreement within the quality parameters for NMR solution structure calculation.

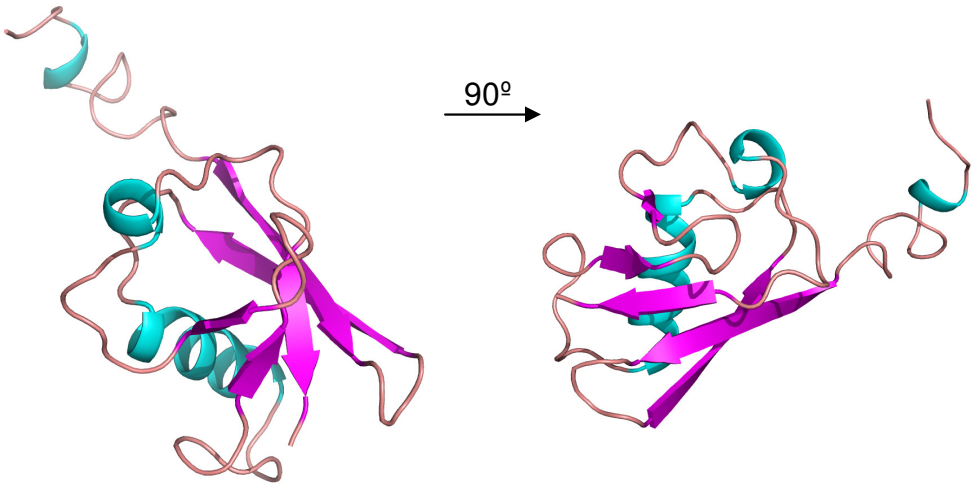

Figure 3.5. A ribbon diagram of the structure of Kindlin 2 1-105. The α helices are depicted in cyan color and the beta strands in magenta. The structure shows 2 distinct helices spanning across residues 48-59 and 86-89. A helix like feature is apparent in the N-terminus across residues 15-19. Five beta strands with varying length partially covers α1 helix.

	parameters
NOE distance restraints	
All	1304
Sequential, |i-j|=1	436
Medium range, 1<|i-j|<6	222
Long range, |i-j|>= 6	295
Intraresidue	445
RMSD from idealized covalent geometry	
Bonds (Å)	0.0057 +/- 0.000
Angles (deg)	0.6873 +/- 0.018
Impropers (deg)	0.5258 +/- 0.012
Total energy (kcal/mol)	811.28
Ramachandran plot	
Most favored region (%)	69%
Additionally and generously allowed region (%)	31%
Disallowed region (%)	0%
Average RMSD residues 8-100	
Backbone atoms (Å)	1.745 +/- 0.470
Heavy atoms (Å)	2.087 +/- 0.418
Average RMSD residues 23-100	
Backbone atoms (Å)	0.425 +/- 0.105
Heavy atoms (Å)	1.002 +/- 0.125

Table 3.2. Structural statistics of Kindlin 2 1-105 structure calculation.

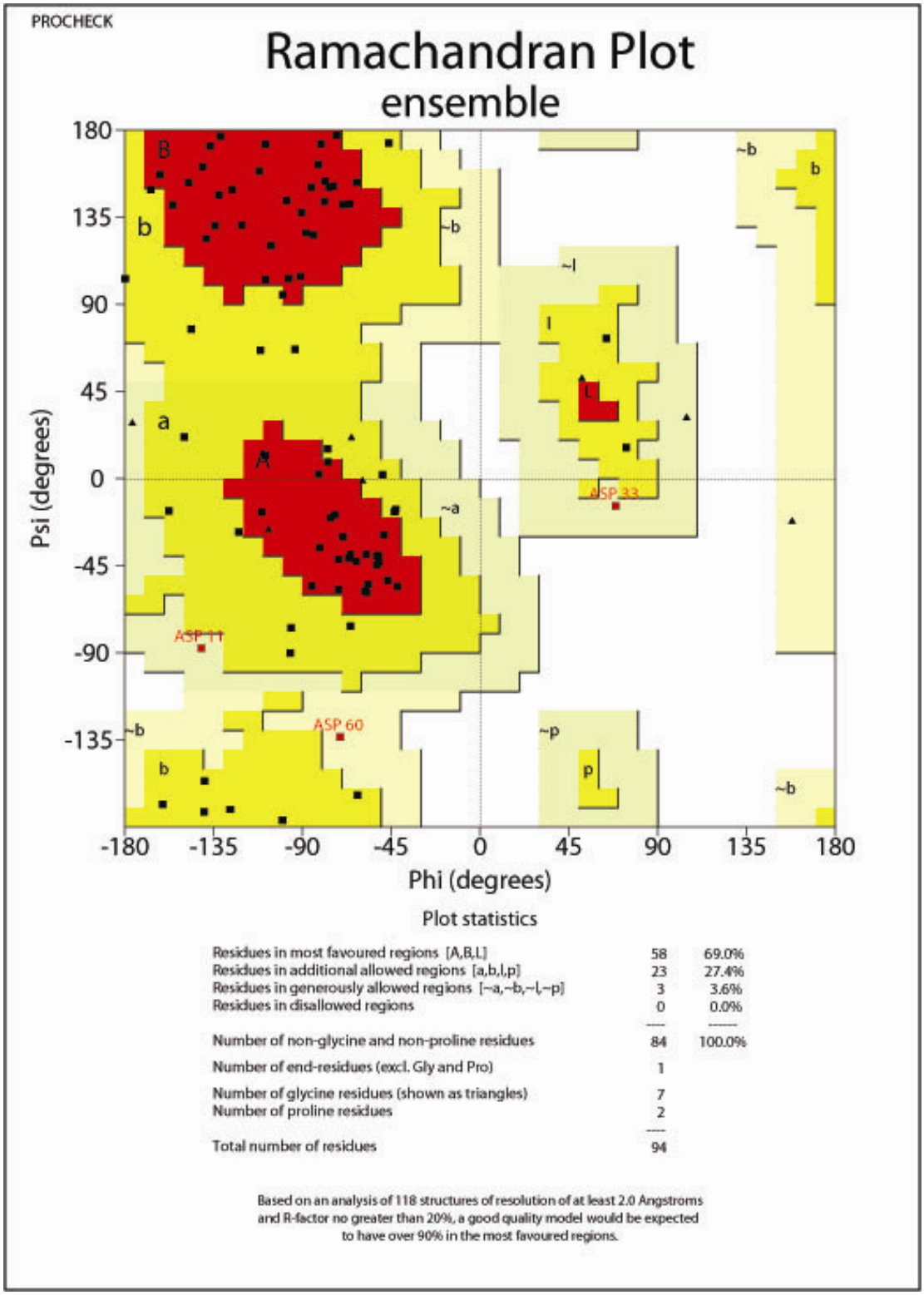

Figure 3.6. Ramachandran plot of Kindlin 2 1-105 of the 20 lowest energy structures.

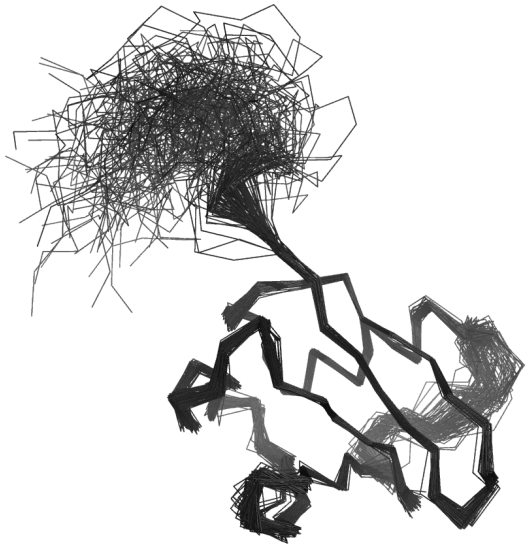

Figure 3.7. The overlay of the 100 lowest energy structures.

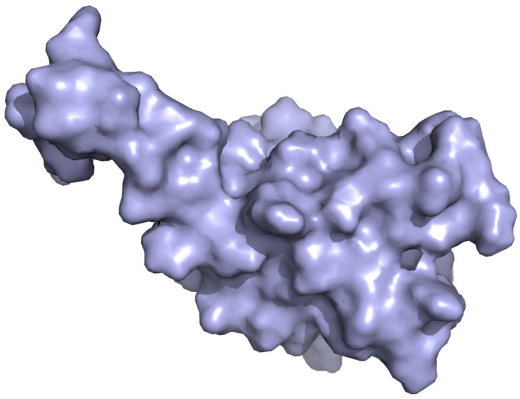

Figure 3.8. Surface representation of the charges of the structure of Kindlin 2 1-105.

3.4. Structural comparison of Kindlin 1 and Kindlin 2 F0 domains.

Kindlin 1 and 2 full length proteins share 62% sequence identity. The N-term residues 1-105 including the F0 domain of both proteins have a sequence similarity of 62 %. Figure 3.13.(a) shows a sequence comparison between all N-term 1-105 sequences of Kindlin proteins.

A closer look at the multiple sequence alignment of Kindlin proteins show a considerable similarity between residues 18-105 among all three sequences. The core structure is well conserved among Kindlin F0 domain within orthologs (Goult et al., 2009). A considerable difference is seen within the first 18 residues of Kindlin 2 compared to the first 11 residues in Kindlin 1 and the first 16 residues in Kindlin 3. These sequences are drastically different in length and composition compared to the core structure and might account for potential differences in binding patterns.

The N-terminal 1-18 residues show a right handed helical feature spanning residues 6-12 (13-19 residues in our construct). This feature is not present in Kindlin 1 structure, in which the corresponding region is disordered. In addition to the helical feature in the N-terminus, there are two other significant differences between Kindlin 1 and 2 structures: First is the turn between β1 and β2 strands. In Kindlin 2 it is a tight turn of four residues whereas in Kindlin 1 it comprise of nine residues. See figure 3.9.(b). The assignment of residue D33 in the turn of Kindlin 2 is missing. The helices α1 and α2 have equal lengths in Kindlin 1 and 2 F0 domain, which are 13 and 5 residues respectively. Both helices are right handed with similar orientation angles. The second major

```
CLUSTAL W (1.83) multiple sequence alignment

K1              ----MLSSTDFTFAS--WELVVRVDHPNEEQQKDVTLRVSGDLHVGGVMLKLVEQINISQ 54
K2              MALDGIRMPDGCYAD-GTWELSVHVTDVN----RDVTLRVTGEVHIGGVMLKLVEKLDVKK 56
K3              --MAGMKTASGDYID-SSWELRVFVGEEDPE-AESVTLRVTGESHIGGVLLKIVEQINRKQ 57
                     :  ..  : .  *** * * . :    ..*****:*: *:***:**:**::: .:

K1              DWSDFALWWEQKHCWLLKTHWTLDKYGVQADAKLLFTPQHKMLRLRLPN 103
K2              DWSDHALWWEKKRTWLLKTHWTLDKYGIQADAKLQFTPQHKLLRLQLPN 105
K3              DWSDHAIWWEQKRQWLLQTHWTLDKYGILADARLFFGPQHRPVILRLPN 106
                ****.*:***:*: ***:*********: ***:* * ***: : *:***
```

(a)

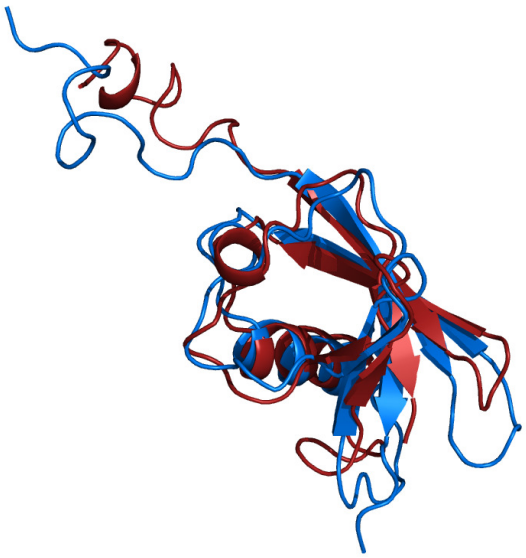

(b)

Figure 3.9. (a) Multiple sequence alignments of residues 1-105 of Kindlin proteins. K1=Kindlin 1, K2=Kindlin 2, K3=Kindlin 3. The sequence alignment was obtain using Clustal W software, which is the most commonly used softare for the alignment of multiple residues. **(b) Overlay of Kindlin 1 and 2 solution NMR structures.** Blue-Kindlin 1 and red-Kindlin 2 F0 domains. Despite the 60% sequence similarity, the globular fold is the same. Minor differences are observed between the two structures.

difference between Kindlin 1 and 2 F0 structures is the length and position angle of the beta strands. β1 and β2 beta strands in Kindlin 1 and 2 have equal lengths and orientations except the beta hairpin turn, which is different in the number of amino acids. In Kindlin 2 F0 domain, the β3, β4 and β5 strands are slightly different in orientation angles and lengths compared to Kindlin 1 F0 domain. Minor differences between the two structures *may* account for the functional differences between the F0 sub-domains of the two proteins.

3.5. A Model 3D structure for full length Kindlin 2 protein.

Kindlin 2 is a relatively novel protein, which has not been studied extensively although it plays a significant role in homeostasis. Neither its structural details nor structure based functions have been reported so far making it difficult to evaluate its function at a molecular level. The current information available on the full length Kindlin 2 protein is its primary sequence and its predicted secondary structure. It is difficult to understand the potential function of Kindlin 2 merely from its primary and secondary structure. A tertiary structure of a protein gives much more insight to its function. Determining the tertiary structure of a protein is a complex process which requires time and expertise skills. Generating or predicting model 3D structures from the protein sequence has become a common task. Model structures give insight to the structure, may help us to understand its function/potential function and assist in designing projects accordingly. With the increasing availability of free accessible web servers and fast computers, obtaining model structures for proteins is nowadays a common task.

Robetta/Rosetta and i-Tasser are few of those widely used servers for computer generated prediction of model structures from the primary protein sequence.

To have a better view on the full length Kindlin 2 protein, we obtained a model structure from Robetta protein structure prediction server at http://robetta.bakerlab.org. The full length amino acid sequence residues 1-680 of Kindlin 2 was submitted to the server for automated structure prediction. The server uses comparative modeling and de nova structure prediction methods to create subdomain models, which are pooled together to create the lowest energy models structures. (Kim et al., 2004). Several lowest energy model structures were generated and are shown in Figure 3.10. All structures show similar domain structures but slightly different orientations. These models show a multiple domain globular fold structure. The putative PH domain is surrounded by other domains of Kindlin 2. The F2 subdomain is split by the PH domain which is consistent in all model structures and comparable with literature. The bipartite F2 and F3 show tight packing against the PH domain. The model structure shows close proximity between the Kindlin 2 F0 domain and F2 subdomain.

Model 1 is the lowest energy structure. We are interested to understand which of these models may be the closest to the accurate structure. Dr. Koichi Fukuda, a member in our laboratory, was able to obtain Kindlin 2 PH domain protein and kindly provided it for my experiments. The only two subdomain proteins of Kindlin 2 available are the F0 and the PH domain. The proximity of the PH and F0 domain is different in each model structure and we questioned whether there is an interaction between the two subdomains.

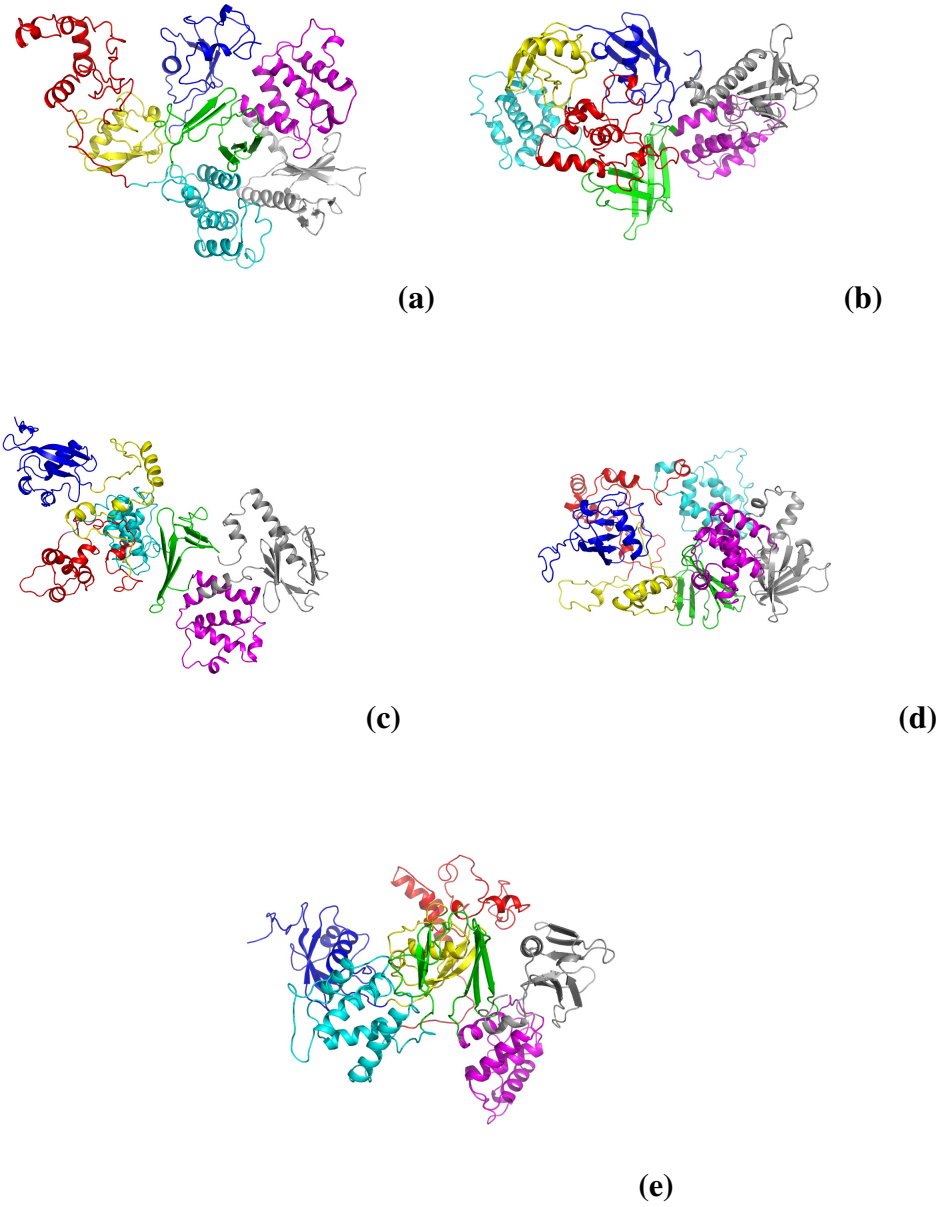

Figure 3.10. Lowest energy model structures for Kindlin 2 Full length protein predicted from the Robetta server. (a) Model 1 (b) Model 2 (c) Model 3 (d) Model 4 (e) Model 5. Blue-F0 domains yellow and red-F1 domain, Cyan and magenta- F2, green- PH domain and grey-F3 subdomain.

To evaluate whether there is an intermolecular interaction between F0 and PH domain, we performed a HSQC NMR experiment. The HSQC spectra were recorded for 0.1mM ^{1}H-^{15}N Kindlin 2 1-105 and in the presence of 0.2mM Kindlin 2 PH domain. The superimposed spectra are shown in Figure 3.19 and display no significant peak perturbations. This implies that the interaction between PH domain and F0 domain is not significant. Observing all the model structures we excluded the possibility that model 1 is precise since the PH domain and the F0 domains are in close contact in model 1 structure. It leaves us with the possibility that model 2-5 may be close to the actual structure of Kindlin 2. However, it could also be reasoned that although spatially close there might be no significant interaction between Kindlin 2 F0 and PH domains.

3.6. Summary of chapter 3 results.

To summarize, Kindlin 2 1-105 solution structure is the first piece of atomic level information obtained for Kindlin 2 protein. The difficulty of getting soluble and high yielding protein for the full length protein and its subdomains slows down structural and functional analyses. Despite the 60% sequence similarity, Kindlin 2 1-105 structure adopts a similar fold to Kindlin 1 1-95 structure. The fold of both proteins is an ubiquitin-like beta grasp fold with a 10 residues long alpha helix which is surrounded with 5 beta strands. The solution structures of Kindlin 1 and 2 N terminal F0 domains show minor differences from each other and these structural differences may be useful to relate them to their potential function/s.

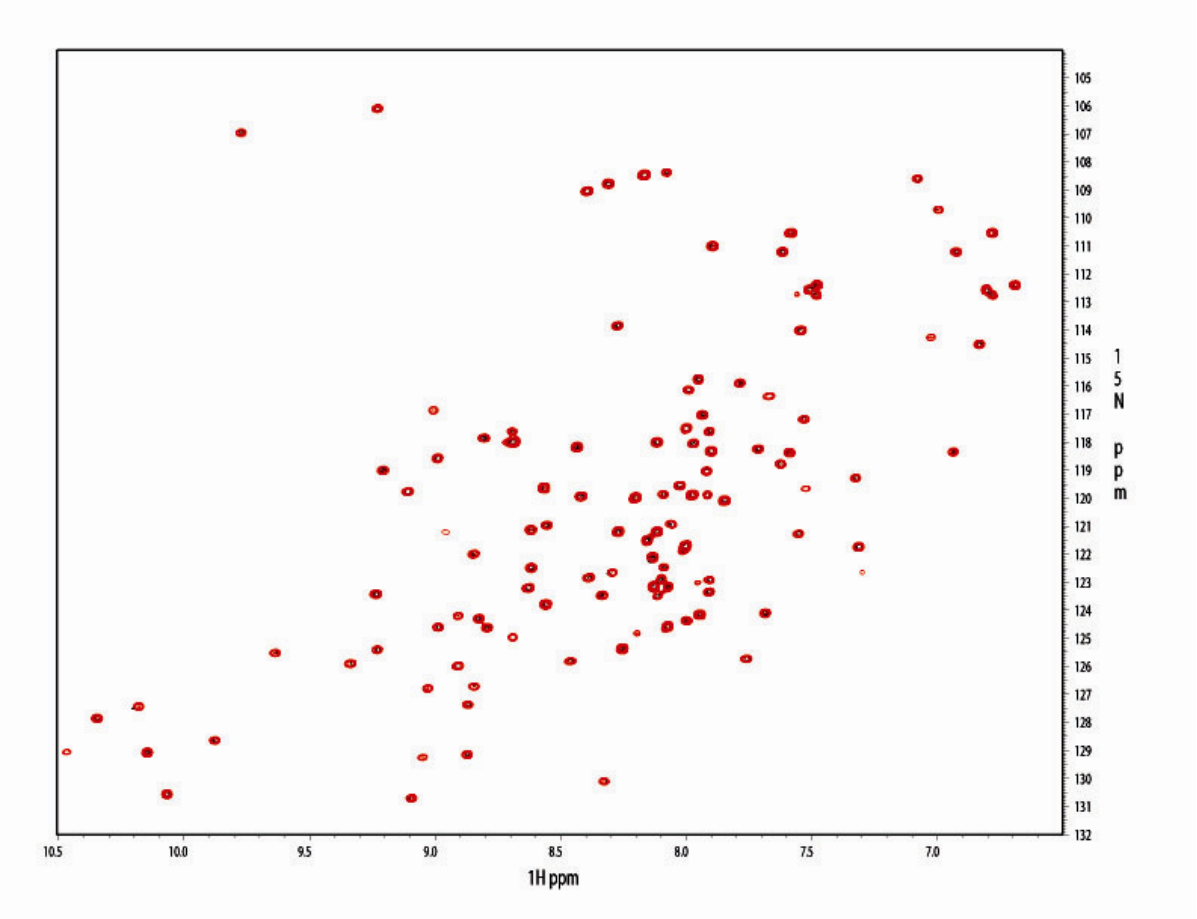

Figure 3.11. ^{1}H-^{15}N HSQC spectra of ^{15}N Kindlin 2 0.1 mM 1-105 in the absence (black) and presence (red) of 0.2mM Kindlin 2 PH domain showing no interaction of 15N Kindlin 2 1-105 and Kindlin 2 PH domain.

CHAPTER IV

INTERACTIONS OF KINDLIN 2 F0 DOMAIN

4.1. Overview

The function of a protein is related to its three dimensional structure of the protein. We have solved the solution structure of Kindlin 2 F0 domain. Kindlin 1 and 2 F0 domains share > 60% sequence homology and adopts a similar 3D fold. It could be assumed that the functions of the Kindlin 1 and 2 F0 domains are similar. However, the function of Kindlin 1 F0 domain (Goult, B. T., 2009) has not been elucidated up-to-date. Having the structure the next step is to understand the function/s of the F0 domain.

This chapter describes several binding interactions of Kindlin 2 F0 domain. Altogether, we suggest a potential role of Kindlin 2 F0 domain in the process of integrin activation.

4.2. Kindlin 2 N-terminal – a domain essential for Kindlin and Talin mediated integrin activation

The N-ter region of Kindlin 2 is known to interact with ILK and Migfilin (Tu et al., 2003). However the role of the F0 domain of Kindlin 2 has not been functionally characterized and there is no information in literature about the function of Kindlin N terminal or F0 domain.

Kindlin proteins (in particular the C terminal FERM domain) bind to integrin β CT and play a cofactor role in integrin activation (Goult et al., 2009; Harburger et al., 2009; Larjava et al., 2008; Ma et al., 2008; Montanez et al., 2008; Moser et al., 2009). To understand whether there is a functional significance of Kindlin 2 F0 domain in integrin activation, an integrin activation assay was performed in collaboration with Dr. Yang-Qing Ma in Dr. Ed. Plow laboratory.

In here, a particular focus was given to compare the effect of the full length Kindlin protein and F0 domain deleted full length Kindlin 2 in integrin activation. We transferred the corresponding constructs into EGFP vectors. The constructs were transfected into CHO cells, which stably express αIIbβ3 integrins. Activation of integrins was measured based on PAC1 binding, an antibody which only binds to activated integrins. To understand the role of Kindlin 2 in Talin induced integrin activation, Talin-H-EGFP constructs were co-transfected to CHO cells. Talin H domain is a considerably stronger co-activator of integrin than full length Talin (Goksoy et al., 2008).

The data summarized in Figure 4.1. are results from 3 independent experiments showing that there is more than a two fold activation of integrins in the presence of Kindlin 2 compared to Talin H alone. Integrin activation with Kindlin 2 alone shows a

much weaker activation than Talin H alone (Ma et al., 2008). By comparison, there is a substantial decrease in integrin activation in residues 11-143 deleted Kindlin 2 construct. The same was true for 1-105 deleted Kindlin construct (data not shown). Previous studies have indicated that Kindlin-2 1-263 was important for integrin activation but now we further narrowed down to 1-105 region. These data have highlighted the importance of Kindlin N-ter in integrin activation. Further it is evidenced that Kindlin F0 plays a central role in integrin activation.

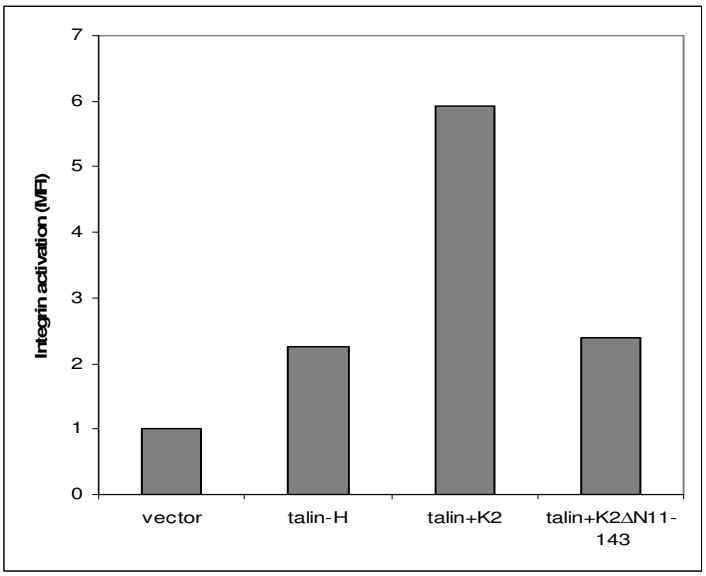

Figure 4.1. The effect of Talin head domain, Talin head - Kindlin 2 and Talin head – Kindlin 2 Δ 11-143 in integrin activation. CHO cells which are stably expressing αIIbβ3, were transfected with cDNAs of Talin head domain, Talin head- Kindlin 2 and Talin head – Kindlin 2 Δ 11-143. The EGFP positive cells were gated and used to monitor PAC-1 binding/integrin activation (Ma et al., 2008).

4.3. Kindlin 2 N-ter and integrin interaction

Knowing the structure of Kindlin 2 1-105 and its functional significance *in vivo*, we questioned the role of Kindlin 2 N-ter in integrin activation. There is evidence from literature for direct interaction of Kindlin 2 C-ter with integrin (Shi et al., 2007; Ma et al., 2008; Bledzka et al., 2010). Deletion of Kindlin 2 1-218 or 1-345 from full length Kindlin disrupts the interaction with integrin CT (Ma et al., 2008). To investigate whether Kindlin 2 F0 domain (1-105 residues) interact with the integrin CT, we performed a series of experiments using NMR. HSQC-NMR is the most simple, quick, informative and straightforward experiment to examine the interaction between two proteins.

Integrin CT peptide residues K716-T764, has been widely known for its low solubility at physiological salt concentration. Thus, the wild type peptide is difficult to use for NMR experiments with Kindlin proteins as the stabilizing buffer is 50mM Sodium phosphate and 100mM Sodium Chloride. Several modifications on the CT have been done to improve solubility and stability of the peptide (Goksoy et al., 2008; Wegener et al., 2007). One such modification from one of our group members, Dr. Jianmin Liu, was to mutate several N terminal hydrophobic membrane proximal Leucine residues. This has dramatically improved the stability and solubility of the peptide.

Figure 4.2 shows the HSQC of two superimposed spectra, the HSQC of 0.1 mM ^{15}N-D β3 integrin mutant CT in the presence of 0.2mM Kindlin 2 1-105 in red and in black the free form (^{15}N-D β3 mutant). Several peaks have been shifted giving direct evidence for interaction between the two molecules. The same peaks have perturbed for Kindlin 2 11-143 interaction (data not shown). Mapping the perturbed residues on

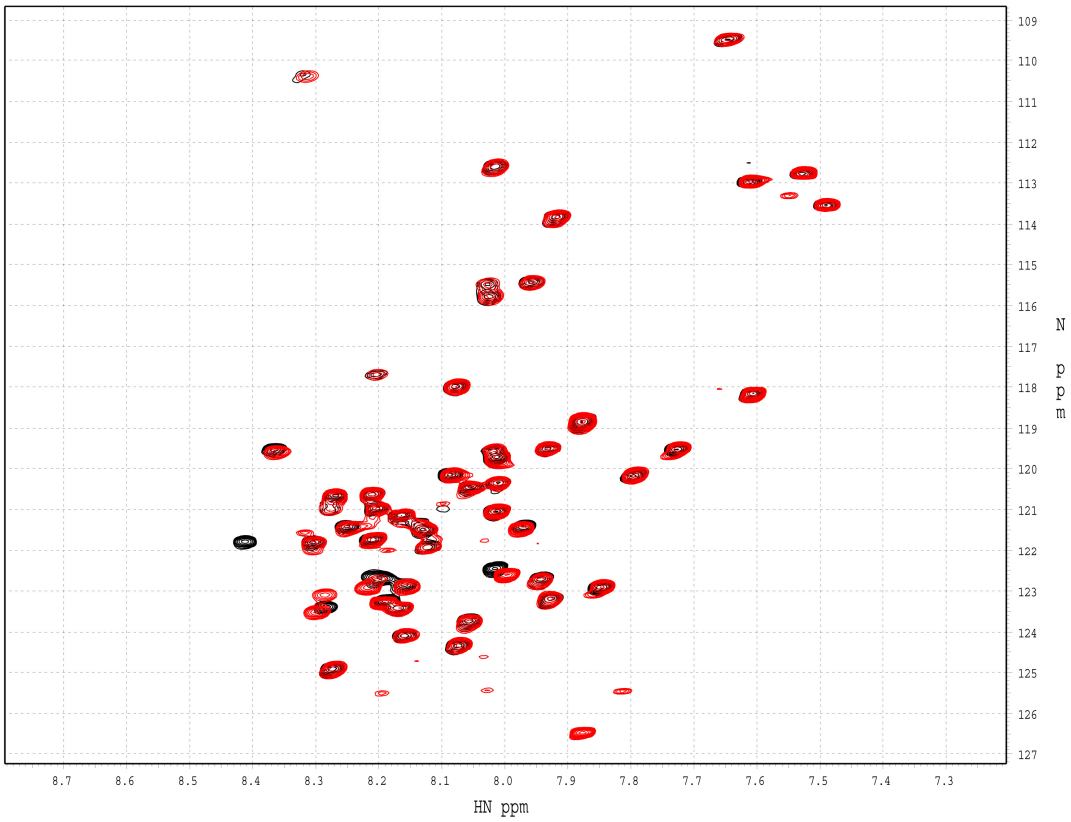

Figure 4.2. ^{1}H-^{15}N HSQC spectrum of integrin ^{15}N-D β3mutant CT and Kindlin 2 1-105 interaction. An overlay of the ^{1}H-^{15}N HSQC spectra of β3 integrin CT mutant (in black) and β3 mutant in the presence of Kindlin 2 1-105 (in red) at 1:2 molar ratio.

integrin revealed that the very N-terminal stretch of residues and several residues in the linker region are involved in the interaction (Shown in Figure 4.3.).

The reverse NMR experiment of ^{15}N Kindlin 2 1-105 and unlabelled β3 integrin CT mutant was performed at a 1 to 2 excess molar ratio. Data shown in Figure 4.4 suggests a very weak interaction with small peak shifts. β3 integrin CT wild type His fusion protein and β3 integrin wt MBP fusion protein have a similar peak perturbation

pattern (data not shown). The perturbed residues on Kindlin 2 1-105 are shown in Figure 4.3.

GSSHHHHHHS SGLVPRGSHM ^{716}KKKITIHDRK EFAKFEEERA AKWDTANNP LYKEATSTFT NITYRGT

Figure 4.3. Perturbed residues of integrin CT sequence. The linker region is underlined. The β3 CT starts with ^{716}K. The stretches of 716KKKITIH and GLVP in the linker are essentially perturbed by Kindlin 2 1-105 interaction highlighted in red.

Although very weak, these data suggest that Kindlin 2 1-105 may be partially involved in binding to integrin (in addition to the major binding site by Kindlin-2 C-terminal PTB domain). The full structure of Kindlin-2 is not available, however, examination of the model structures suggest that the N- and C-terminus of Kindlin-2 are spatially close (Fig 3.10) so integrin β3 CT might bind to both regions. Such binding mode may enhance the tighter association of Kindlin 2 with integrin.

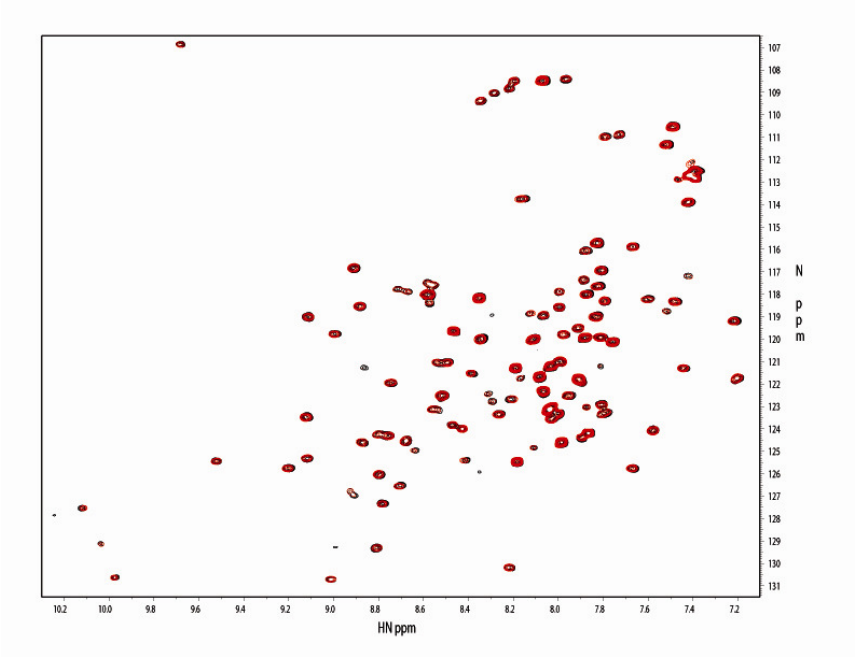

Figure 4.4. ^{1}H-^{15}N HSQC superimposed spectra of 15N Kindlin 2 1-105 and unlabeled β3 integrin CTmutant interaction. The red peaks correspond to ^{15N} Kindlin 2 1-105 in the presence of β3 CT at 1:2 molar ratio. The black peaks correspond to ^{15}N Kindlin 2 1-105 HSQC spectrum. The peaks shifts are observed at 1:2 excess molar ratio are small but consistent among repeated experiments.

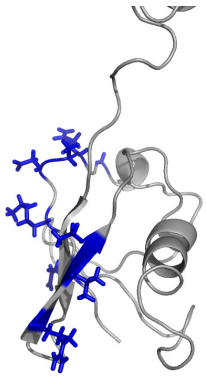

Figure 4. 5. Ribbon diagram of Kindlin 2 1-105 highlighting perturbed residues due to integrin interaction. The most perturbed peaks are confined to one area of the molecule.

4.4. Kindlin 2 N' and membrane interaction

As revealed above, functional data show that Kindlin 2 1-105 plays an important role in integrin activation and *in vitro* NMR data supports that integrin CT interacts with Kindlin 2 F0 domain. The membrane N-ter residues that have perturbed belong to the very proximal residues of the integrin beta3 CT. For such interactions *in vivo*, Kindlin 2 F0 domain should come in close contact with the membrane. We reasoned whether there is a secondary interaction between the membrane and Kindlin F0 which may help to stabilize the interaction between Kindlin F0 and integrin.

To investigate our hypothesis, we used NMR as our tool for analysis. In order to create a membrane mimetic environment, LUV, large unilamellar vesicles of phosphoinositides with 25% PIP2 were provided from one of our group members, Dr. Jun Yang. These form the necessary membrane surface for analysis. We added LUV at 1:5, 1:10 and 1:20 molar ratios to ^{15}N labeled Kindlin 2 1-105 protein and HSQC spectra of Kindlin were recorded in the presence and absence of LUV's. Data are shown in Figure 4.6 reveal a weak interaction between the membrane and Kindlin F0 even at low molar ratio.

This piece of information confirms that Kindlin 2 F0 domain interacts with the membrane weakly. This supports our hypothesis that Kindlin 2 F0 may stabilize the interaction between integrin and Kindlin F0 by tethering to the membrane. As mentioned above, Kindlin 2 also contains a PH-like domain that may bind to phosphoinositides to facilitate the kindlin-2/membrane association. Our collaborator Cary Wu has recently found that Kindlin 2 does potently bind to PIP3 and such binding seems to be important

for Kindlin 2 mediated integrin activation (Qu et al., submitted). I therefore measured the Kindlin 2 PH

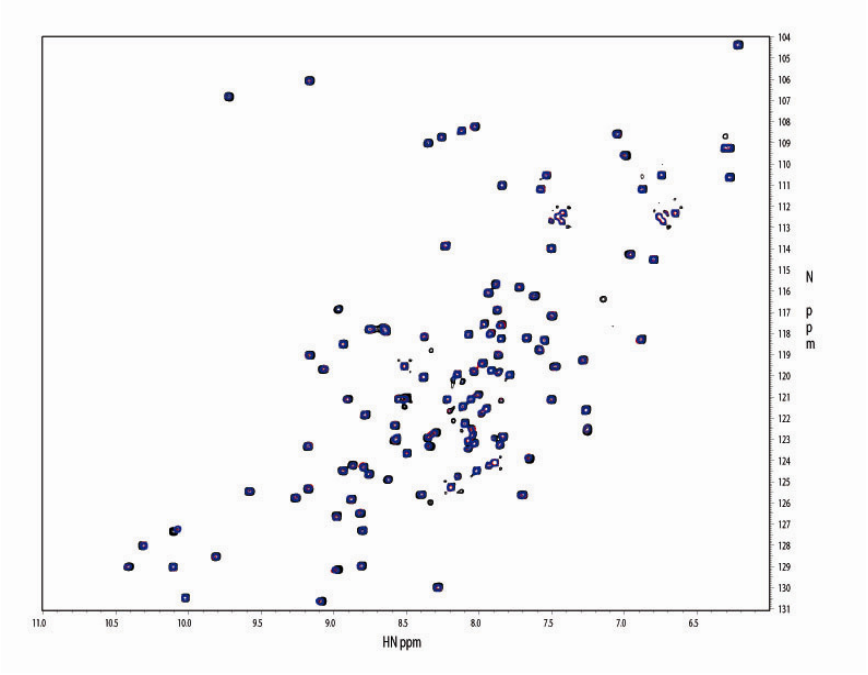

(a)

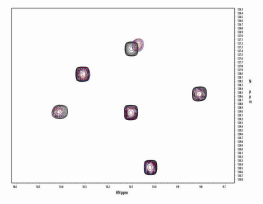

(b)

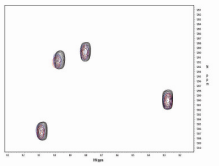

(c)

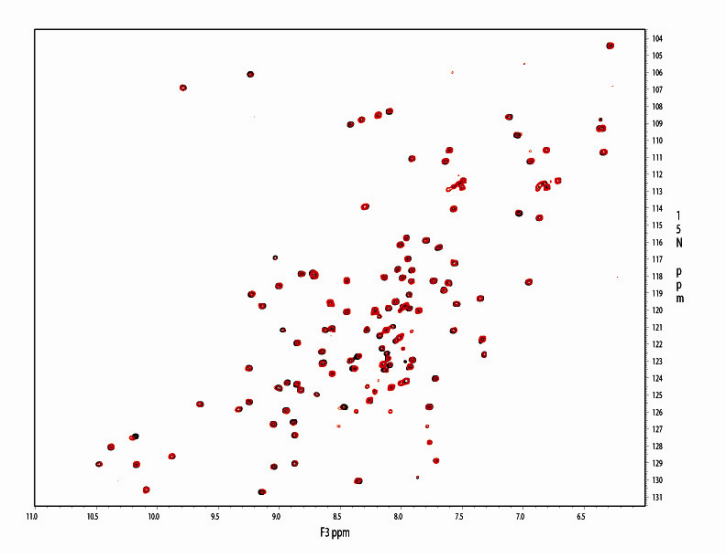

(d)

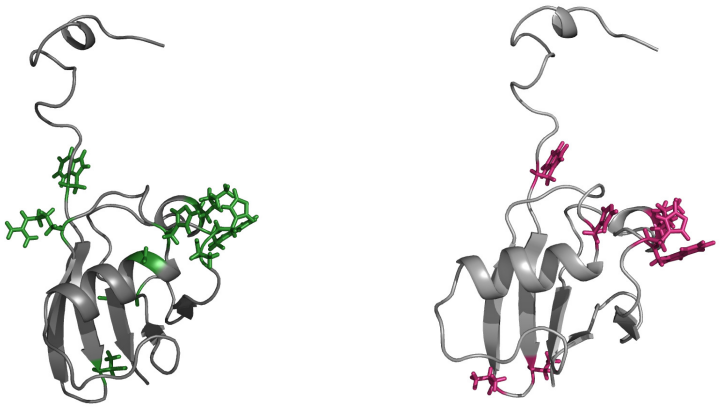

(e)

Figure 4.6. ^{1}H-^{15}N HSQC spectra showing interaction of ^{15}N Kindlin 2 1-105 and LUV/PIP2. (a) An overlay of spectra of black – free form of Kindlin 1-105, red – complex of Kindlin 2 1-105 and LUV at 1-5 molar ratio, green – complex of Kindlin 2 1-105 and LUV at 1-10 molar ratio, blue - complex of Kindlin 2 1-105 and LUV at 1-20 molar ratio. (b) and (c) zoomed images of (a). (d) is the ^{1}H-^{15}N HSQC of the interaction between Kindlin 2 1-105 and PIP3(C16). (e) Ribbon diagrams Kindlin 2 1-105 representing and highlighting perturbed residue side chains due to membrane interaction in green and PIP3 interaction in pink.

domain, (kindly provided by Dr. Koichi Fukuda) binding to PIP3 using SPR experiment, which revealed the Kd~1μM (Appendix 5). Thus, Kindlin 2 may use its multiple domains including F0 and PH-like domain to associate with membrane to facilitate the Kindlin-2/integrin interaction. Structural and functional analysis of filamin/integrin complex (Kiema et al., 2006) showed that filamin is a negative regulator of integrin activation. Interestingly, the filamin binding site on integrin seems to mask both Talin and Kindlin 2

binding (Figure 4.7.). Thus, one possible mechanism for the co-activation of Kindlin 2 and Talin is that they both compete with Filamin and promote the integrin activation. The membrane association of Kindlin 2 may tether the Kindlin 2 binding to integrin tail to enhance the kindlin-2 effect (Figure 4.7.).

Figure 4.7. Integrin beta CT sequences showing Talin, Filamin and Kindlin binding sites. Filamin binding site on integrin partially overlaps with Kindlin PTB and talin binding sites (slide adopted from Dr. Mitali Das).

4.5. Summary of chapter 4 results

To summarize, as described throughout the chapter, Kindlin 2 F0 domain plays a significant role in integrin activation. Deletion of F0 domain abolished the contributory effect in Talin induced integrin activation due to full length Kindlin 2. Thus F0 domain itself plays a very important role in integrin activation. How F0, PH and F3 domains cooperate in integrin activation needs to be further investigated at atomic level.

From binding interaction studies Kindlin 2 F0 domain interacts with PIP2/membrane and integrin β3 CT tails. Interestingly the interaction sites or residues of Kindlin 2 F0 domain are non-overlapping.

CHAPTER V

INTERACTIONS STUDIES OF KINDLIN 2 AND MIGFILIN

This chapter addresses aim 3. The role of Kindlin 2, together with its potential interacting partners, is evaluated in the complex process of integrin activation. The first section (5.1.) investigates the interaction between Kindlin 2 and Migfilin. A detail analysis of Kindlin 2 and Migfilin interaction/s is evaluated to understand its role in the focal adhesion complex. The second section (4.2.) investigates the global role of Migfilin, Kindlin 2 and Talin H in integrin activation.

5.1. Kindlin 2 and Migflin interaction – a necessary link in focal adhesions.

5.1.1. Introduction

It has been shown in literature that Kindlin 2 interacts with Migfilin (Tu et al., 2003; Wu, 2005). The interaction between Kindlin 2 N-ter and Migfilin is required to recruit Migfilin to focal adhesion site (Tu et al., 2003). Based on our model of integrin activation (Chapter 1, Figure 1.6.), the recruitment of Migfilin is a necessary step for the removal of bound Filamin from the integrin β CT. The accessibility of integrin CT for

binding is the most important and initial step in the process of integrin activation. Migfilin N-terminal 1-36 residues bind to Filamin, removing Filamin from the CT. At resting/inactive states of integrins Filamin is bound to integrin CT and masks Talin H and Kindlin 2 binding sites on the integrin tail demonstrating the negative regulatory effect of Filamin in integrin activation (Kiema et al., 2006; Ithychanda et al., 2009a and b; Wu, 2005). Removal of Filamin from integrin allows Talin H and Kindlin to bind to CT and promote subsequent activation of integrins (Chapter 1, Figure 1.6).

Based on the facts in literature, (a) Kindlin 2 plays a role in recruiting Migfilin to focal adhesion site and (b) Kindlin 2 may also play a role in integrin activation. It is not clear how Kindlin performs both these functions. As the initial step of understanding the central role of Kindlin 2 in the complex process of integrin activation, we investigated the interaction between Kindlin 2 N-terminal and Migfilin. To pinpoint the binding surfaces and further understand the role of Kindlin 2 N-terminal sequences we initiated to investigate the interaction between Kindlin 2 and Migfilin using Kindlin 2 F0 domain protein as a starting point. The following sub-chapter provides an outline of the experiments and results of the binding interactions of Kindlin 2 and Migfilin.

5.1.2. Kindlin 2 N-ter and Migflin interaction

The interaction between Kindlin 2 and Migfilin is mediated through the LIM domains of Migfilin (Tu et al., 2003). Unpublished *in vivo* data from our collaborator, Dr. Cary Wu, show that the interaction is abolished upon deletion of residues 1-218 of Kindlin 2. This demonstrates that Kindlin 2 N-terminal region is responsible for the interaction between Kindlin 2 and Migfilin.

The N-term region of residues 1-218 of Kindlin 2 mainly comprises of the F0 sub-domain and partial F1 sub-domain. As a starting point, to investigate the interaction between Kindlin 2 and Migfilin, we speculated whether there is an interaction between Kindlin 2 and Migfilin via the N-terminal 1-105 residues (F0) of Kindlin 2 and LIM domains of Migfilin. We used NMR as our tool for initial analysis.

We cloned Migfilin LIM domains separately and in all possible combinations into pHis-1 and pGEX-4T-1 vector. These are: Migfilin LIM123, LIM23, LIM12, LIM1, LIM2 and LIM3. All His fusion tag constructs were completely insoluble. The GST fusion proteins were soluble and further optimization revealed that 15 ° C inductions gave a very high yield of soluble protein. Figure 5.1 shows the HSQC spectra of all LIM domain proteins of Migfilin. The spectra of LIM1 and LIM2 proteins show well spread peak distribution implying a properly structured protein. Surprisingly, the peaks of the HSQC spectrum of Migfilin LIM3 are confined into a narrow range around 8ppm of the ^{1}H-scale. This demonstrates that LIM3 is an unstructured protein. More interestingly, the HSQC spectrum of LIM23 domain does not show peak crowding around the center 8ppm (see figure 5.3.(e)). The spectrum of Migfilin LIM23 shows almost a twice as much of peaks compared to LIM2 domains itself. This shows that LIM3 domain adopts a structured fold in the presence of LIM2 domain. Therefore all experiments were carried out using Migfilin LIM23 domain instead of LIM2 and LIM3 separately.

To investigate the potential interaction between Kindlin 2 1-105 and Migfilin LIM domains we performed a series of ^{1}H-^{15}N 2D HSQC experiments. HSQC is the most sensitive experiment, which is able to detect interactions between wide ranges of binding

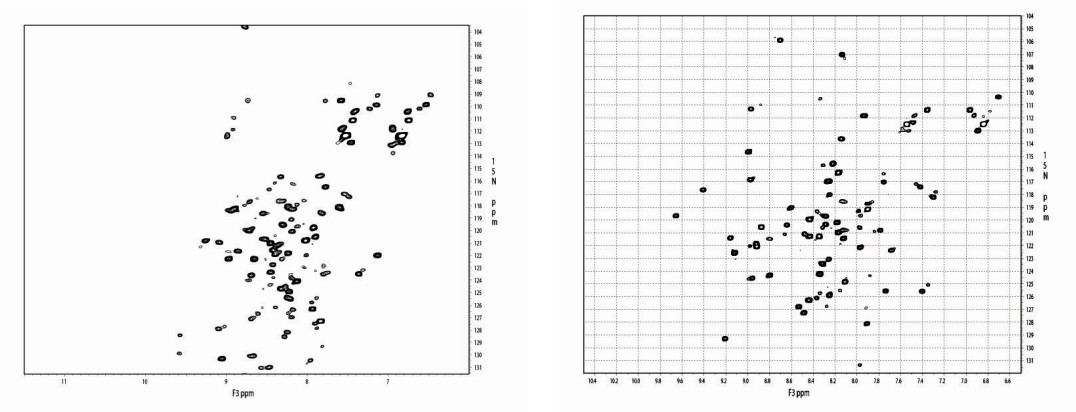

(a) (b)

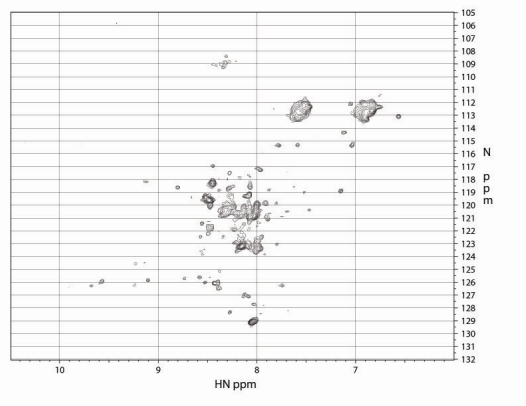

(c)

Figure 5.1. ^{1}H-^{15}N HSQC of all Migfilin LIM domains. (a) shows the HSQC spetrum of Migfilin LIM 1 domain (b) of Migfilin LIM2 domain and (c) of Migfilin LIM 3 domain respectively. (a) and (b) spectrums show a distribution of peaks which correlates to a well folded protein whereas in (c) spectrum most peaks are centered around 8 ppm which implies a partially unstructured protein.

affinities from milli molar to nano molar. To initiate the experiments I added an unlabeled Migfilin LIM23 domain protein into ^{15}N labeled Kindlin 2 1-105 protein at a 1:2 molar ratio. Each peak in the HSQC spectrum for Kindlin 2 1-105 corresponds an

amino acid in the protein, more precisely each peak in the HSQC spectrum reflects a correlation between amide proton and directly attached ^{15}N group of the protein. Any change in peak position, peak broadening or peak disappearance of Kindlin 2 1-105 HSQC spectrum upon adding the interacting partner Migfilin LIM23, resembles a change in the chemical environment of the residue. This implies an interaction between the two interacting partners. Our assumption was that if there is any interaction between Kindlin 2 1-105 and Migflin LIM23 proteins, it should reflect as peak perturbations or peak broadening or disappearances in the HSQC spectrum. The recorded HSQC spectrum is shown in figure 5.2. No significant peak perturbations were observed between Kindlin 2 1-105 and Migfilin LIM23 / LIM1 domains at 1-2 molar ratios suggesting no interaction between Kindlin 2 1-105 and Migfilin LIM 23/1 domains.

To further confirm our conclusion we performed a series of NMR experiments by performing the reverse experiments. I recorded HSQC experiments of ^{15}N labeled Migfilin LIM1 and LIM23 in the presence and absence of unlabeled Kindlin 2 1-105 protein. The superimposed spectra were evaluated for peak position changes. These data show no significant peak perturbations, confirming that there is no interaction between Kindlin 2 1-105 and Migfilin LIM domains.

To summarize, NMR data from figure 5.2., reveal that there is no interaction of the first 105 residues of Kindlin 2 and Migfilin LIM domain. However, *in vivo* assays have shown a strong interaction between Kindlin 2 1-218 (data not shown) and Migfilin

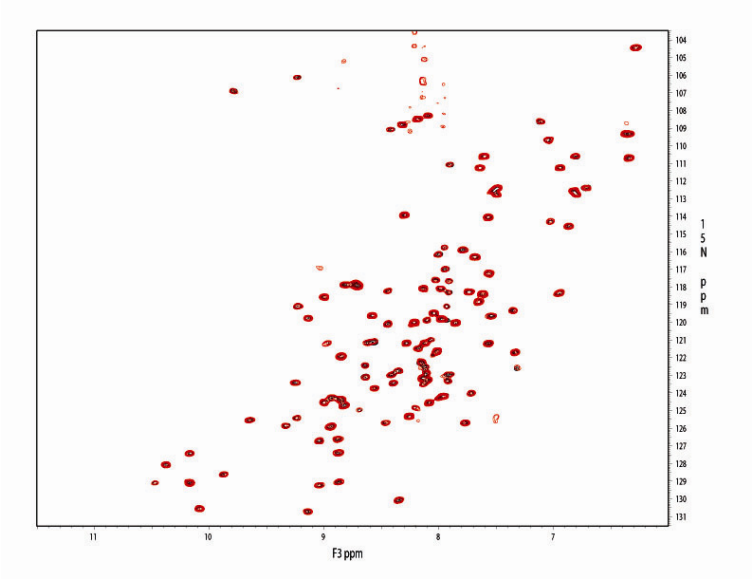

(a)

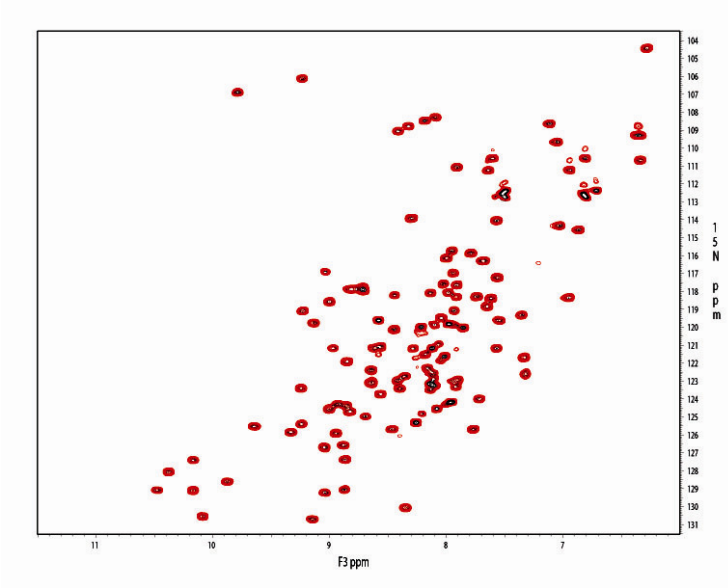

(b)

Figure 5.2. ^{1}H-^{15}N HSQC of Kindlin 1-105 and Migfilin LIM domains. (a) Interaction between ^{15}N labeled Kindlin 2 1-105 and unlabeled Migfilin LIM23 domain. (b) Interaction between ^{15}N labeled Kindlin 2 1-105 and unlabeled Migfilin LIM1. Both spectra show no significant peak perturbation implying no significant interaction between the proteins.

LIM domains. Therefore, we assume that the interacting site between Migfilin and Kindlin 2 is beyond residues 105 of Kindlin 2.

To evaluate the effect of the residues between 105 and 218 of Kindlin 2 on the interaction with Migfilin LIM domains, we engineered a number of protein expression constructs beyond this region. All these constructs were engineered carefully selecting boundaries according to the model structure of Kindlin 2. The constructs details, their expression and solubility are summarized in table 3.1. Most of the constructs within 105-218 of Kindlin 2 had either low expression of the target protein or the expressed protein was in the insoluble fraction of the cell. Kindlin 2 11-143 construct had a low expression and a yield of <1mg per Liter of LB culture. The ^{15}N labeled protein yield was even lesser but we are able to obtain a sufficient amount for NMR experiments by growing cultures in larger scales. To test our hypothesis, a series of HSQC experiments were performed using ^{15}N labeled Kindlin 2 11-143 and Migfilin LIM23 domains and vive versa. The results are shown in figure 5.3.

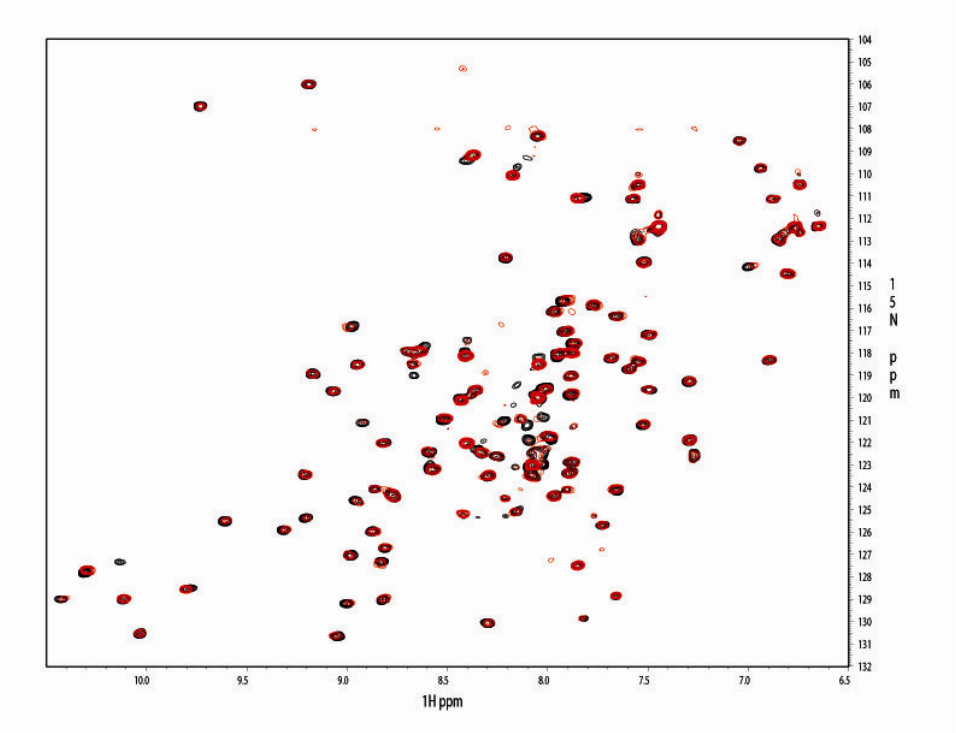

(a)

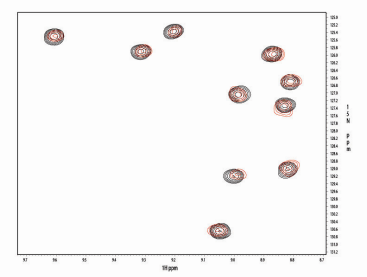

(b)

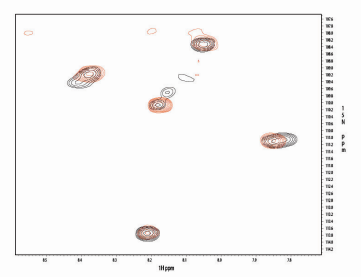

(c)

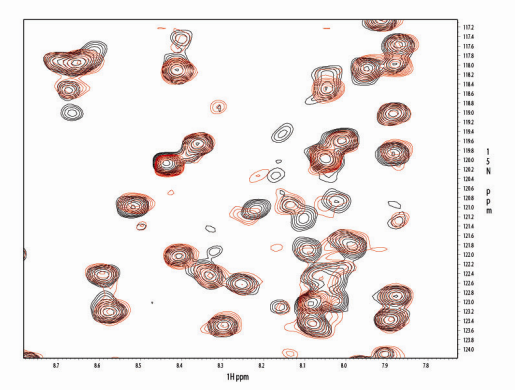

(d)

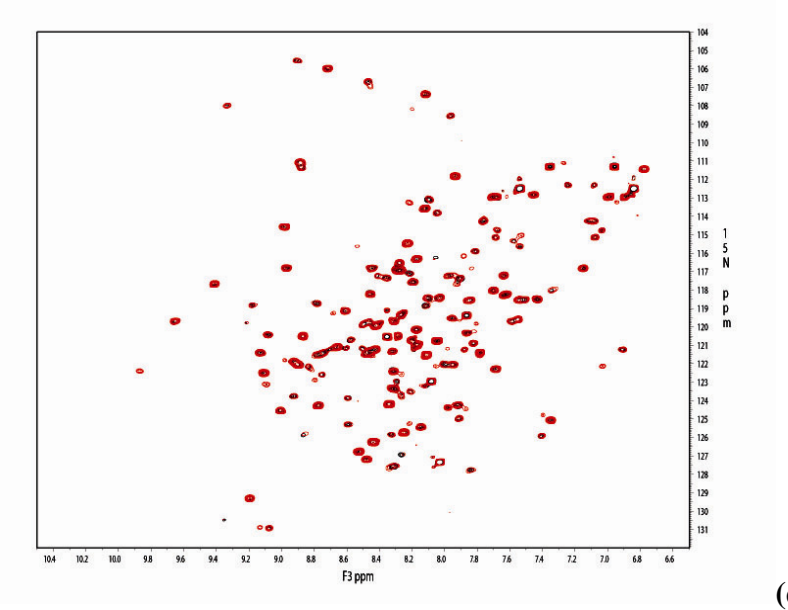

(e)

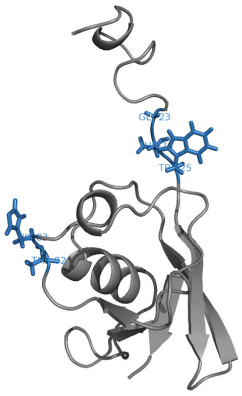

(f)

Figure 5.3. ^{1}H-^{15}N HSQC between Kindlin 2 11-143 and Migfilin Lim23 at 1:2 molar ratios. All experiments were performed at pH 6.89 in 50mM sodium phosphate and 100mM Sodium chloride. Spectrum (a) shows the interaction between 15 N labeled Kindlin 2 11-143 and unlabeled Migfilin LIM23 domains. Spectrum (b), (c) and (d) are zoomed images of (a). (e) Shows the reverse experiment using ^{15}N labeled Migfilin Lim23 domain and unlabeled Kindlin 2 11-143 protein. (f) Ribbon diagram of Kindlin2 1-105 highlighting *some* perturbed residues (23-25 and 83-85 residues) due to Migfilin LIM23 interaction. The HSQC spectra of Kindlin 2 1-105 and 11-143 are not 100% overlapping.

The spectrum shown in 5.3.(a) and zoomed images (b), (c) and (d), clearly show significant peak perturbations. A 1:1 molar ratio interaction perturbed the same peaks as in 1:2 but to a lesser extend. Thus the interaction occurs in a dose dependant manner. This clearly evidences weak interaction between Kindlin 2 11-143 and Migfilin LIM23 fragments with a weak affinity between the two molecules.

The HSQC spectra of Kindlin 2 11-143 and 1-105 are different. However there are some peaks that are overlapping. We correlated some of the perturbed peaks to Kindlin 2 1-105 structure. We could clearly see, as shown in Figure 5.3.(f), that peak clusters of residues 23-25 and 83-85 are perturbed.

To investigate whether Migfilin LIM1 has an effect (in addition to LIM23) on the interaction between Kindlin 2 11-143 and Migfilin LIM domains, we cloned all LIM domains (LIM123) into pGEX-4T-1 vector. Although the expression was reasonable, the protein was unstable and tends to precipitate during the purification process. We were unable to obtain a sufficient amount to perform NMR experiments. However, Migfilin LIM 1 itself is a stable protein. Next, we were interested to understand whether LIM 1 domain of Migfilin has a contributory effect for the interaction between Migfilin and Kindlin 2 11-143. The HSQC spectrum of ^{15}N Kindlin 2 11-143 and that in the presence of a two fold excess molar ratio of Migfilin LIM 1 were superimposed and analyzed for any apparent peak perturbations. The spectra shown in figure 5.4 clearly show that there are no peak perturbation implying that the interaction between Kindlin 2 11-143 fragment and Migfilin LIM 1 domain is insignificant. This experiment narrows down the binding domains of Migfilin to LIM23 and residues 11-143 on Kindlin 2.

In vivo assays have shown a strong interaction between Kindlin 2 1-218 (data not shown) and Migfilin LIM domains. To evaluate whether the binding site is further expanded beyond residue 143 in Kindlin 2, we needed an expression construct encompassing residues 143-218.

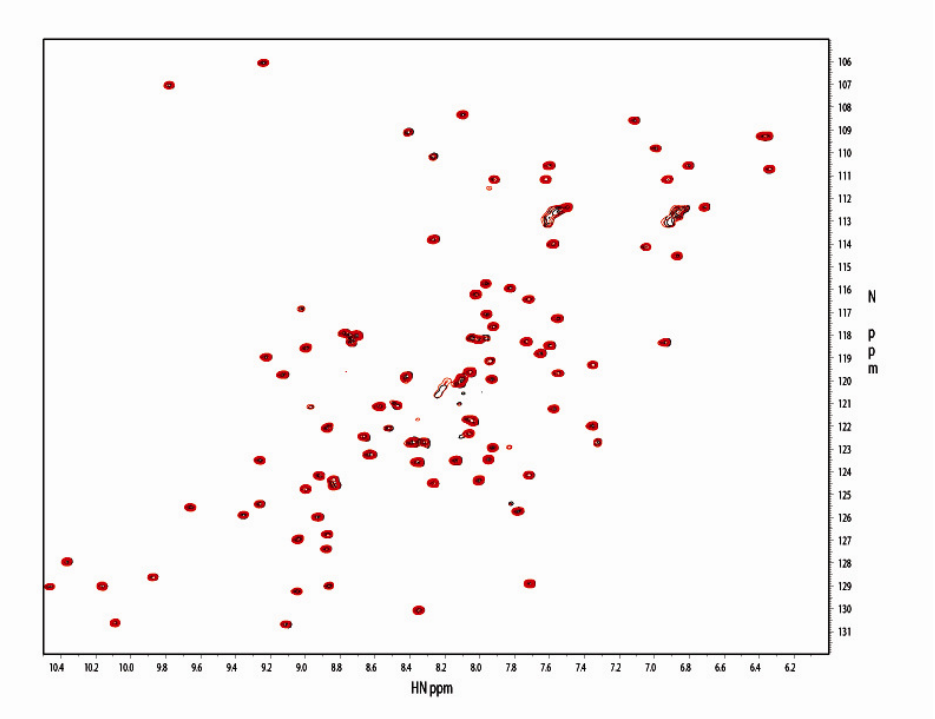

Figure 5.4. ^{1}H-^{15}N HSQC superimposed spectra showing the interaction between Kindlin 2 11-143 and Migfilin LIM 1 at 1:2 molar ratio. The black spectrum corresponds to ^{1}H-^{15}N HSQC of Kindlin 2 11-143 and red spectrum is the HSQC acquired of Kindlin 2 11-143 in the presence of Migfilin LIM 1 domain.

An expression construct for Kindlin 2 95-268, engineered using pGST-1 vector, a pGEX-4T-1 derived vector, had a very poor expression of the protein. Residues 95-268 of Kindlin 2 consist of partial F1 sub-domains and parts of F2. Optimization on temperature of induction, time of induction etc, did not improve the expression. I made

two smaller constructs by subdividing residues 95-268 into 95-168 and 168-268. I chose these boundaries according to the Kindlin 2 model structure. Kindlin 2 95-168 protein was a complete aggregate in size exclusion chromatography (with and without the fusion tag). We were able to isolate Kindlin 2 168-268 as a GST fusion protein at its dimeric state. To investigate the interaction between Migfilin and Kindlin 2, I performed a 2D HSQC experiment. The spectra of Migfilin LIM23 were recorded in the absence and presence of Kindlin 2 168-286-GST fusion protein. The data are shown in Figures 5.5.

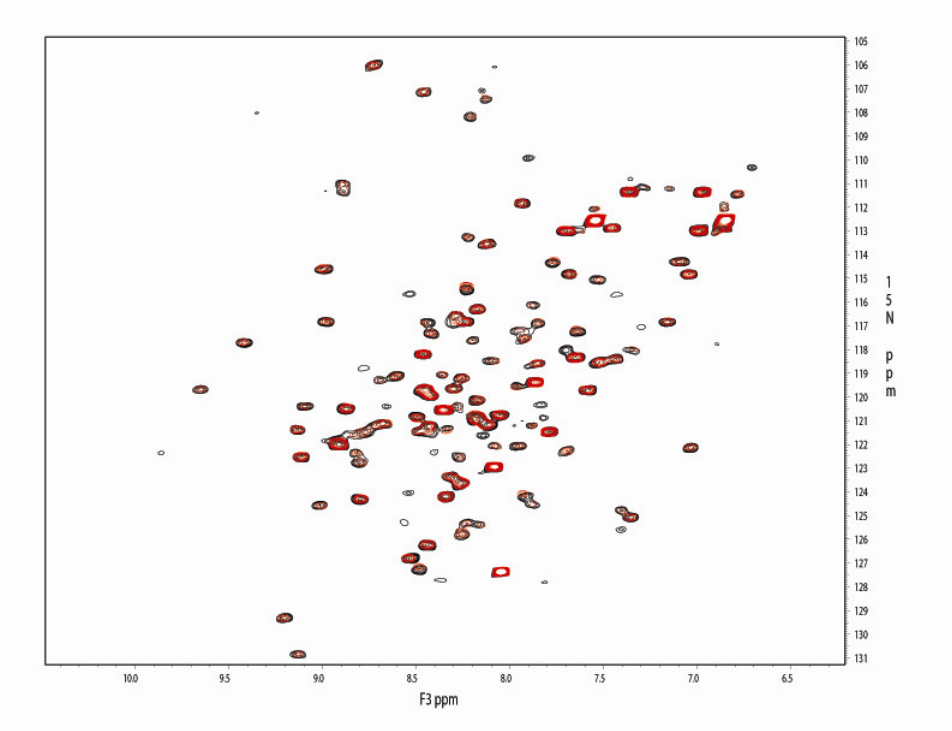

Figure 5.5. ^{1}H-^{15}N HSQC superimposed spectra of the interaction between ^{15}N Migfilin LIM23 and Kindlin 2 168-268-GST

As a control experiment, I recorded a HSQC experiment with GST protein as the interacting partner, at a 1:2 molar ratio in the presence of ^{15}N Migfilin LIM23. A

prominent chemical shift pattern is seen in the control spectra representing the influence of the GST tag on Migfilin LIM23 domain.

After cleavage of the GST tag from Kindlin 2 168-268-GST fusion protein, a majority of the cleaved protein tend to aggregate, while a much smaller fraction co-eluted with the dimerized GST tag when subjected to size exclusion chromatography. Although low in yield, Kindlin 2 168-268 protein is a tetramer.

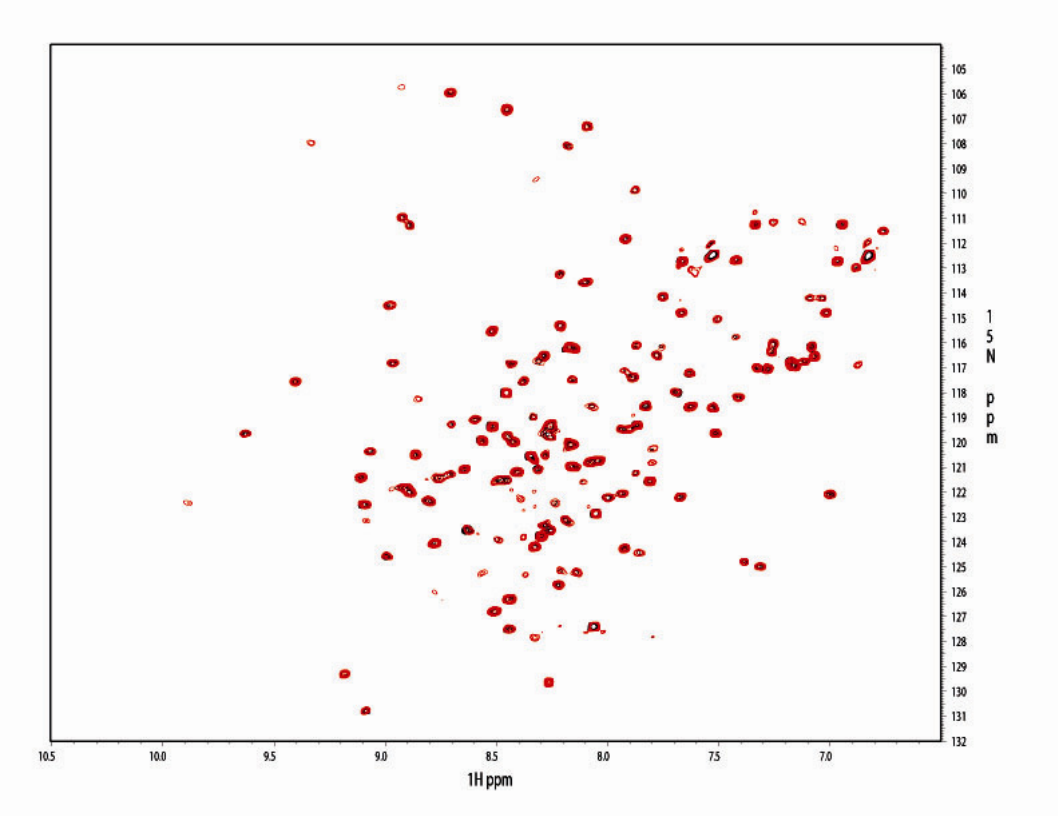

Figure 5.6. ^{1}H-^{15}N HSQC superimposed spectra of ^{15} N Migfilin LIM23 in black and ^{15} N Migfilin LIM23 in the presence of Kindlin 2 168-268 in red.

The superimposed HSQC spectra between ^{15}N Migfilin LIM23 and Kindlin 2 168-268 in the presence of ^{15}N Migfilin LIM23 are shown in Figure 5.6. No significant peak perturbations are observed in figure 5.6 which again implies that there is no significant

interaction between Kindlin 2 168-268 and Migfilin LIM23 domains. The positive effect seen earlier in figure 4.5 was due to the GST fusion tag.

Since, *in vivo* assays have shown an interaction between Kindlin 2 N-ter and Migfilin LIM domains, we predicted that the remaining untested fragments of Kindlin 2 N-ter are responsible for the interaction. Unfortunately, Kindlin 2 95-168 fragment, which is a region untested for the interaction, is completely aggregating. A closer look at the amino acid sequence of Kindlin 2 95-168 revealed that there is a stretch of positively charged lysines followed by alternating negatively charged amino acids. We rationalized that this region may be the leading cause for aggregation. I made two shorter constructs of Kindlin 2, residues 95-154 consists of the positively charged amino acid stretch whereas residues 155-268 contains the negatively charged amino acids. Surprisingly, the expressed protein of Kindlin 2 95-154 aggregates completely, being unavailable for further analysis. Kindlin 2 155-268 behaves the same way as Kindlin 2 168-268 and is a tetramer in size exclusion chromatography. A HSQC experiment with ^{15}N Migfilin LIM23 and Kindlin 2 155-268 revealed no interaction.

The only stretch of amino acids of Kindlin 2 N-terminal region that have not been tested for interaction with Migfilin LIM domains are residues 143-154. Having strong *in vivo* data from our collaborators for positive and strong interaction between Kindlin N-terminal and Migfilin, we reasoned that residues 143 to 154 may impose binding. To test our hypothesis we synthesized a peptide of residues 143-154 which comprise of amino acids: KKPRDPTKKKKKKK. To investigate the nature of interaction between Migfilin LIM23 domain and the synthesized peptide, we performed a HSQC experiment, which is capable in detecting very weak interactions. Multiple HSQC spectra of ^{15}N Migfilin

LIM23 domain protein with increasing molar ratios of the peptide were recorded. The results shown in Figure 5.6 revealed no significant peak perturbations even at 1:4 molar ratios.To summarize, we tested residue 1-268 of Kindlin 2 for the interaction with Migfilin Lim domains. Among all the experiments, we have seen a weak interaction between Kindlin 2 11-143 and Migfilin LIM23 domains.

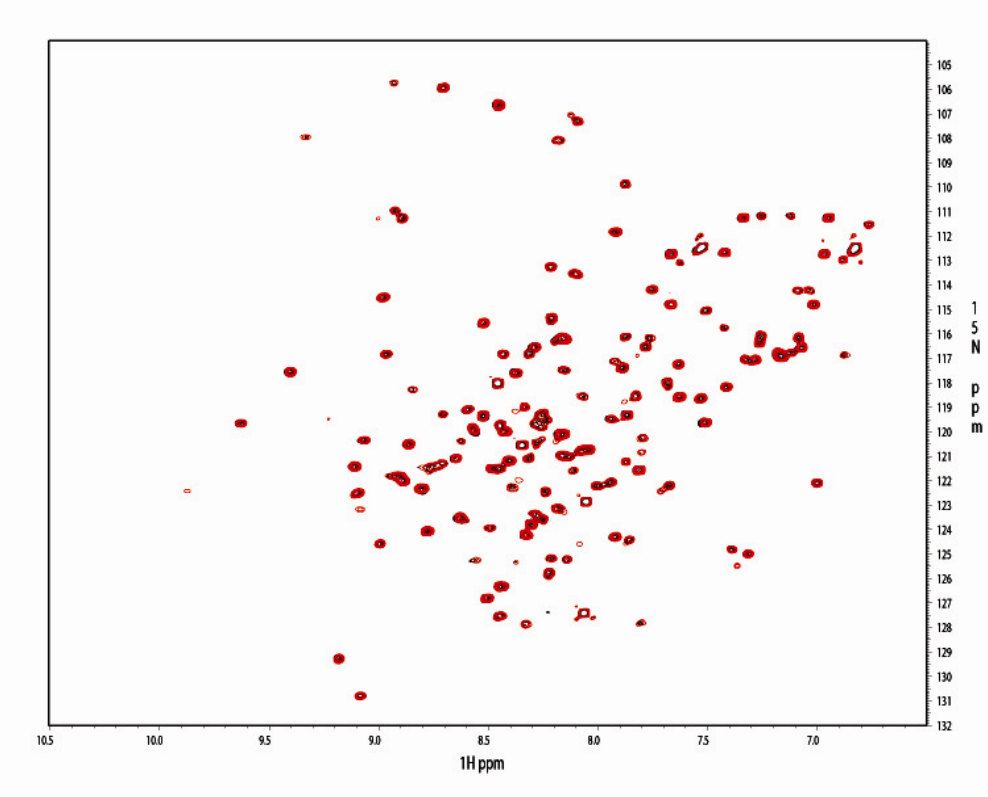

Figure 5.7. Migfilin LIM23 with Kindlin 2 143-154 peptide. This is an overlay of HSQC spectra between ^{15}N Migfilin Lim23 domain and that in the presence of Kindlin 2 143-154 synthetic peptide.

The HSQC spectra of Kindlin 2 1-105 and 11-143 are not identical, but there are certain peaks that are partially overlapping. In order to get a vague idea of the distribution of the perturbed peaks by correlating them to the Kindlin 2 105 structure, we have seen that most of the perturbed peaks are common to both constructs. This leaves us with the

question whether the C-terminal residues 105-143 on Kindlin 2 has an effect on the functional structure. Tracing back some of the perturbed residues on Kindlin 2 11-143spectrum to the solution structure of Kindlin 2 1-105 reveals that peak clusters have been perturbed. These are residues 23-25 and 83-85. A closer observation of the two sequences in the Kindlin 2 model structure shows that the C-terminal residues of 95-143 are structured. As shown in figure 5.8, the F0 domain is highlighted in blue and parts of F1 sub-domain in yellow. Figure5.8.(a) is the model structure Kindlin 2 1-105. Residues 95-105 in (a) denote a C-terminal single beta strand whereas in (b), Kindlin 2 11-43 construct, the C-terminal 95-143 sequences are structured in to an anti-parallel beta sheet

(a) (b)

Figure 5.8. (a) Kindlin 2 1-105 model structure and (b) Kindlin 2 11-143 model structures in ribbon diagrams, obtained from Kindlin 2 model 1 structure. The residues in blue correspond to 1-95 F0 domain and the residues in yellow correspond to 96-105 in (a) and 95-143 in (b).

and a short helix. According to the solved 3D structure of Kindlin 2 1-105 (Chapter III), residues 100-105 are unstructured. There is a possibility that the C-terminal residues highlighted in yellow in (b) may influence a functional conformation on F0 domain. If so,

this might be a reason for the positive interaction between Kindlin 2 11-143 / Migfilin Lim23 domains and negative interaction between Kindlin 2 1-105 / Migfilin LIM23 domains. It is quite evident that Kindlin 2 N-ter has a positive influence for Migfilin LIM domain interaction. *In vivo* studies used a larger fragments for analysis. But due to size limitation in NMR, fragmentation was a necessity. We cloned larger fragments of Kindlin 2, but unfortunately, Kindlin 2 1-218 had no expression.

To summarize, all data above suggest that there is a very weak interaction between Kindlin 2 full length/N-terminal and Migfilin LIM domains. According to our schematic representation of integrin activation, the link between Migfilin and Kindlin play a crucial role in the establishment of the link between the actin cytoskeleton and the extracellular matrix. Continuing evidence from *in vivo* studies from our collaborators has strong support for the interaction between Kindlin 2 N-ter and Migfilin. However, or NMR studies did not record a significant binding interaction further analysis are required to pin-point the binding interfaces.

5.2. The role of Kindlin 2 and Migfilin in integrin activation.

5.2.1.Introduction

Migfilin and Kindlin are key molecules in the process of integrin activation. Talin H domain of Talin is a well known activator of integrins and the mechanism of Talin H in integrin activation has been widely accepted (Calderwood, 2004; Garcia-Alvarez et al., 2003; Vinogradova et al., 2002) The importance of Kindlin in integrin activation has been recently implicated (Ma et al., 2008). Migfilin is known to bind to Filamin and Kindlin. The importance of the interaction between Migfilin and Filamin is well

established. The interaction between Migfilin and Kindlin is important to recruit Migfilin to the focal adhesion site (Tu et al., 2003). Besides, it is interesting to know how the interaction between Migfilin and Kindlin may affect in the process of integrin activation.

To understand the role of Migfilin/Kindlin in the complex process of integrin activation, in collaboration, we performed a series of NMR, ITC, SPR and *in vivo* functional experiments, which will be analyzed and discussed throughout the next sub-chapter.

5.2.2. In vivo functional evidence for the role of Migfilin in Talin and Kindlin 2 induced integrin activation.

A very recent *in vivo* study performed by Dr. Ma Yang-Qing in Dr. Ed. Plow Lab revealed a few important facts on the role of Migfilin in Talin and Kindlin 2 induced integrin activation. The results of the integrin activation assays are summarized in Figures 5.9 and 5.10 below. Each experiment shows the median of 3 experiments of PAC1 binding. PAC1 is a ligand for the binding of activated αIIbβ3 integrins. Figure 5.8 shows that there is an enhanced activation of integrin in the presence of Migfilin-Talin H–Kindlin2 compared to Talin H-Kindlin 2 or Talin H alone. This clearly shows the positive role of full length Migfilin in Talin H and Kindlin2 induced integrin activation.

Figure 5.8 further shows that integrin αIIbβ3 activation is diminished in the presence of over-expression of only Migfilin-Kindlin2 (last lane). This further supports the well-established role of Talin H in integrin activation and confirms that Talin H is the key molecule to propagate integrin activation.

The functional role of Kindlin2 in Talin induced integrin activation was heightened in Figure 5.9.-lane 5. Over-expression of Migfilin and Talin H show the same level in PAC1 binding to activated integrins compared to Talin H. This implies that Migfilin has no effect on enhancing the effect of integrin activation without Kindlin 2. In other words, the interaction between Kindlin and Migfilin may play a significant role in integrin activation.

To summarize the data in figure 5.9: TalinH is sufficient for the activation of integrins. Kindlin and Migfilin have a cofactor effect for the role in Talin induced integrin activation. The interaction between Kindlin and Migfilin is necessary to show the effect of Migfilin in integrin activation.

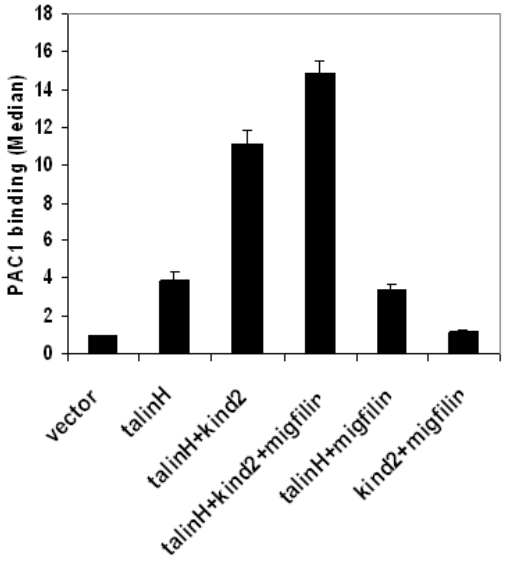

Figure 5.9. Integrin activation assay. Effect of Migfilin on Talin and Kindlin 2 induced integrin activation. CHO cells are stably expressing αIIbβ3, transfected with cDNAs of each Talin head domain, Talin head-Kindlin 2, Talin head – Kindlin 2-Migfilin, TalinH-Migfilin and Kindlin2 and Migfilin (Ma et al., 2008).

Migfilin is an adaptor protein comprising of 373 amino acids. Structurally, the C-terminal LIM domains have shown to mediate the interaction with Kindlin (Tu et el, 2003). The unstructured N-terminal region interacts with Filamin and act as a negative regulator in integrin activation (Ithychanda et al., 2009b; Ithychanda et al., 2009c). The central proline rich region has two binding sites for Src and VASP. Migfilin is the initiator of the Src pathway and prevents and protect against apoptosis (Zhao et al., 2009). To investigate the effect of each domain of Migfilin in the role of Migfilin in integrin activation, another integrin activation assay was performed by Dr. Ma, Yang-Qing, incorporating Migfilin sub-domain proteins (Figure 5.10.).

Migfilin(s) is an isoform of Migfilin, which lacks the proline rich region. To evaluate the functional role of the proline rich region in integrin activation Migfilin(s) isoform was overexpressed and the extent of αIIbβ3 binding was monitored. Similarly, the effect of Migfilin 1-85 and the C-terminal LIM domains were monitored and the data are shown in Figure 5.10. According to the figure, a significant decrease in PAC1 binding could not be observed for Migfilin(s), demonstrating that the proline rich region of Migfilin has no contributory effect in integrin activation.

Figure 5.10 shows deletion of N and/or C terminal domains, reduce PAC1 binding heightening the importance of both regions as a cooperate role in integrin inside-out signaling mechanism.

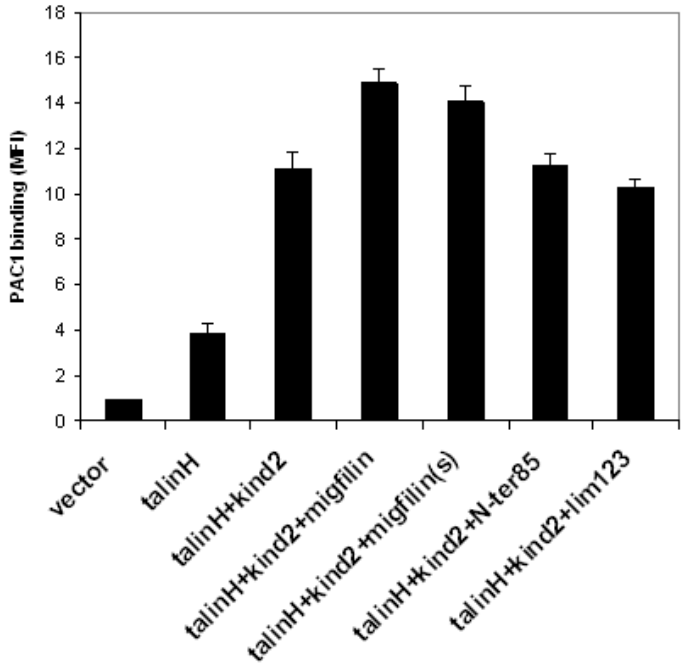

Figure 5.10. Integrin activation assay. Effect of Migfilin subdomains on Talin and Kindlin 2 induced integrin activation. CHO cells are transfected with cDNAs of each Talin head domain, Talin head- Kindlin 2, Talin head – Kindlin 2-Migfilin(s), TalinH-Migfilin and Kindlin2 and Migfilin Nterminal 1-85residues, TalinH-Migfilin and Kindlin2 and Migfilin C-terminal LIM domains (Ma et al., 2008)

Migfilin N-terminal 1-85 residues are well known to bind to Filamin, thereby removing Filamin from integrin CT and makes integrin available for potent activation by Talin and Kindlin 2 (Ithychanda et al., 2009a; Ithychanda et al., 2009b) (Lad et al., 2008; lad et al., 2007). Over expressing Migfilin N-terminal 1-85 in CHO cells would remove Filamin from integrin tails allowing the CT available for potential activation by Talin and Kindlin. Being the only negative regulator identified to remove Filamin from integrin CT tail; Migfilin N-terminal region plays a very important role to initiate the process of

integrin activation. Interestingly, the LIM domains of Migfilin show an equal importance in integrin activation. The only known link of Migfilin LIM domains is its interaction mediated by Kindlin 2. Kindlin 2 protein recruits Migfilin to the focal adhesion site, allowing it to regulate the inhibitory effect of Filamin (Tu et el, 2003).

To summarize, this assay demonstrates the functional importance of both C and N terminal of Migfilin for integrin activation and deleting either of it would substantially diminish integrin activation.

Despite the role in recruiting Migfilin to FA, Kindlin also interacts with integrin to heighten the effect of integrin activation. In focal adhesions, Talin H, Kindlin 2 and Migfilin are spatially close. NMR data have shown that there is no interaction between Kindlin F0 and Talin H domain. We questioned, whether there is a secondary interaction between Migfilin and Talin H. We hypothesized, whether Migfilin bridges Talin H and Kindlin N-ter and thereby forming a ternary complex, which may stabilize the interaction with integrin. The next subchapter evaluates our hypothesis through a series of NMR and SPR experiments.

5.2.3. The relationship between Migfilin and Talin interaction

To test our hypothesis introduced in the previous subchapter, we performed a series of HSQC, in vivo and SPR experiments. These help us to understand the interaction between Talin H and Migfilin subdomains.

The first step was to obtain Talin H and subdomain proteins to perform interaction experiments. I subcloned Talin H domain and its subdomains into pHis-1 vector as explained in chapter II -methods and materials section. After expression and purification of the proteins, I performed a 2D-HSQC experiments between ^{15}N labeled Talin His fusion proteins and unlabeled Migfilin LIM and vice versa. Data summarized in figure 5.11 show a site specific interaction between Migfilin LIM domains and all ^{15}N labeled his tag-Talin subdomains: TalinH, TalinF0F1, TalinF0 and TalinF1. The chemical shifts were dose dependant. The reverse experiments of ^{15}N labeled Migfilin LIM domains and unlabeled Talin subdomains were positive. To further confirm this interaction, I performed an SPR analysis. The results revealed a very weak interaction between Talin F0F1 and Migfilin LIM domains with a 40μM and 3μM affinity for Talin F0F1 and F0 domains respectively.

I performed another group of experiments without the His tag of Talin subdomain proteins and Migfilin LIM domains. Interestingly, the interaction was completely

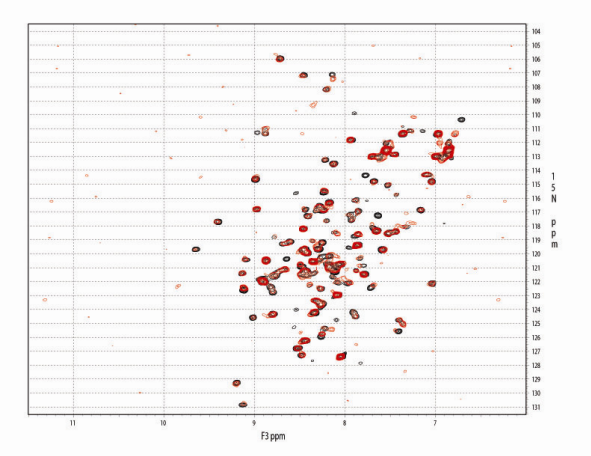

(a)

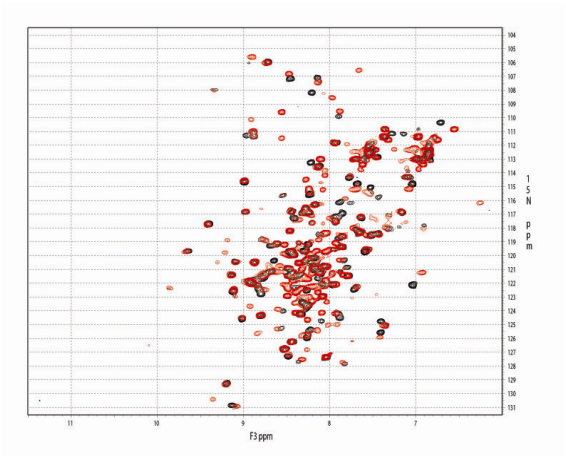

(b)

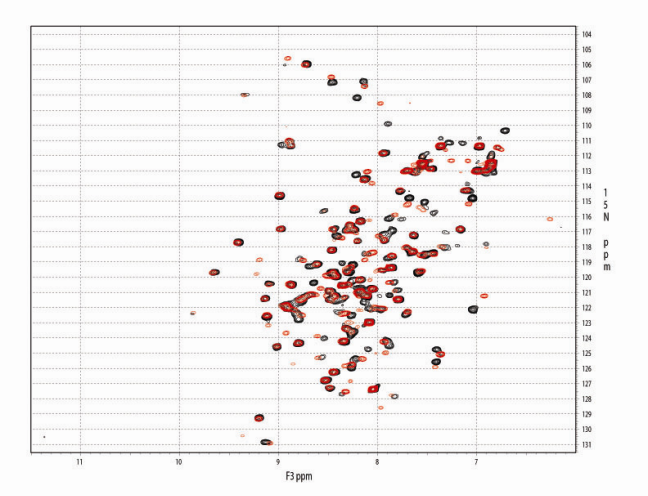

(c)

Figure 5.11. ^{1}H-^{15}N HSQC of ^{15}N Migfilin LIM domains and Talin subdomains. Figure (a) shows the interaction between ^{15}N Migfilin LIM 23 domain and unlabeled Talin head domain. Spectrum (b) shows the interaction between Migfilin LIM 23 domain and Talin F0F1 subdomains. Figure (c) shows the interaction between Migfilin LIM23 domains and Talin F0 domain. All spectra show significant chemical shift perturbation.

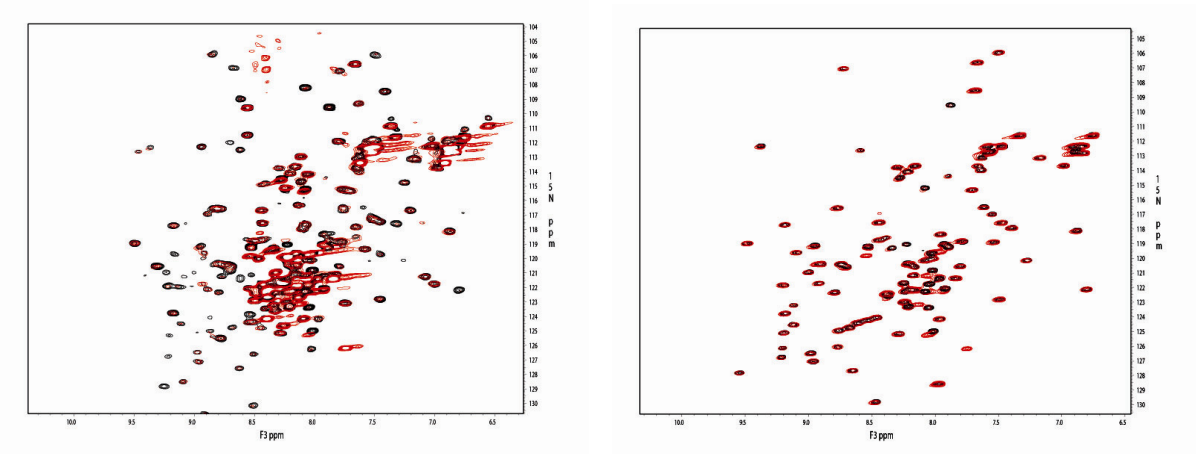

(a) **(b)**

Figure 5.12. ^{1}H-^{15}N HSQC of ^{15}N Talin subdomains and Migfilin LIM domains. Figure (a) shows the interaction between ^{15}N Talin F0F1 and Migfilin LIM 23 domain. Spectrum (b) shows the interaction between Talin F0 and Migfilin LIM 23 domain. All spectra show significant chemical shift perturbation.

abolished (Figure 5.13). These experiments heighten the effect of the His tag on LIM domain proteins. However, further analyses are necessary to validate our results.

Although we have eliminated the possibility between the interaction of Talin H domain and Migfilin LIM domains, we questioned whether the rest of Migfilin, the proline rich region and/or the N-ter 1-85 residues may have an effect on Talin H binding. Migfilin 1-85 and 1-36 were kindly provided by Dr. Sujay Itchichanda. We performed 2D HSQC experiments to evaluate our hypothesis.

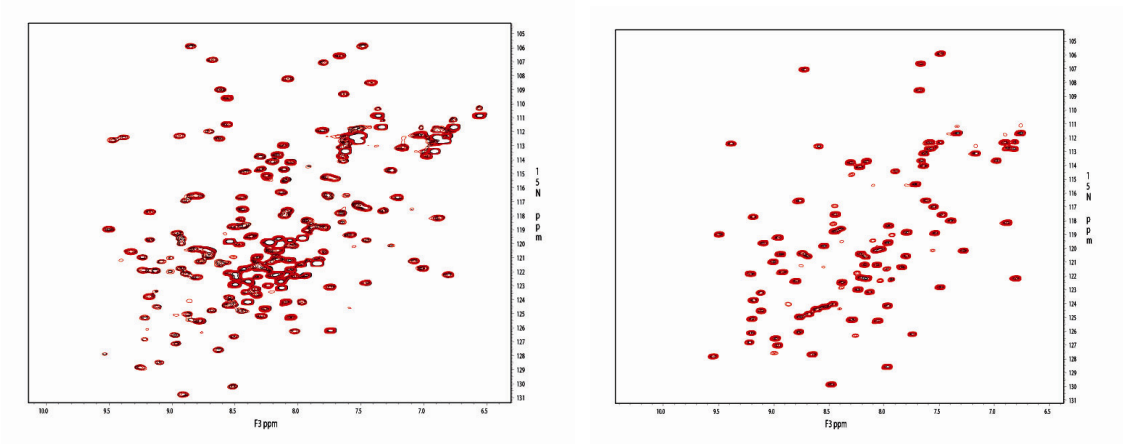

(a) **(b)**

Figure 5.13. ^{1}H-^{15}N HSQC of ^{15}N Talin subdomains without the HIS tag and Migfilin LIM domains. Figure (a) shows the interaction between ^{15}N Talin F0F1(after cleavage of HIS tag) and Migfilin LIM 23 domain. Spectrum (b) shows the interaction between Talin F0 (after cleavage of HIS tag) and Migfilin LIM 23 domain. All spectra show no significant chemical shift perturbation.

We analyzed the interactions of ^{15}N Migfilin 1-86 - Talin F0F1/F1 and ^{15} N Talin F0/F0F1 – Migfilin 1-36mer by NMR-HSQC. We were not able to observe any significant chemical shift perturbations evidencing no interaction between Talin and Migfilin N-ter. An *in vivo* experiment performed by our collaborators showed a negative interaction between Migfilin proline rich region and Talin H.

5.3. Summary of chapter 5 results.

NMR, SPR, ITC and *in vivo* assays have been used through out this thesis work, to understand the molecular role of Kindlin 2 in the process of integrin activation. Among the binding partners of Kindlin 2, the link between Kindlin 2 and Migfilin plays an indispensible role in integrin activation. To understand and validate the interaction between Kindlin 2 N-ter and Migfilin (obtained from in vivo assays), NMR was used as our primary method of analysis.

To summarize, a very weak interaction was observed between Kindlin 2 full length/N-terminal 11-143 and Migfilin LIM domains. Continuing evidence from *in vivo* studies from our collaborators has strong support for the interaction between Kindlin 2 N-ter and Migfilin. According to our schematic representation of integrin activation, the link between Migfilin and Kindlin play a crucial role in the establishment of the link between the actin cytoskeleton and the extracellular matrix.

Integrin activation assays demonstrated the functional importance of both C and N terminal of Migfilin for integrin activation and deleting either of it would substantially diminish integrin activation. Our experiments have not recorded any interaction between Talin H domain and Migfilin full length protein. This eliminates our hypothesis on the formation of a ternary complex between Migfilin-Talin H-Kindlin 2 N-ter, which may help to stabilize activated integrin and enhance the effect of integrin activation.

CHAPTER VI

KINDLIN C-TER AND INTEGRIN INTERACTION

6.1. Introduction.

Kindlin 2 C-term plays a significant role in integrin activation (Shi et al., 2007; Ma et al., 2008). A number of health related issues have been linked to the failure of C-term Kindlin to interact with integrin CT. Thus, to investigating its role in integrin activation is becoming an area of interest. Up to date, there is no structural information available to evaluate the role of Kindlin proteins in integrin activation. Kindlin 2 F3 subdomain and Talin F3 subdomain have similar homology. Through homology modeling, Ma et al. have mapped the interaction between Kindlin F3 and integrin CT (Shi et al., 2007; Ma et al., 2008; Bledzka et al., 2010). A structure based analysis of the interaction between Kindlin and integrin CT, would be necessary to understand and evaluate its mechanism in integrin activation. Up to date, there is no information available for the C-ter or full length structure of Kindlin. Lack of structural information

of Kindlin makes it difficult to evaluate the molecular role of Kindlin 2 C-ter in integrin activation.

In order to evaluate and perceive an atomic level understanding of the interaction between Kindlin C-ter and integrin, we undertook an extensive analysis of Kindlin 2 C-term. The next subchapter evaluates the attempt taken to obtain Kindlin 2 C-ter protein/s.

6.2. Expression of Kindlin 2 C-terminal.

To investigate the role of Kindlin 2 C-ter, obtaining the 3D structure of the protein is a necessity. As described in chapter 2, to initiate the process of recombinant protein expression, a prediction of the secondary structure of Kindlin 2 C-ter is helpful. In the process of cloning subdomain structures of Kindlin 2, the predicted secondary structural information would be beneficial in choosing the correct boundaries for the prospective protein (Appendix 1- Secondary structure prediction of Kindlin 2).

The boundaries that have been chosen were selected within the coiled region of high probability without disturbing the predicted secondary structure. Several boundaries been chosen are: residues 565-658, 565-680, 485-680 and 567-662. Their fusion tag, bacterial strain, solubility etc are summarized in Table 4.2.

All the constructs of the C-terminal F3 subdomain, have either no expression or a very low expression. The expressed protein is completely in the insoluble fraction of the cell. We reasoned that poor expression of F3 could be due to the presence of multiple rare codons in the sequence. To evaluate this we expressed the protein in Rosetta 2 and RIP bacterial host strains, which are supplemented with additional plasmids for the expression

of rare tRNA codons in *E.coli*. A significant increase in the level of expression could not be seen even in Rosetta 2 bacterial host strain.

The next approach was to obtain F2 subdomain of Kindlin 2. Although the C-terminal F2 constructs have a higher level of expression, the expressed protein tends to be

MIG-2 BOUNDARIES	FUSION TAG	BACTERIAL HOST STRAIN	PROTEIN EXPRESSION	PROTEIN SOLUBILTY	GEL FILTRATION
565-658	GST	BL21 (DE3)	no expression		
	MBP-HIS	BL21 (DE3)	no expression		
		BL21 (DE3)pLys	no expression		
		Rosetta (DE3)	no expression		
		Rosetta 2 (DE3)	low expression	in pellet	
567-662	HIS	Rosetta 2	low expression	in pellet	
	GST	Rosetta 2	low expression	in pellet	
567-665	HIS	Rosetta 2	low expression	soluble	Aggregate
567-680					
394-567	GST	Rosetta 2	low expression	soluble	Aggregate

Table 6.1. Summary of Kindlin 2 C-terminal constructs, their expression vectors, expression conditions and gel filtration data.

a complete aggregate when subjected to size exclusion chromatography. We reasoned, with evidence with the model structure, that F2 subdomain is packed against the potential PH domain and isolating F2 subdomain itself may expose hydrophobic residues/patches that might have initiated aggregation of F2. However, a construct including PH-F2 domains did not substantially reduce the aggregation evidencing that the PH domain alone may not help the problem. To understand whether aggregation is due to improper folding of the protein we assisted protein folding by introducing chaperones during protein expression. However, we were not able to observe any sort of an oligomeric state other than an aggregate when subjected to gel filtration. A close analysis of the sequence revealed multiple cysteine residues. We rationalized that intermolecular disulfide bond

formation may promote protein aggregation at an early stage of the protein purification process. A site directed mutation of C471A and C520S of Kindlin 2 459-567 construct of F2 subdomain did not prevent aggregation at all. To further reason out the effect of buffer interferences we performed the purification process in multiple buffers. PBS buffer at pH 7.0 was used for most protein purification protocols. We change the buffer to MES at pH 6.4 and Tris-HCl at pH 8.0. Results showed that change in buffer did not help in preventing or reducing the fact that the protein is aggregating. As an additional step we reasoned that protein stabilizing agents like cryotropes, kosmotropes, detergents etc may help to prevent aggregation when added throughout the protein purification process. I performed an aggregation assay (Saunders et el., 2008) using a wide variety of buffer additives. None of the additives helped except 1% sarkosyl. Sarkosyl is a very strong detergent, which is known to rupture the tertiary structure of the protein. Since sarkosyl helped partially to prevent/reduce aggregation we think that aggregation is initiated through hydrophobic contacts. We are limited by choosing additives because of NMR compatibility. None of the approaches helped so far to shift the Kindlin 2 F2 domain protein from being an aggregate to a lower order oligomer or monomer.

To summarize, we have cloned Kindlin 2 C-ter extensively. However we were not able to obtain any subdomain protein due to various difficulties in expression and aggregation of the protein.

6.3.Summary of chapter 6 results

The attempts of obtaining the C-terminal subdomain protein of Kindlin 2 failed due to varying degrees of difficulties in expression constructs. Certain approaches are outlined in chapter v, which could be useful in future to guide through to obtain Kindlin 2 C-ter protein for prospective functional analyses.

CHAPTER VII

DISCUSSION AND FUTURE DIRECTIONS

This thesis work has been concerned with understanding the role of Kindlin 2 in integrin activation. Our primary focus is to understand the function of Kindlin 2 in a structural point of view, which will give us more insight to understand the mechanism of Kindlin 2 at atomic level. Initial trials of full length Kindlin 2 protein expression were low and we were not able to obtain sufficient amounts for structural analyses. However, we were able to obtain subdomain proteins of Kindlin 2 after extensive subcloning. Currently, we have Kindlin 2 F0 domain (residues 1-105 and 11-143), Kindlin 2 F1 fragment (residues 155-268 and 143-154 peptide) and Kindlin 2 PH domain. The F0 domain is a high yielding and stable protein suitable for NMR studies. We have obtained the structure of Kindlin 2 F0 domain through solution NMR. Kindlin 2 155-268 is a tetramer and NMR structure determination would not be feasible. However, X-ray crystallography could be the method of choice for Kindlin 2 155-268 structure.

Kindlin 1 and 2 F0 domains have a similar beta grasp fold. The structures show minor but distinct differences that lead us consider with the possibilities of functional differences between Kindlin 1 and 2 F0 domains. Thus evolutionary, the structural differences in the F0 domains may have developed for potential functional differences. There are no facts in literature that show functional differences between the F0 domains. As a future step it would be interested to investigate whether these minor differences in structure may impose significant differences in their function.

A remarkable finding during this thesis work is that Kindlin 2 F0 domain plays a fundamental role in integrin activation. Deletion of F0 domain from full length Kindlin 2 substantially reduced integrin activation (due to PAC1 binding) in comparison to full length Kindlin 2. One goal of this thesis was to understand how Kindlin 2 F0 contributes in the integrin activation mechanism i.e. to find the structural determinants of Kindlin F0 domain and understand its central role in integrin activation. We have observed a weak interaction of the F0 domain with the membrane, PIP3 and integrin β3 CT membrane proximal residues and a 1μM affinity of PH and PIP3. All these data show that F0 and PH domains of Kindlin 2 interact with the membrane surface. Based on our and our collaborators data we proposed that Kindlin F0 and PH domain tether to the membrane to enhance the effect of Kindlin 2 in integrin activation (Figure 7.1.).

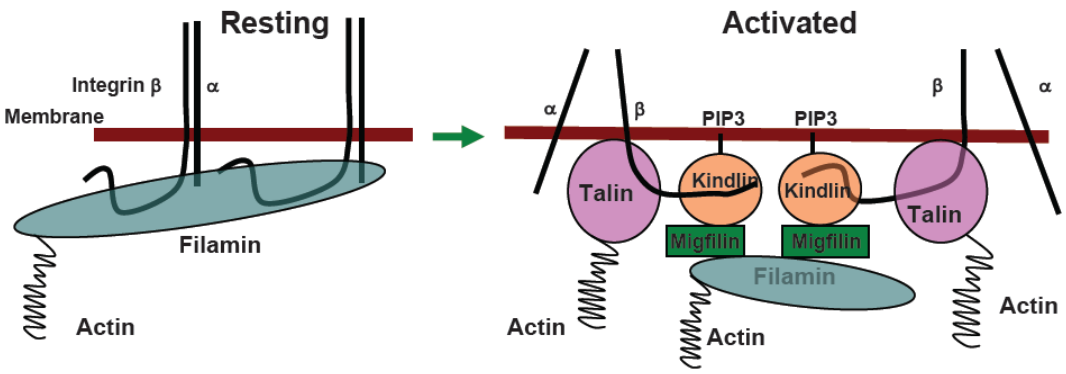

Figure 7.1. Schematic diagram of the proposed model of integrin activation. This shows that integrin CT is associated with Filamin through multiple binding sites and maintains integrin at the resting state or inactive state. Upon activation, Talin binds to the membrane proximal β3 CT, Kindlin is tethered to the membrane via the PH domain and facilitates the interaction between Kindlin C-ter F3 and integrin CT.

A closer look at the N-terminal sequence of Kindlin 2 shows a stretch of multiple positive charges encompassing the nuclear localization signal between the PH domain and F0 domain. There is a possibility, that these positive charges on Kindlin 2 may help the full length protein to anchor to the negatively charged membrane surface. This may further strengthen our hypothesis, where multiple domains of Kindlin 2 or in part may interact with the membrane surface essentially to tether Kindlin 2 to the membrane to facilitate the effect of Kindlin 2 in integrin activation. A future direction to validate our hypothesis is a thorough analysis using structure based mutagenesis and functional assays. Papayannopoulos et al. have shown that a polybasic motif in N-WASP directly binds to PIP2 and regulates its activity (Papayannopoulos et al., 2003). There is a

possibility that the polybasic motif of Kindlin 2 may also has some regulatory significance. It would be interesting to analyze whether this poly basic stretch of residues in Kindlin 2 play a role in membrane anchoring or has a regulatory function.

According to our data and literature, both F0 domain and F3 domain of Kindlin 2 and Talin F3 domain interact with the integrin β3 CT. It is quite interesting how all these proteins may bind to the ~50 amino acid length β3 cytoplasmic tail of integrin. Observing the model structures of Kindlin 2, it is clear that Kindlin 2 N-ter F0 and C-ter F3 domains are spatially close. In a 3D space, it is possible that all above mentioned domains have contact with the β3 CT.

The binding sites on Kindlin 2 F0 domain structure, due to integrin interaction in blue and membrane interaction in magenta is shown below. It is clear from figure 7.2. that the interaction sites are not overlapping. This supports our hypothesis that Kindlin F0 domain interacts with the membrane and partly facilitates the effect of Kindlin 2 in integrin activation.

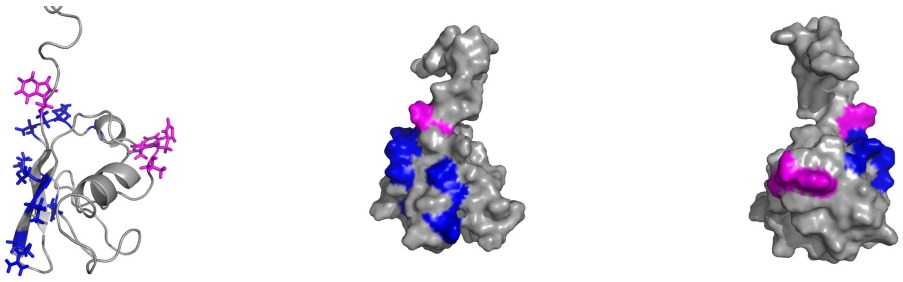

(a) (b) (c)

Figure 7.2. Kindlin 2 F0 dmain structure. Highlighted residues are due to integrin interaction (partly) in blue and PIP/membrane interaction in magenta. (a) Ribbon diagram (b) surface view (c) surface view after 180 deg rotation from (b).

Another aspect in this multi-collaborative-project is to understand the significance of Migfilin and Kindlin 2 interaction. Among the binding partners of Kindlin 2, the interaction between Kindlin N-ter and Migfilin plays an indispensible role in recruiting Migfilin to focal adhesion (Tu et al., 2003). To validate the interaction obtained from *in vivo* assays and understand the interaction specifics between Kindlin 2 N-ter and Migfilin, NMR was used as our primary method of analysis.

Our results show an interaction between Kindlin 2 11-143 residues with Migfilin LIM23 domains. However, further truncation of the protein abolished the interaction between Kindlin and Migfilin. We postulate that the F1 subdomain (F1 fragment), which is C terminally located from the F0 domain, may impose an effect on the core F0 domain structure and facilitates the interaction with Migfilin LIM domains. Evidence from our collaborators has reported a positive interaction between the Kindlin 2 N-ter 1-218 and Migfilin LIM domains. The facts that:

1. We only observed an interaction between Kindlin 2 11-143 and Migfilin LIM domains although we screened all fragments of Kindlin 2 1-268 protein *in vitro.*
2. Truncation of Kindlin 2 11-143 abolished the interaction with Lim domains *in vitro.*
3. A larger fragment of 1-218 show a positive interaction *in vivo*

supports our hypothesis of a 3D functional structure, which is distorted during truncation of larger a fragment into smaller sub-domain proteins of Kindlin 2.

All model structures of Kindlin 2 show that the F0 and F1 fragments (highlighted in yellow and red) residues 1-276 form a well defined core structure (see below). The core (shown by an arrowhead) is surrounded by localized positive and negative charges. It is

possible that this structure is the functional structure that mediates Migfilin LIM domain interaction. Truncation may distort the functional structure and abolish interaction, which is consistent with our data.

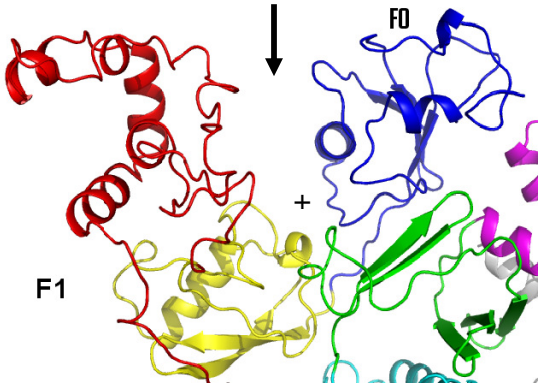

Figure 7.3. Part of the full length Kindlin 2 Model 1 highlighting F0 domain in blue and F1 fragments in yellow and red.

An expression construct made for Kindlin 2 1-276 had no significant protein expression. We were able to obtain F0 (blue) and 155-268 residues (red and part of yellow) separately. Expression constructs with incorporation of the positive charges, Kindlin 2 1-154, 1-177, 11-158, are either insoluble or are soluble aggregates. If the interaction between Migfilin and Kindlin 2 is mediated via the F0-F1 core structure, obtaining the protein would be a necessary step.

Model structures of Kindlin 2 display that the F0 subdomain of Kindlin 2 holds a central position in the structure. It forms a core structure together with F1 subdomain fragments on one side and is in close contact with other domains in the structure. This positioning of F0 domain may stabilize all interacting domains of the structure. There is a possibility that deleting F0 domain from the full length protein may perturb the 3D structure. This may influence the interaction/association with integrin and other proteins

like Migfilin. The integrin activation assay shown in figure 4.1. in chapter 4 shows that deletion of the F0 domain from the full length Kindlin 2 abolish integrin activation, demonstrating the central role of Kindlin 2 F0 domain. In order to understand the position of the F0 domain in the full length protein, the 3D structure of Kindlin 2 is necessary.

Kindlin 2 is a phosphor protein where residues 159 and 181 are phosphorylated. In vivo assays have demonstrated a positive interaction for Kindlin 2 1-218. The two potential phosphorylation sites are located within 1-218 residues. Kindlin 2 for *in vivo* analysis was purified from mammalian cells and for *in vitro* analysis from bacterial expression systems. Bacteria lack the bio mechanism for many types of post-translational modifications. If a post-translational modification such as a phosphorylation is necessary for the interaction between Kindlin 2 and Migfilin, *in vitro* experiments would not detect the interaction. There are many examples in literature to support this kind of phenomenon. One example is the interaction between the integrin cytoplasmic tail and Dok1 protein. Dok1 is cytoplasmic protein and is involved in many signaling pathways. It also plays an important role in cell migration (Yamanashi et el, Cell 1997; Noguchi et el, EMBO J 1999). Both Talin PTB and Dok1 PTB domains binds to the central $NPxY^{747}$ motif of the β3 integrin CT. The major difference of this interaction is that Dok1 negatively regulate integrin activation and Talin activates integrin (Wegener, K.L. et el, cell 2007). This contrasting role of function occurs due to one simple modification in the sequence. Phosphorylation of Tyr^{747} residue shows a dramatic change in binding affinities. Another more recent example explains that Kindlin 2 PTB domain itself shows a higher affinity for non-phosporylated Y^{759} on integrin CT than the phophorylated tail

(Bledzka et al., 2010). There are many types of post-translational modifications that can occur in mammalian cells and not found in bacterial cell machineries. Phosphorylation is one such mechanism that change or control the behavior of the protein. Kindlin and Migfilin are relatively large proteins with multiple phosphorylation sites. So the only way to incorporate potential PTM is to grow the protein in a mammalian expression system, insect cell expression systems or the more common baculovirus insect cell expression system.

Although an interaction between Kindlin 2 N-term and Migfilin LIM domains was observed in biological assays, we were not able to pin down the exact binding interface/s using in-vitro studies (NMR, SPR and ITC experiments). As described above, the possibilities of (1) a distortion in the function 3D structure through subcloning, (2) a post-translational modification at the binding surface in Kindlin or Migfilin (3) a central role of F0 domain in the full length protein could be reasoned, and investigating and evaluating these possibilities would be a future necessary step for the molecular level understanding of the role of Kindlin and Migfilin in integrin activation.

The interaction between Kindlin 2 and Migfilin plays a significant role in cell adhesion processes. In addition to the structural role in the cell by forming a connection via the ECM and actin cytoskeleton, Kindlin-2 and Migfilin have become essential elements in the process of integrin activation. Our data on integrin activation assays in figures Fig 5.9 and 5.10 have emphasized the significance of both Kindlin and Migfilin in Talin induced integrin activation. How does Migfilin contribute to enhance integrin activation? Our hypothesis of the formation of a ternary complex via *Migfilin-Kindlin N-ter-Talin H* interactions would stabilize the interaction with integrin CT thereby

heightening the effect of activated integrins was evaluated giving particular interest to Migfilin and Talin H interaction. Our data have eliminated the possibility of this interaction using NMR. How does Migfilin overexpression enhance the effect of integrin activation? From literature it is evident that Migfilin N-ter removes the negative regulatory effect of Filamin from the integrin CT. Kindlin 2 and Migfilin interaction recruits Migfilin to the focal adhesion site allowing Migfilin N-ter to interact with Filamin. Further analyses are necessary to evaluate and understand the cooperate role of Migfilin/Kindlin/TalinH in integrin activation.

The role of Kindlin C-term F3 domain in Talin induced integrin activation has been demonstrated in literature. However, up-to-date there are no structural studies on Kindlin 2 C term been reported. As a goal of this thesis work, we have been extensively subcloning and optimizing the C-term Kindlin 2 in order to obtain a soluble protein for structure based analysis. Despite the varying number of bacterial expression systems, vectors, fusion tags, mutations, optimization strategies, we were not able to obtain a soluble monomeric protein for the C-term of Kindlin 2. For the molecular level understanding of integrin activation, the structure of Kindlin is a necessary component. In future work, it is beneficial to further subclone changing the boundaries of the protein in the scope of obtaining a suitable protein. As an immediate future step, subcloning from lower species like mouse and *C. elegans* would be helpful. The mouse and human Kindlin 2 amino acid sequences have a 98% similarity while the DNA sequences show 87% homology. Obtaining the Kindlin 2 C-term protein will allow us to evaluate the interaction between Kindlin C-term and integrin and investigate the prospective auto

inhibitory mechanism. Certain approaches outlined here, could be useful in future to guide to obtain Kindlin 2 C-ter protein for prospective functional analyses.

Modeling studies suggest that there is a possible interaction between the N-ter and FERM domain of Kindlin 2. A similar interaction is seen in Talin. (Goksoy et al., 2008). Talin rod domain and PTB domain interaction keeps Talin in its inactive dimeric conformation. PIP2 disrupts the binding interface between the rod domain and PTB domain and opens up the binding interface for integrin activation. Having similar structural architecture and binding patterns, we assume that similar to Talin, Kindlin obtains an inactive conformation through N-ter and C-ter interaction. In vivo data from on-going studies have clearly shown that Kindlin 2 interacts with PIP3. Based on this data we further hypothesize that the active conformation is revealed through potent PIP3 interaction.

In addition to Talin, N-WASP, an actin polymerization protein, is another protein where the C-ter and N-term interaction is disrupted by potent PIP2 and Cdc42 binding. PIP2 binds to a polybasic stretch in the sequence which perturbs the C and N terminal interaction thereby revealing the active form of N-WASP (Venizelos Papayannopoulos et el, 2007, Molecular cell). A similar sequence motif of positively charged residues is found in Kindlin 2, residues 148-154. The fact hat modeling structures suggest that there is a Kindlin C-ter and N-ter interaction and PIP3 disrupts the interaction may support our hypothesis on the proposed autoinhibition mechanism for Kindlin 2. Obtaining the C-terminal protein will be first step to conduct a detailed analysis in order to support the prospective auto-inhibitory mechanism of Kindlin 2.

To conclude, Kindlins play an indispensable role in integrin activation. The role of Kindlin 2 C-ter has been determined (Ma, Yang-Qing et al., 2008). However, up-to-date there is a lack of information in literature about the role of the N-ter domains of Kindlin 2. Here we have elucidated certain interacting partners of Kindlin 2 N-ter and hypothesized its role in integrin activation. In brief, we have solved the structure of the F0 domain of Kindlin 2 and have elucidated specific non-overlapping binding sites on F0 due to integrin β3 and PIP3 binding. In support with other *in vivo* and *in vitro* data, we hypothesized that the Kindlin 2 N-terminal domain/s interacts with the membrane and helps the full length Kindlin 2 protein to anchor to the membrane surface. This interaction may stabilize Kindlin 2 and helps to facilitate the effect of Kindlin 2 in integrin activation. In addition, we have elucidated that the F0 domain has partially overlapping binding sites with the membrane and Migfilin LIM domains. Kindlin 2 F0 deletion constructs completely abolishes integrin activation, further heightening the significance of Kindlin 2 F0 domain. Overall, this work has given a better understanding of the of Kindlin 2 N-ter.

REFERENCES

An, Z., Dobra, K., Lock, J.G., Stromblad, S., Hjerpe, A., and Zhang, H. (2010). Kindlin-2 is expressed in malignant mesothelioma and is required for tumor cell adhesion and migration. Int. J. Cancer

Anthis, N.J., Wegener, K.L., Ye, F., Kim, C., Goult, B.T., Lowe, E.D., Vakonakis, I., Bate, N., Critchley, D.R., Ginsberg, M.H., and Campbell, I.D. (2009). The structure of an integrin/talin complex reveals the basis of inside-out signal transduction. EMBO J. *28,* 3623-3632.

Arita, K., Wessagowit, V., Inamadar, A.C., Palit, A., Fassihi, H., Lai-Cheong, J.E., Pourreyron, C., South, A.P., and McGrath, J.A. (2007). Unusual molecular findings in Kindler syndrome. Br. J. Dermatol. *157,* 1252-1256.

Ashton, G.H. (2004). Kindler syndrome. Clin. Exp. Dermatol. *29,* 116-121.

Ashton, G.H., McLean, W.H., South, A.P., Oyama, N., Smith, F.J., Al-Suwaid, R., Al-Ismaily, A., Atherton, D.J., Harwood, C.A., Leigh, I.M.*, et al.* (2004). Recurrent mutations in kindlin-1, a novel keratinocyte focal contact protein, in the autosomal recessive skin fragility and photosensitivity disorder, Kindler syndrome. J. Invest. Dermatol. *122,* 78-83.

Barczyk, M., Carracedo, S., and Gullberg, D. (2010). Integrins. Cell Tissue Res. *339,* 269-280.

Bialkowska, K., Ma, Y.Q., Bledzka, K., Sossey-Alaoui, K., Izem, L., Zhang, X., Malinin, N., Qin, J., Byzova, T., and Plow, E.F. (2010). The integrin co-activator kindlin-3 is expressed and functional in a non-hematopoietic cell, the endothelial cell. J. Biol. Chem.

Bialkowska, K., Ma, Y.Q., Bledzka, K., Sossey-Alaoui, K., Izem, L., Zhang, X., Malinin, N., Qin, J., Byzova, T., and Plow, E.F. (2010). The integrin co-activator Kindlin-3 is expressed and functional in a non-hematopoietic cell, the endothelial cell. J. Biol. Chem. *285,* 18640-18649.

Bledzka, K., Bialkowska, K., Nie, H., Qin, J., Byzova, T., Wu, C., Plow, E.F., and Ma, Y.Q. (2010). Tyrosine phosphorylation of integrin beta3 regulates kindlin-2 binding and integrin activation. J. Biol. Chem. *285,* 30370-30374.

Burch, J.M., Fassihi, H., Jones, C.A., Mengshol, S.C., Fitzpatrick, J.E., and McGrath, J.A. (2006). Kindler syndrome: a new mutation and new diagnostic possibilities. Arch. Dermatol. *142,* 620-624.

Calderwood, D.A. (2004). Integrin activation. J. Cell. Sci. *117,* 657-666.

Calderwood, D.A., Yan, B., de Pereda, J.M., Alvarez, B.G., Fujioka, Y., Liddington, R.C., and Ginsberg, M.H. (2002). The phosphotyrosine binding-like domain of talin activates integrins. J. Biol. Chem. *277,* 21749-21758.

Chivian, D., Kim, D.E., Malmstrom, L., Bradley, P., Robertson, T., Murphy, P., Strauss, C.E., Bonneau, R., Rohl, C.A., and Baker, D. (2003). Automated prediction of CASP-5 structures using the Robetta server. Proteins *53 Suppl 6,* 524-533.

Chivian, D., Kim, D.E., Malmstrom, L., Schonbrun, J., Rohl, C.A., and Baker, D. (2005). Prediction of CASP6 structures using automated Robetta protocols. Proteins *61 Suppl 7,* 157-166.

Cornilescu, G., Delaglio, F., and Bax, (1999) A. Protein backbone angle restraints from searching a database for chemical shift and sequence homology. J. Biomol. NMR *13,* 289-302.

Cox, D., Brennan, M., Moran, N. (2010) Integrins as therapeutic targets: lessons and opportunities. Nature Reviews Drug Discovery 9, 804-820.

Curtis, K.A., Kindlin, C.M., Reich, K.M., and White, D.E. (1995). Functional reach in wheelchair users: the effects of trunk and lower extremity stabilization. Arch. Phys. Med. Rehabil. *76,* 360-367.

Delaglio, F., Grzesiek, S., Vuister, G.W., Zhu, G., Pfeifer, J., and Bax, A. (1995). NMRPipe: a multidimensional spectral processing system based on UNIX pipes. J. Biomol. NMR *6,* 277-293.

Dephoure N., Zhou C., Villen J., Beausoleil S.A., Bakalarski C.E., Elledge S.J., Gygi S.P. (2008). A quantitative atlas of mitotic phosphorylation.Proc. Natl. Acad. Sci. U.S.A. 105:10762-10767

Dowling, J.J., Gibbs, E., Russell, M., Goldman, D., Minarcik, J., Golden, J.A., and Feldman, E.L. (2008). Kindlin-2 is an essential component of intercalated discs and is required for vertebrate cardiac structure and function. Circ. Res. *102,* 423-431.

Dowling, J.J., Vreede, A.P., Kim, S., Golden, J., and Feldman, E.L. (2008). Kindlin-2 is required for myocyte elongation and is essential for myogenesis. BMC Cell Biol. *9,* 36.

D'Souza, M.A., Kimble, R.M., and McMillan, J.R. (2010). Kindler syndrome pathogenesis and fermitin family homologue 1 (kindlin-1) function. Dermatol. Clin. *28,* 115-118.

Fukuda, K., Gupta, S., Chen, K., Wu, C., and Qin, J. (2009). The Pseudoactive Site of ILK Is Essential for Its Binding to α-Parvin and Localization to Focal Adhesions. Mol. Cell *36,* 819-830.

Garcia-Alvarez, B., de Pereda, J.M., Calderwood, D.A., Ulmer, T.S., Critchley, D., Campbell, I.D., Ginsberg, M.H., and Liddington, R.C. (2003). Structural determinants of integrin recognition by talin. Mol. Cell *11,* 49-58.

Garcia-Alvarez, B., de Pereda, J.M., Calderwood, D.A., Ulmer, T.S., Critchley, D., Campbell, I.D., Ginsberg, M.H., and Liddington, R.C. (2003). Structural determinants of integrin recognition by talin. Mol. Cell *11,* 49-58.

Garrett, D.S., Powers, R., Gronenborn, A.M., and Clore, G.M. (1991). A common-sense approach tp peak picking in two-, three- and dimensional spectra using aotomatic computer analysis of contour diagrams. J. Magn. Reson. 214-220.

Giancotti, F.G., and Ruoslahti, E. (1999). Integrin signaling. Science *285,* 1028-1032.

Goksoy, E., Ma, Y.Q., Wang, X., Kong, X., Perera, D., Plow, E.F., and Qin, J. (2008). Structural basis for the autoinhibition of talin in regulating integrin activation. Mol. Cell *31,* 124-133.

Gong, X., An, Z., Wang, Y., Guan, L., Fang, W., Stromblad, S., Jiang, Y., and Zhang, H. (2010). Kindlin-2 controls sensitivity of prostate cancer cells to cisplatin-induced cell death. Cancer Lett.

Goult, B.T., Bouaouina, M., Elliott, P.R., Bate, N., Patel, B., Gingras, A.R., Grossmann, J.G., Roberts, G.C., Calderwood, D.A., Critchley, D.R., and Barsukov, I.L. (2010). Structure of a double ubiquitin-like domain in the talin head: a role in integrin activation. EMBO J. *29,* 1069-1080.

Goult, B.T., Bouaouina, M., Harburger, D.S., Bate, N., Patel, B., Anthis, N.J., Campbell, I.D., Calderwood, D.A., Barsukov, I.L., Roberts, G.C., and Critchley, D.R. (2009). The structure of the N-terminus of kindlin-1: a domain important for alphaiibbeta3 integrin activation. J. Mol. Biol. *394,* 944-956.

Goult, B.T., Bouaouina, M., Harburger, D.S., Bate, N., Patel, B., Anthis, N.J., Campbell, I.D., Calderwood, D.A., Barsukov, I.L., Roberts, G.C., and Critchley, D.R. (2009). The structure of the N-terminus of kindlin-1: a domain important for alphaiibbeta3 integrin activation. J. Mol. Biol. *394,* 944-956.

Hannigan, G.E., Leung-Hagesteijn, C., Fitz-Gibbon, L., Coppolino, M.G., Radeva, G., Filmus, J., Bell, J.C., and Dedhar, S. (1996). Regulation of cell adhesion and anchorage-dependent growth by a new beta 1-integrin-linked protein kinase. Nature *379,* 91-96.

Harburger, D.S., Bouaouina, M., and Calderwood, D.A. (2009). Kindlin-1 and -2 directly bind the C-terminal region of beta integrin cytoplasmic tails and exert integrin-specific activation effects. J. Biol. Chem. *284,* 11485-11497.

Harburger, D.S., and Calderwood, D.A. (2009). Integrin signalling at a glance. J. Cell. Sci. *122,* 159-163.

Has, C. (2009). Kindler syndrome. A new bullous dermatosis. Hautarzt *60,* 622-626.

Has, C., Herz, C., Zimina, E., Qu, H.Y., He, Y., Zhang, Z.G., Wen, T.T., Gache, Y., Aumailley, M., and Bruckner-Tuderman, L. (2009). Kindlin-1 Is required for RhoGTPase-mediated lamellipodia formation in keratinocytes. Am. J. Pathol. *175,* 1442-1452.

Has, C., Wessagowit, V., Pascucci, M., Baer, C., Didona, B., Wilhelm, C., Pedicelli, C., Locatelli, A., Kohlhase, J., Ashton, G.H., *et al.* (2006). Molecular basis of Kindler syndrome in Italy: novel and recurrent Alu/Alu recombination, splice site, nonsense, and frameshift mutations in the KIND1 gene. J. Invest. Dermatol. *126,* 1776-1783.

He, Y., Esser, P., Schacht, V., Bruckner-Tuderman, L., and Has, C. (2010). Role of Kindlin-2 in Fibroblast Functions: Implications for Wound Healing. J. Invest. Dermatol.

Herz, C., Aumailley, M., Schulte, C., Schlotzer-Schrehardt, U., Bruckner-Tuderman, L., and Has, C. (2006). Kindlin-1 is a phosphoprotein involved in regulation of polarity, proliferation, and motility of epidermal keratinocytes. J. Biol. Chem. *281,* 36082-36090.

Hynes, R.O., Lively, J.C., McCarty, J.H., Taverna, D., Francis, S.E., Hodivala-Dilke, K., and Xiao, Q. (2002). The diverse roles of integrins and their ligands in angiogenesis. Cold Spring Harb. Symp. Quant. Biol. *67,* 143-153.

Ithychanda, S.S., Das, M., Ma, Y.Q., Ding, K., Wang, X., Gupta, S., Wu, C., Plow, E.F., and Qin, J. (2009). Migfilin, a molecular switch in regulation of integrin activation. J. Biol. Chem. *284,* 4713-4722.

Ithychanda, S.S., Hsu, D., Li, H., Yan, L., Liu, D., Das, M., Plow, E.F., and Qin, J. (2009). Identification and characterization of multiple similar ligand-binding repeats in filamin: implication on filamin-mediated receptor clustering and cross-talk. J. Biol. Chem. *284,* 35113-35121.

Jeener, J., Meier, B.H., Bachmann, P., and Ernst, R.R. (1979). Investigation of exchange processes by two-dimensional NMR spectroscopy. J. Chem Phy. *71,* 11.

Johnson, B.A., and Blevins, R.A. (1994). NMR View: A computer program for the vialization and analysis of NMR data. J. Mol. Biol. *4,* 603-614.

Jurk, K., Schulz, A.S., Kehrel, B.E., Rapple, D., Schulze, H., Mobest, D., Friedrich, W., Omran, H., Deak, E., Henschler, R., Scheele, J.S., and Zieger, B. (2010). Novel integrin-dependent platelet malfunction in siblings with leukocyte adhesion deficiency-III (LAD-III) caused by a point mutation in FERMT3. Thromb. Haemost. *103,*

Kay, L.E., Keifer, P., and Saarinen, T. (1992). Pure absorption gradient enhanced heteronuclear single quantum correlation spectroscopy with improved sensitivity. J. Am. Chem. Soc. *114,* 10663-10665.

Kay, L.E., Xu, G.Y., Singer, A.U., Muhandiram, D.R., and Forman-Kay, J.D. (1993). A gradient enhanced HCCH-TOCSY experiment for recording side-chain H-1 and C13 correlations in H2O samples of proteins. J. Magn. Reson. *101,* 333-337.

Keller, R.S., Shai, S.Y., Babbitt, C.J., Pham, C.G., Solaro, R.J., Valencik, M.L., Loftus, J.C., and Ross, R.S. (2001). Disruption of integrin function in the murine myocardium leads to perinatal lethality, fibrosis, and abnormal cardiac performance. Am. J. Pathol. *158,* 1079-1090.

Kim, D.E., Chivian, D., and Baker, D. (2004). Protein structure prediction and analysis using the Robetta server. Nucleic Acids Res. *32,* W526-31.

Kong, X., Wang, X., Misra, S., and Qin, J. (2006). Structural basis for the phosphorylation-regulated focal adhesion targeting of type Igamma phosphatidylinositol phosphate kinase (PIPKIgamma) by talin. J. Mol. Biol. *359,* 47-54.

Kruger, M., Moser, M., Ussar, S., Thievessen, I., Luber, C.A., Forner, F., Schmidt, S., Zanivan, S., Fassler, R., and Mann, M. (2008). SILAC mouse for quantitative proteomics uncovers kindlin-3 as an essential factor for red blood cell function. Cell *134,* 353-364.

Kuijpers, T.W., van de Vijver, E., Weterman, M.A., de Boer, M., Tool, A.T., van den Berg, T.K., Moser, M., Jakobs, M.E., Seeger, K., Sanal, O.*, et al.* (2009). LAD-1/variant syndrome is caused by mutations in FERMT3. Blood *113,* 4740-4746.

Lai-Cheong, J.E., Parsons, M., and McGrath, J.A. (2010). The role of kindlins in cell biology and relevance to human disease. Int. J. Biochem. Cell Biol. *42,* 595-603.

Lai-Cheong, J.E., Ussar, S., Arita, K., Hart, I.R., and McGrath, J.A. (2008). Colocalization of kindlin-1, kindlin-2, and migfilin at keratinocyte focal adhesion and relevance to the pathophysiology of Kindler syndrome. J. Invest. Dermatol. *128,* 2156-2165.

Larjava, H., Plow, E.F., and Wu, C. (2008). Kindlins: essential regulators of integrin signalling and cell-matrix adhesion. EMBO Rep. *9,* 1203-1208.

Lau, T.L., Kim, C., Ginsberg, M.H., and Ulmer, T.S. (2009). The structure of the integrin alphaIIbbeta3 transmembrane complex explains integrin transmembrane signalling. EMBO J. *28,* 1351-1361.

Lee, H.S., Lim, C.J., Puzon-McLaughlin, W., Shattil, S.J., and Ginsberg, M.H. (2009). RIAM activates integrins by linking talin to ras GTPase membrane-targeting sequences. J. Biol. Chem. *284,* 5119-5127.

Lin, X., Qadota, H., Moerman, D.G., and Williams, B.D. (2003). C. elegans PAT-6/actopaxin plays a critical role in the assembly of integrin adhesion complexes *in vivo*. Curr. Biol. *13,* 922-932.

Ma, Y.Q., Qin, J., Wu, C., and Plow, E.F. (2008). Kindlin-2 (Mig-2): a co-activator of beta3 integrins. J. Cell Biol. *181,* 439-446.

Mackinnon, A.C., Qadota, H., Norman, K.R., Moerman, D.G., and Williams, B.D. (2002). C. elegans PAT-4/ILK functions as an adaptor protein within integrin adhesion complexes. Curr. Biol. *12,* 787-797.

Mackinnon, A.C., Qadota, H., Norman, K.R., Moerman, D.G., and Williams, B.D. (2002). C. elegans PAT-4/ILK functions as an adaptor protein within integrin adhesion complexes. Curr. Biol. *12,* 787-797.

Malinin, N.L., Plow, E.F., and Byzova, T.V. (2010). Kindlins in FERM adhesion. Blood

Manevich-Mendelson, E., Feigelson, S.W., Pasvolsky, R., Aker, M., Grabovsky, V., Shulman, Z., Kilic, S.S., Rosenthal-Allieri, M.A., Ben-Dor, S., Mory, A.*, et al.* (2009). Loss of Kindlin-3 in LAD-III eliminates LFA-1 but not VLA-4 adhesiveness developed under shear flow conditions. Blood *114,* 2344-2353.

Martin-Bermudo, M.D., Dunin-Borkowski, O.M., and Brown, N.H. (1998). Modulation of integrin activity is vital for morphogenesis. J. Cell Biol. *141,* 1073-1081.

McDowall, A., Svensson, L., Stanley, P., Patzak, I., Chakravarty, P., Howarth, K., Sabnis, H., Briones, M., and Hogg, N. (2010). Two mutations in the KINDLIN3 gene of a new leukocyte adhesion deficiency III patient reveal distinct effects on leukocyte function *in vitro*. Blood *115,* 4834-4842.

McDowall, A., Svensson, L., Stanley, P., Patzak, I., Chakravarty, P., Howarth, K., Sabnis, H., Briones, M., and Hogg, N. (2010). Two mutations in the KINDLIN3 gene of a new leukocyte adhesion deficiency-III patient reveal distinct effects on leukocyte function *in vitro*. Blood

McGrath, J.A. (2004). Translational benefits from research on rare genodermatoses. Australas. J. Dermatol. *45,* 89-93.

McPherson, A., Malkin, A.J., and Kuznetsov, Y.G. (1995). The science of macromolecular crystallization. Structure *3,* 759-768.

Meves, A., Stremmel, C., Gottschalk, K., and Fassler, R. (2009). The Kindlin protein family: new members to the club of focal adhesion proteins. Trends Cell Biol. *19,* 504-513.

Montanez, E., Ussar, S., Schifferer, M., Bosl, M., Zent, R., Moser, M., and Fassler, R. (2008). Kindlin-2 controls bidirectional signaling of integrins. Genes Dev. *22,* 1325-1330.

Montelione, G.T., Zheng, D., Huang, Y.J., Gunsalus, K.C., and Szyperski, T. (2000). Protein NMR spectroscopy in structural genomics. Nat. Struct. Biol. *7 Suppl,* 982-985.

Mory, A., Feigelson, S.W., Yarali, N., Kilic, S.S., Bayhan, G.I., Gershoni-Baruch, R., Etzioni, A., and Alon, R. (2008). Kindlin-3: a new gene involved in the pathogenesis of LAD-III. Blood *112,* 2591.

Moser, M., Bauer, M., Schmid, S., Ruppert, R., Schmidt, S., Sixt, M., Wang, H.V., Sperandio, M., and Fassler, R. (2009). Kindlin-3 is required for beta2 integrin-mediated leukocyte adhesion to endothelial cells. Nat. Med. *15,* 300-305.

Moser, M., Nieswandt, B., Ussar, S., Pozgajova, M., and Fassler, R. (2008). Kindlin-3 is essential for integrin activation and platelet aggregation. Nat. Med. *14,* 325-330.

Muhandiram, D.R., and Kay, L.E. Gradient-Enhanced Triple-Resonance Three-Dimensional NMR Experiments with Improved Sensitivity . J. Magn. Reson. *103,* 203-216.

Nieswandt, B., Varga-Szabo, D., and Elvers, M. (2009). Integrins in platelet activation. J. Thromb. Haemost. *7 Suppl 1,* 206-209.

Nofal, E., Assaf, M., and Elmosalamy, K. (2008). Kindler syndrome: a study of five Egyptian cases with evaluation of severity. Int. J. Dermatol. *47,* 658-662.

Nussbaum, C., Moser, M., and Sperandio, M. (2010). Leukocyte adhesion deficiency-III: when leukocytes cannot stop. Pediatr. Res. *67,* 339.

Nussbaum, C., Moser, M., and Sperandio, M. (2010). Leukocyte adhesion deficiency-III: when leukocytes cannot stop. Pediatr. Res. *67,* 339.

Oxley, C.L., Anthis, N.J., Lowe, E.D., Vakonakis, I., Campbell, I.D., and Wegener, K.L. (2008). An integrin phosphorylation switch: the effect of beta3 integrin tail phosphorylation on Dok1 and talin binding. J. Biol. Chem. *283,* 5420-5426.

Papachristou, D.J., Gkretsi, V., Tu, Y., Shi, X., Chen, K., Larjava, H., Rao, U.N., and Wu, C. (2007). Increased cytoplasmic level of migfilin is associated with higher grades of human leiomyosarcoma. Histopathology *51,* 499-508.

Petricca, G., Leppilampi, M., Jiang, G., Owen, G.R., Wiebe, C., Tu, Y., Koivisto, L., Hakkinen, L., Wu, C., and Larjava, H. (2009). Localization and potential function of kindlin-1 in periodontal tissues. Eur. J. Oral Sci. *117,* 518-527.

Petrich, B.G., Marchese, P., Ruggeri, Z.M., Spiess, S., Weichert, R.A., Ye, F., Tiedt, R., Skoda, R.C., Monkley, S.J., Critchley, D.R., and Ginsberg, M.H. (2007). Talin is required for integrin-mediated platelet function in hemostasis and thrombosis. J. Exp. Med. *204,* 3103-3111.

Plow, E.F., Qin, J., and Byzova, T. (2009). Kindling the flame of integrin activation and function with kindlins. Curr. Opin. Hematol. *16,* 323-328.

Qin, J., Vinogradova, O., and Plow, E.F. (2004). Integrin bidirectional signaling: a molecular view. PLoS Biol. *2,* e169.

Sabnis, H., Kirpalani, A., Horan, J., McDowall, A., Svensson, L., Cooley, A., Merck, T., Jobe, S., Hogg, N., and Briones, M. (2010). Leukocyte adhesion deficiency-III in an African-American patient. Pediatr. Blood Cancer.

Sadler, E., Klausegger, A., Muss, W., Deinsberger, U., Pohla-Gubo, G., Laimer, M., Lanschuetzer, C., Bauer, J.W., and Hintner, H. (2006). Novel KIND1 gene mutation in Kindler syndrome with severe gastrointestinal tract involvement. Arch. Dermatol. *142,* 1619-1624.

Sambrook, J., Fritsch, E.F., and Maniatis, T. (1989). Molecular Cloning 2nd Ed.*3,* p. A. 3.

Shattil, S.J., Kim, C., and Ginsberg, M.H. (2010). The final steps of integrin activation: the end game. Nat. Rev. Mol. Cell Biol. *11,* 288-300.

Shattil, S.J., Kim, C., and Ginsberg, M.H. (2010). The final steps of integrin activation: the end game. Nat. Rev. Mol. Cell Biol. *11,* 288-300.

Shuker, S.B., Hajduk, P.J., Meadows, R.P., and Fesik, S.W. (1996). Discovering high-affinity ligands for proteins: SAR by NMR. Science *274,* 1531-1534.

Siegel, D.H., Ashton, G.H., Penagos, H.G., Lee, J.V., Feiler, H.S., Wilhelmsen, K.C., South, A.P., Smith, F.J., Prescott, A.R., Wessagowit, V.*, et al.* (2003). Loss of kindlin-1, a human homolog of the Caenorhabditis elegans actin-extracellular-matrix linker protein UNC-112, causes Kindler syndrome. Am. J. Hum. Genet *73,* 174-187.

Smith, L., Page, R.C., Xu, Z., Kohli, E., Litman, P., Nix, J.C., Ithychanda, S.S., Liu, J., Qin, J., Misra, S., and Liedtke, C.M. (2010). Biochemical Basis of the Interaction between Cystic Fibrosis Transmembrane Conductance Regulator and Immunoglobulin-like Repeats of Filamin. J. Biol. Chem. *285,* 17166-17176.

Svensson, L., Howarth, K., McDowall, A., Patzak, I., Evans, R., Ussar, S., Moser, M., Metin, A., Fried, M., Tomlinson, I., and Hogg, N. (2009). Leukocyte adhesion deficiency-III is caused by mutations in KINDLIN3 affecting integrin activation. Nat. Med. *15,* 306-312.

Tadokoro, S., Shattil, S.J., Eto, K., Tai, V., Liddington, R.C., de Pereda, J.M., Ginsberg, M.H., and Calderwood, D.A. (2003). Talin binding to integrin beta tails: a final common step in integrin activation. Science *302,* 103-106.

Takafuta, T., Saeki, M., Fujimoto, T.T., Fujimura, K., and Shapiro, S.S. (2003). A new member of the LIM protein family binds to filamin B and localizes at stress fibers. J. Biol. Chem. *278,* 12175-12181.

Tu, Y., Wu, S., Shi, X., Chen, K., and Wu, C. (2003). Migfilin and Mig-2 link focal adhesions to filamin and the actin cytoskeleton and function in cell shape modulation. Cell *113,* 37-47.

Uhrin, P., Zaujec, J., Breuss, J.M., Olcaydu, D., Chrenek, P., Stockinger, H., Fuertbauer, E., Moser, M., Haiko, P., Fassler, R.*, et al.* (2010). Novel function for blood platelets and podoplanin in developmental separation of blood and lymphatic circulation. Blood

Ussar, S., Moser, M., Widmaier, M., Rognoni, E., Harrer, C., Genzel-Boroviczeny, O., and Fassler, R. (2008). Loss of Kindlin-1 causes skin atrophy and lethal neonatal intestinal epithelial dysfunction. PLoS Genet *4,* e1000289.

Ussar, S., Wang, H.V., Linder, S., Fassler, R., and Moser, M. (2006). The Kindlins: subcellular localization and expression during murine development. Exp. Cell Res. *312,* 3142-3151.

Vinogradova, O., Vaynberg, J., Kong, X., Haas, T.A., Plow, E.F., and Qin, J. (2004). Membrane-mediated structural transitions at the cytoplasmic face during integrin activation. Proc. Natl. Acad. Sci. U. S. A. *101,* 4094-4099.

Vinogradova, O., Vaynberg, J., Kong, X., Haas, T.A., Plow, E.F., and Qin, J. (2004). Membrane-mediated structural transitions at the cytoplasmic face during integrin activation. Proc. Natl. Acad. Sci. U. S. A. *101,* 4094-4099.

Vinogradova, O., Velyvis, A., Velyviene, A., Hu, B., Haas, T., Plow, E., and Qin, J. (2002). A structural mechanism of integrin alpha(IIb)beta(3) "inside-out" activation as regulated by its cytoplasmic face. Cell *110,* 587-597.

Wang, H., Lim, D., and Rudd, C.E. (2010). Immunopathologies linked to integrin signalling. Semin. Immunopathol.

Wegener, K.L., Partridge, A.W., Han, J., Pickford, A.R., Liddington, R.C., Ginsberg, M.H., and Campbell, I.D. (2007). Structural basis of integrin activation by talin. Cell *128,* 171-182.

White, S.J., and McLean, W.H. (2005). Kindler surprise: mutations in a novel actin-associated protein cause Kindler syndrome. J. Dermatol. Sci. *38,* 169-175.

Wiebe, C.B., Petricca, G., Hakkinen, L., Jiang, G., Wu, C., and Larjava, H.S. (2008). Kindler syndrome and periodontal disease: review of the literature and a 12-year follow-up case. J. Periodontol. *79,* 961-966.

Wiliamson, M.P., Havel, T.F., and Wüthrich, K. (1985). Solution conformation of proteinase inhibitor IIa from bull seminal plasma by 1H nuclear magnetic resonance and distance geometry. J. Mol. Biol. *182,* 295-315.

Wozniak, M.A., Modzelewska, K., Kwong, L., and Keely, P.J. (2004). Focal adhesion regulation of cell behavior. Biochim. Biophys. Acta *1692,* 103-119.

Wuthrich, K. (1991). Six years of protein structure determination by NMR spectroscopy: What we have learned? Protein Conformation 139-146.

Wuthrich, K. (1989). The development of nuclear magnetic resonance spectroscopy as a technique for protein structure determination. Acc Chem Res *22,* 36-44.

Wuthrich, K. (1989). Protein structure determination in solution by nuclear magnetic resonance spectroscopy. Science *243,* 45-50.

Wuthrich, K., Wider, G., Wagner, G., and Braun, W. (1982). Sequential Resonance assignments as a basis for determination of spatial protein structures by high resolution proton nuclear magnetic resonance. J. Mol. Biol. *155,* 311-319.

Xiong, J.P., Stehle, T., Diefenbach, B., Zhang, R., Dunker, R., Scott, D.L., Joachimiak, A., Goodman, S.L., and Arnaout, M.A. (2001). Crystal structure of the extracellular segment of integrin alpha Vbeta3. Science *294,* 339-345.

Xiong, J.P., Stehle, T., Zhang, R., Joachimiak, A., Frech, M., Goodman, S.L., and Arnaout, M.A. (2002). Crystal structure of the extracellular segment of integrin alpha Vbeta3 in complex with an Arg-Gly-Asp ligand. Science *296,* 151-155.

Xiong, Y.M., Haas, T.A., and Zhang, L. (2002). Identification of functional segments within the beta2I-domain of integrin alphaMbeta2. J. Biol. Chem. *277,* 46639-46644.

Xu, X., Rongali, S.C., Miles, J.P., Lee, K.D., and Lee, M. (2006). pat-4/ILK and unc-112/Mig-2 are required for gonad function in Caenorhabditis elegans. Exp. Cell Res. *312,* 1475-1483.

Xu, X., Rongali, S.C., Miles, J.P., Lee, K.D., and Lee, M. (2006). pat-4/ILK and unc-112/Mig-2 are required for gonad function in Caenorhabditis elegans. Exp. Cell Res. *312,* 1475-1483.

Xu, Y., Wang, X., Yang, J., Vaynberg, J., and Qin, J. (2006). PASA--a program for automated protein NMR backbone signal assignment by pattern-filtering approach. J. Biomol. NMR *34,* 41-56.

Yang, J., Ma, Y.Q., Page, R.C., Misra, S., Plow, E.F., and Qin, J. (2009). Structure of an integrin alphaIIb beta3 transmembrane-cytoplasmic heterocomplex provides insight into integrin activation. Proc. Natl. Acad. Sci. U. S. A. *106,* 17729-17734.

APPENDICES

APPENDIX 1

Kindlin 2 Full Length human PSIPRED PREDICTION RESULTS

Conf: Confidence (0=low, 9=high)
Pred: Predicted secondary structure (H=helix, E=strand, C=coil)
AA: Target sequence

PSIPRED HFORMAT (PSIPRED V2.5 by David Jones)

```
Conf: 973631256777403402368996278854799998145147999999988768543221
Pred: CCCCCEECCCCCEECCEEEEEEEECCCCCEEEEEEEECCCHHHHHHHHHHHHCCCCCCCC
  AA: MALDGIRMPDGCYADGTWELSVHVTDVNRDVTLRVTGEVHIGGVMLKLVEKLDVKKDWSD
            10        20        30        40        50        60

Conf: 000218534033531112353012326330113357616998599977899974270079
Pred: CCCCHHHHCCHHHHHHHHHHHCCCCCCCCCCCCCCCCCEEEEECCCCCCEEEEEEECCCHHH
  AA: HALWWEKKRTWLLKTHWTLDKYGIQADAKLQFTPQHKLLRLQLPNMKYVKVKVNFSDRVF
            70        80        90       100       110       120

Conf: 999998888087871000123578551332102464323432101688745778877565
Pred: HHHHHHHHHCCCCCCHHHCCCCCCCCHHHHHHCCCCCCCCCCCCCCCCCCCCCCCCCCCC
  AA: KAVSDICKTFNIRHPEELSLLKKPRDPTKKKKKKLDDQSEDEALELEGPLITPGSGSIYS
          130       140       150       160       170       180

Conf: 888876767866666788746776545677532456776324589988855753146726
Pred: CCCCCCCCCCCCCCCCCCCCCCCCCCCCCCCCCCCCCCCCCCCCCCCCCCCCCHHHHHCCCCH
  AA: SPGLYSKTMTPTYDAHDGSPLSPTSAWFGDSALSEGNPGILAVSQPITSPEILAKMFKPQ
          190       200       210       220       230       240

Conf: 688987323576787840120686999789999802245124888672553101245565
Pred: HHHHHHHCCCCCCCCCCCHHHCCCCCCCEEEEEEECEEEECCCCCCCCEEEEEHHHHHHH
  AA: ALLDKAKINQGWLDSSRSLMEQDVKENEALLLRFKYYSFFDLNPKYDAIRINQLYEQAKW
          250       260       270       280       290       300

Conf: 663488556899998860300112102456776777666610343787500121670178
Pred: HHHCCCCCCCHHHHHHHHHHEEEEECCCCCCCCCCCCCCCCHHHHHHHHHCCCEEEECCC
  AA: AILLEEIECTEEEMMMFAALQYHINKLSIMTSENHLNNSDKEVDEVDAALSDLEITLEGG
          310       320       330       340       350       360

Conf: 767520022000766320100152122334430368999706365430732327572334
Pred: CCCCCCHHHHCCHHHHCCCHHCCCCCCCCCCCCEEEEEEEECCEEEEEECHHHCCCCCHHH
  AA: KTSTILGDITSIPELADYIKVFKPKKLTLKGYKQYWCTFKDTSISCYKSKEESSGTPAHH
          370       380       390       400       410       420

Conf: 156762451010004662017998304898426999448756688787750333165300
Pred: CCCCCCEEECCCCCCCCCCEEEEEEECCCCCCEEEEEECCCHHHHHHHHHHHHHHHCCCCC
  AA: MNLRGCEVTPDVNISGQKFNIKLLIPVAEGMNEIWLRCDNEKQYAHWMAACRLASKGKTM
          430       440       450       460       470       480
```

```
Conf: 012205899999999971699987432731246677820034378828875002468999
Pred: CCCCCHHHHHHHHHHHHHCCCCCCCCCCCCCCCCCCCCCCCCCHHHHHHHHCCCCCCHHHH
  AA: ADSSYNLEVQNILSFLKMQHLNPDPQLIPEQITTDITPECLVSPRYLKKYKNKQITARIL
            490       500       510       520       530       540

Conf: 97544228899999999999987450004118999850888633999933141212635 7
Pred: HHHHHHCCCCHHHHHHHHHHHHHHCCCCCCEEEEEEECCCCCCEEEEECHHHEEEECCCC
  AA: EAHQNVAQMSLIEAKMRFIQAWQSLPEFGITHFIARFQGGKKEELIGIAYNRLIRMDAST
            550       560       570       580       590       600

Conf: 977899861200013258985499985167531789999478132477877779888256
Pred: CCEEEEEECCCCCCCCCCCCCEEEEEECCCCCCEEEEEECCCHHHHHHHHHHHHHHHCC
  AA: GDAIKTWRFSNMKQWNVNWEIKMVTVEFADEVRLSFICTEVDCKVVHEFIGGYIFLSTRA
            610       620       630       640       650       660

Conf: 01057300888777415769
Pred: HHHCCCCHHHHHHHHCCCCC
  AA: KDQNESLDEEMFYKLTSGWV
            670       680
```

APPENDIX 2.

Talin and PIP interaction studies.

Activation of integrin heterodynamic receptors is essential for ligand binding and subsequent cellular signaling and cellular processes. Talin H domain has been identified as the key molecule in integrin activation. It has been reported that Talin full length protein has substantially less affect on integrin activation compared to Talin H domain. Goksoy et el have shown through NMR analysis that there is an interaction between the Talin rod domain and Talin H domain that holds Talin in its inactivate conformation, inability to interact with integrin CT and subsequent activation. More precisely the Talin PTB domain (F3 sub-domain) which binds to integrin CT, is masked by Talin rod domain. The interaction between Talin rod domain and H domain is disrupted by PIP2 interaction or by a M319A mutation. Part of this interaction work was published at *Goksoy, E., Ma, Y.Q., Wang, X., Kong, X., Perera, D., Plow, E.F., and Qin, J. (2008). Structural basis for the autoinhibition of talin in regulating integrin activation. Mol. Cell 31, 124-133.*

NMR titration curve: Binding Interaction between Talin F3 subdomain and PIP2

In order to understand the chemical shift perturbation of Talin F3 upon PIP2 binding we performed an NMR titration experiment. The HSQC spectra were recorded with of Talin F3 and PIP2(C4)/PIP2(C8) at increasing molar ratios. The Overlaying HSQC spectra of Talin F3 and PIP2(C8) is shown in figure 1. The protein completely precipitated after 1:1 molar ration of F3 and PIP2(C8). Talin F3 and PIP2(C4) was a much stable complex. Thus the NMR titration experiment was performed with PIP2(C4).

The peak perturbation was recorded for all peaks of Talin F3, upon addition of 1:0.2, 1:0.4 1: 0.6,…1:3.25 of PIP2(C4) molar ratios. The chemical shift perturbation profile of Talin F3 is shown below. The corresponding total chemical shift perturbation table for 1:3.25 molar ratio of Talin F3 vs. PIP2(C4) is shown below.

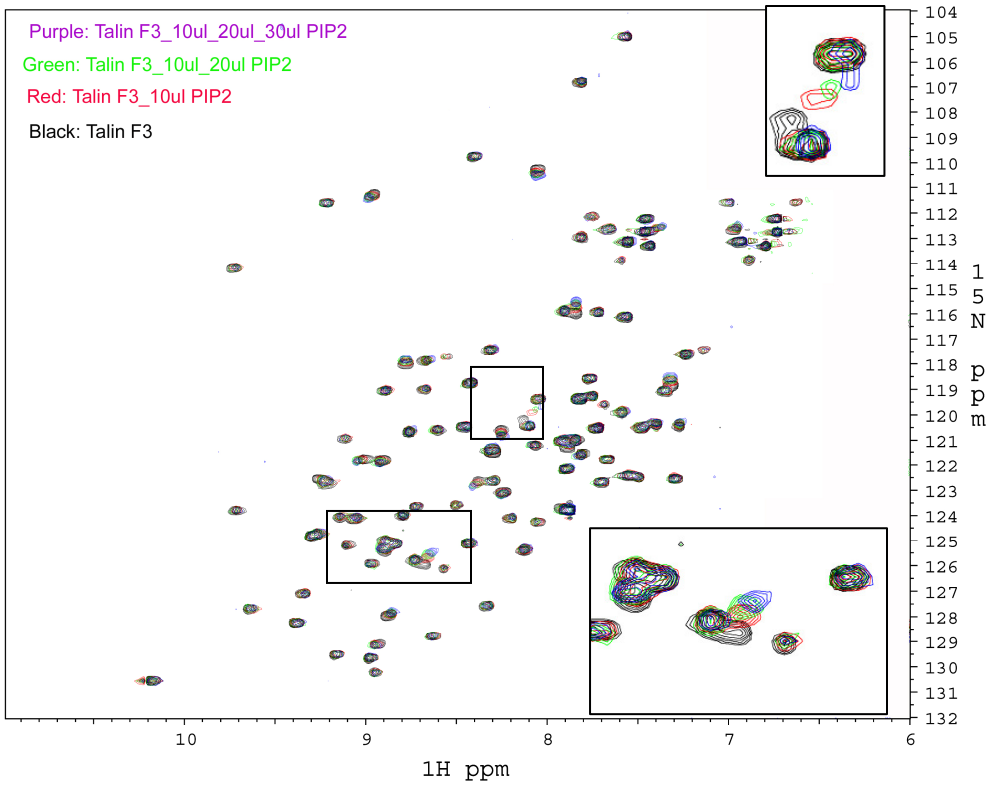

Figure 1. Appendix 2. Overlay of ^{1}H-^{15}N HSQC spectra of Talin F3 and PIP2C8) titration. Black- HSQC Talin F3 free, green-Talin F3 and PIP2 at 1:0.25, red - 1:0.5 and purple - 1:0.75 molar ratios.

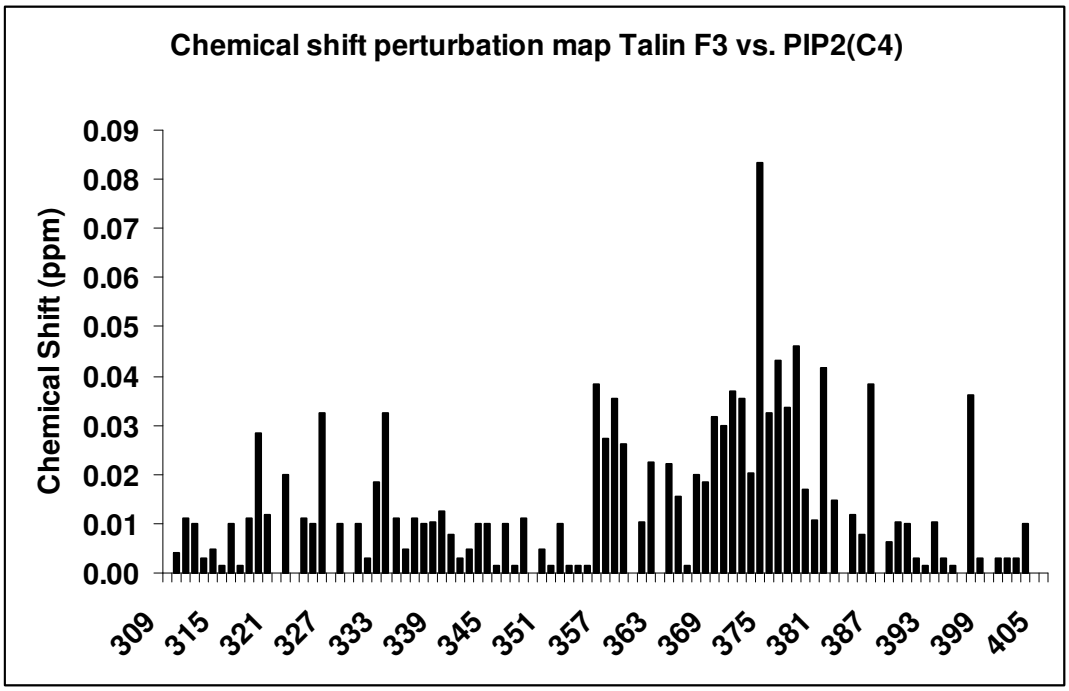

Figure 2. Appendix 2. Chemical shift perturbation profile of all residue of Talin F3 (309-405).

Chemical Shift Purtabations at 1: 3.25 molar ratio for talin F3 vs PIP2C4 titration

	free form		complex							
Res	N	H	N	H	ΔN	ΔH	0.154*ΔN	(0.154*ΔN)2	ΔH^2	δ
309										0.0000
310	120.82	7.71	120.85	7.73	0.03	0.00	0.00462	0.00002	0.00000	0.0042
311	123.27	8.09	123.30	8.12	0.03	-0.01	0.00462	0.00002	0.00010	0.0110
312	122.65	8.56	122.66	8.57	0.01	0.01	0.00154	0.00000	0.00010	0.0101
313	120.01	9.18	120.03	9.20	0.02	0.00	0.00308	0.00001	0.00000	0.0031
314	127.28	9.43	127.31	9.45	0.03	0.00	0.00462	0.00002	0.00000	0.0046
315	123.84	9.34	123.83	9.36	-0.01	0.00	-0.00154	0.00000	0.00000	0.0015
316	116.50	8.37	116.51	8.38	0.01	0.01	0.00154	0.00000	0.00010	0.0101
317	123.11	9.20	123.10	9.22	-0.01	0.00	-0.00154	0.00000	0.00000	0.0015
318	124.47	8.95	124.44	8.98	-0.03	-0.01	-0.00462	0.00002	0.00010	0.0110
319	127.02	8.94	126.89	8.94	-0.13	0.02	-0.02002	0.00040	0.00040	0.0283

320	125.17	8.62	125.13	8.63	-0.04	0.01	-0.00616	0.00004	0.00010	0.0117
321										
322	118.64	7.72	118.64	7.76	0.00	-0.02	0.00000	0.00000	0.00040	0.0200
323										
324	119.45	7.45	119.42	7.48	-0.03	-0.01	-0.00462	0.00002	0.00010	0.0110
325	124.16	8.49	124.15	8.50	-0.01	0.01	-0.00154	0.00000	0.00010	0.0101
326	121.64	9.31	121.72	9.30	0.08	0.03	0.01232	0.00015	0.00090	0.0324
327										
328	123.20	9.13	123.21	9.14	0.01	0.01	0.00154	0.00000	0.00010	0.0101
329	121.67	8.35	121.67	8.37	0.00	0.00	0.00000	0.00000	0.00000	0.0000
330	126.72	9.71	126.73	9.72	0.01	0.01	0.00154	0.00000	0.00010	0.0101
331	113.25	9.79	113.27	9.81	0.02	0.00	0.00308	0.00001	0.00000	0.0031
332	124.16	8.94	124.04	8.96	-0.12	0.00	-0.01848	0.00034	0.00000	0.0185
333	121.64	9.31	121.72	9.30	0.08	0.03	0.01232	0.00015	0.00090	0.0324
334	112.01	7.86	112.04	7.89	0.03	-0.01	0.00462	0.00002	0.00010	0.0110
335	111.70	7.71	111.73	7.73	0.03	0.00	0.00462	0.00002	0.00000	0.0046
336	118.44	8.10	118.47	8.11	0.03	0.01	0.00462	0.00002	0.00010	0.0110
337	118.11	8.95	118.12	8.96	0.01	0.01	0.00154	0.00000	0.00010	0.0101
338	122.89	9.78	122.91	9.81	0.02	-0.01	0.00308	0.00001	0.00010	0.0105
339	122.74	8.77	122.79	8.80	0.05	-0.01	0.00770	0.00006	0.00010	0.0126
340	126.20	9.40	126.25	9.42	0.05	0.00	0.00770	0.00006	0.00000	0.0077
341	127.82	8.69	127.84	8.71	0.02	0.00	0.00308	0.00001	0.00000	0.0031
342	128.61	9.22	128.64	9.24	0.03	0.00	0.00462	0.00002	0.00000	0.0046
343	117.77	8.48	117.77	8.49	0.00	0.01	0.00000	0.00000	0.00010	0.0100
344	108.80	8.45	108.80	8.46	0.00	0.01	0.00000	0.00000	0.00010	0.0100
345	114.98	7.95	114.99	7.97	0.01	0.00	0.00154	0.00000	0.00000	0.0015
346	118.98	7.63	118.98	7.64	0.00	0.01	0.00000	0.00000	0.00010	0.0100
347	124.87	8.78	124.86	8.80	-0.01	0.00	-0.00154	0.00000	0.00000	0.0015
348	129.30	9.01	129.33	9.02	0.03	0.01	0.00462	0.00002	0.00010	0.0110
349	118.11	7.40	118.11	7.42	0.00	0.00	0.00000	0.00000	0.00000	0.0000
350	124.40	8.16	124.37	8.18	-0.03	0.00	-0.00462	0.00002	0.00000	0.0046
351	123.84	9.34	123.83	9.36	-0.01	0.00	-0.00154	0.00000	0.00000	0.0015
352	116.95	8.72	116.96	8.73	0.01	0.01	0.00154	0.00000	0.00010	0.0101
353	126.63	8.38	126.64	8.40	0.01	0.00	0.00154	0.00000	0.00000	0.0015
354	105.85	7.86	105.84	7.88	-0.01	0.00	-0.00154	0.00000	0.00000	0.0015
355	118.31	7.80	118.32	7.82	0.01	0.00	0.00154	0.00000	0.00000	0.0015
356	119.48	7.32	119.72	7.33	0.24	0.01	0.03696	0.00137	0.00010	0.0383
357	128.19	8.99	128.31	9.03	0.12	-0.02	0.01848	0.00034	0.00040	0.0272
358	115.00	7.90	114.77	7.92	-0.23	0.00	-0.03542	0.00125	0.00000	0.0354

359	117.89	7.36	117.72	7.38	-0.17	0.00	-0.02618	0.00069	0.00000	0.0262
360										
361	124.93	9.02	124.91	9.03	-0.02	0.01	-0.00308	0.00001	0.00010	0.0105
362	120.92	8.97	121.05	9.00	0.13	-0.01	0.02002	0.00040	0.00010	0.0224
363										
364	111.18	7.79	111.24	7.83	0.06	-0.02	0.00924	0.00009	0.00040	0.0220
365	114.97	7.76	115.07	7.78	0.10	0.00	0.01540	0.00024	0.00000	0.0154
366	119.67	8.66	119.68	8.68	0.01	0.00	0.00154	0.00000	0.00000	0.0015
367	122.84	8.01	122.84	8.05	0.00	-0.02	0.00000	0.00000	0.00040	0.0200
368	124.16	8.94	124.04	8.96	-0.12	0.00	-0.01848	0.00034	0.00000	0.0185
369	120.37	7.93	120.30	7.92	-0.07	0.03	-0.01078	0.00012	0.00090	0.0319
370	124.16	8.90	124.15	8.89	-0.01	0.03	-0.00154	0.00000	0.00090	0.0300
371	110.35	9.02	110.49	9.07	0.14	-0.03	0.02156	0.00046	0.00090	0.0369
372	121.79	8.45	121.98	8.49	0.19	-0.02	0.02926	0.00086	0.00040	0.0354
373	120.27	8.12	120.25	8.16	-0.02	-0.02	-0.00308	0.00001	0.00040	0.0202
374	118.94	8.14	118.6	8.09	-0.32	0.07	-0.04959	0.00246	0.00449	0.0834
375	119.75	8.30	119.96	8.32	0.21	0.00	0.03234	0.00105	0.00000	0.0323
376	109.40	8.11	109.68	8.13	0.28	0.00	0.04312	0.00186	0.00000	0.0431
377	120.11	7.90	120.21	7.95	0.10	-0.03	0.01540	0.00024	0.00090	0.0337
378	124.89	8.72	124.62	8.72	-0.27	0.02	-0.04158	0.00173	0.00040	0.0461
379	122.16	8.28	122.25	8.31	0.09	-0.01	0.01386	0.00019	0.00010	0.0171
380	117.02	8.82	116.95	8.84	-0.07	0.00	-0.01078	0.00012	0.00000	0.0108
381	120.82	9.07	120.90	9.13	0.08	-0.04	0.01232	0.00015	0.00160	0.0419
382	120.60	7.86	120.67	7.89	0.07	-0.01	0.01078	0.00012	0.00010	0.0147
383	118.06	8.73	118.06	8.75	0.00	0.00	0.00000	0.00000	0.00000	0.0000
384	124.24	9.16	124.28	9.19	0.04	-0.01	0.00616	0.00004	0.00010	0.0117
385	110.65	9.27	110.70	9.29	0.05	0.00	0.00770	0.00006	0.00000	0.0077
386	119.48	7.32	119.72	7.33	0.24	0.01	0.03696	0.00137	0.00010	0.0383
387	119.58	7.52	119.58	7.54	0.00	0.00	0.00000	0.00000	0.00000	0.0000
388	121.53	7.54	121.57	7.56	0.04	0.00	0.00616	0.00004	0.00000	0.0062
389	119.50	8.15	119.52	8.16	0.02	0.01	0.00308	0.00001	0.00010	0.0105
390	115.18	7.61	115.18	7.62	0.00	0.01	0.00000	0.00000	0.00010	0.0100
391	121.59	7.34	121.61	7.36	0.02	0.00	0.00308	0.00001	0.00000	0.0031
392	117.65	7.81	117.66	7.83	0.01	0.00	0.00154	0.00000	0.00000	0.0015
393	120.53	8.34	120.51	8.37	-0.02	-0.01	-0.00308	0.00001	0.00010	0.0105

					0.02	0.01				
394	104.05	7.61	104.07	7.63	0.02	0.00	0.00308	0.00001	0.00000	0.0031
395	121.74	7.74	121.75	7.76	0.01	0.00	0.00154	0.00000	0.00000	0.0015
396	123.02	8.84	123.02	8.86	0.00	0.00	0.00000	0.00000	0.00000	0.0000
397	120.08	7.96	120.21	7.95	0.13	0.03	0.02002	0.00040	0.00090	0.0361
398	116.69	7.28	116.71	7.30	0.02	0.00	0.00308	0.00001	0.00000	0.0031
399	121.47	7.59	121.47	7.61	0.00	0.00	0.00000	0.00000	0.00000	0.0000
400	119.53	8.50	119.55	8.52	0.02	0.00	0.00308	0.00001	0.00000	0.0031
401	118.49	7.87	118.51	7.89	0.02	0.00	0.00308	0.00001	0.00000	0.0031
402	119.60	7.77	119.62	7.79	0.02	0.00	0.00308	0.00001	0.00000	0.0031
403	121.21	7.95	121.22	7.96	0.01	0.01	0.00154	0.00000	0.00010	0.0101
404	123.12	8.24	123.12	8.26	0.00	0.00	0.00000	0.00000	0.00000	0.0000
405	122.84	7.93	122.84	7.95	0.00	0.00	0.00000	0.00000	0.00000	0.0000

Table 1. Appendix 2. Chemical shift perturbation table for Talin F3 and PIP2(C4) interaction. $\delta=[0.154*\Delta N^2+\Delta H^2]1/2$

ITC experiment: Interaction between Talin Rod domain and Talin head domain

Talin is a 270KDa protein. As explained above, understanding the interaction between Talin H domain 50KDa and Rod domain 220KDa through NMR is difficult as it exceeds the size limitation for NMR which is 40KDa. As an alternative method we used ITC to understand the interaction.

ITC has no limitation in size for analysis. The method was explained in chapter 2. It provides a complete thermodynamic profile of the binding interaction.

We have performed an ITC experiment between Talin H and rod domain. A 50µM solution of Talin Rod domain was used in the sample cell and titrated against 1.0 mM solution of Talin head domain. The ITC titration curve is shown in the figure 3 below. The binding affinity between talin H and rod domain is 10µM.

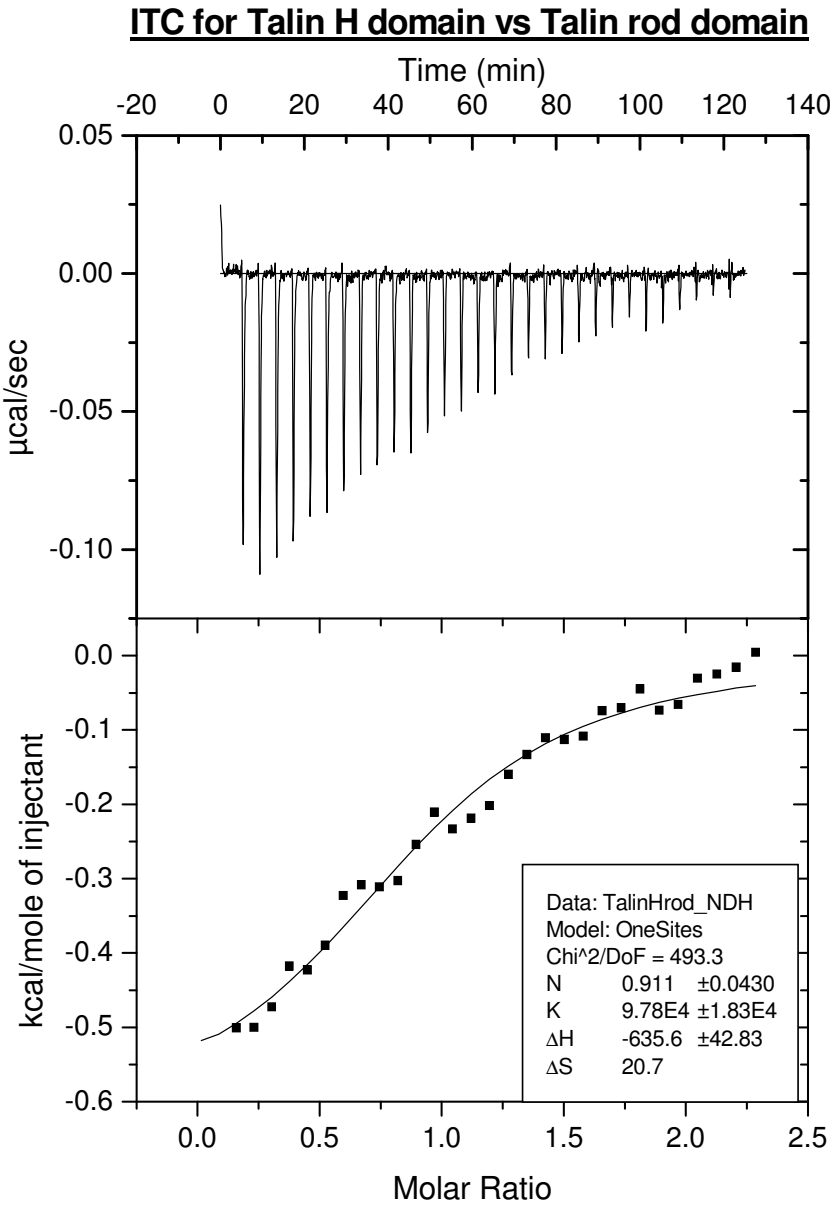

Figure 3. Appendix 2. ITC titration curve for Talin Head domain and Talin Rod domain interaction.

ITC experiment: Talin H, F3, F2F3 domain and PIP2 interaction

These experiments were performed to understand the interaction between Talin H domain and PIP2.

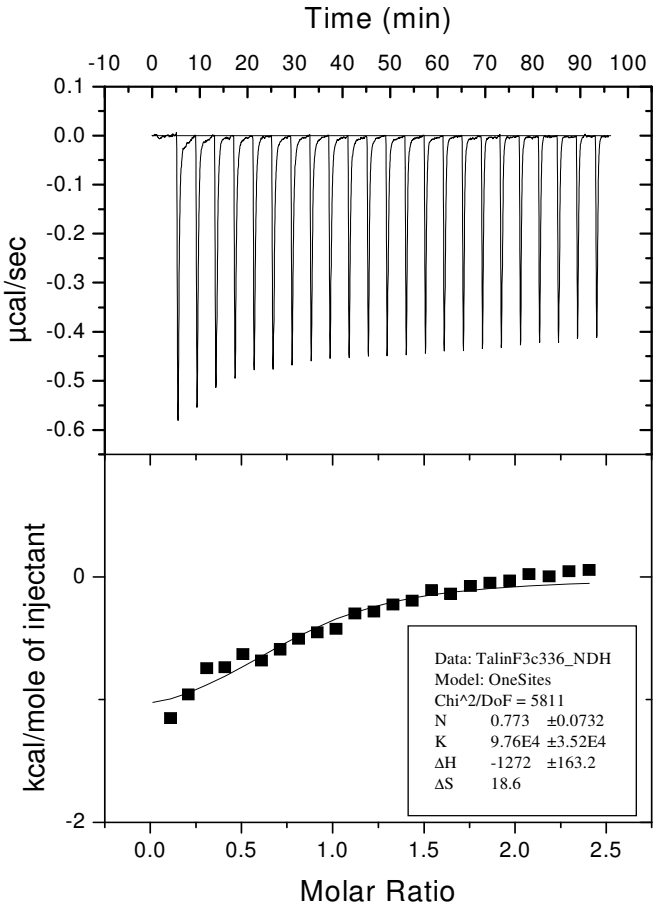

Figure 4. Appendix 2. ITC titration curve for Talin F3 domain and PIP2(C4). Talin F3 domain and PIP2(C4) shows a weak interaction.

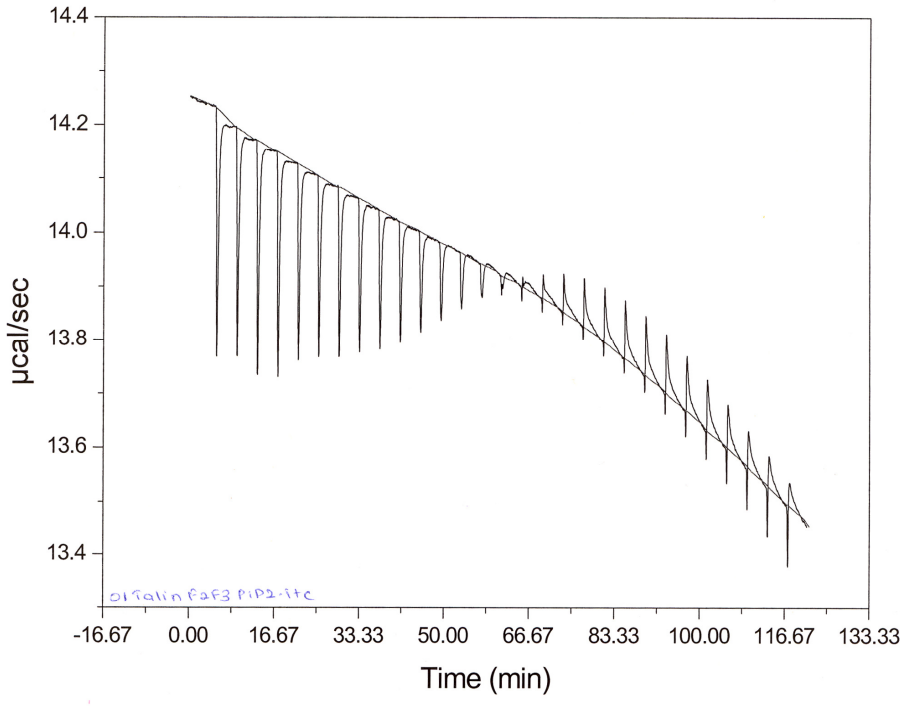

Figure 5. Appendix 2. ITC titration curve for Talin F2F3 domain and PIP2(C6).

The ITC experiment of Talin F2F3 and PIP2(C6) interaction is shown in figure 5. There was a continuous drift in the baseline during the experiment. We are not able to calculate the thermodynamic profile of the binding interaction due to the drift. However it is interesting to note, that the titration between F2F3 and PIP2(C6) starts with an exothermic reaction, switches to an endothermic reaction half way through the titration and finally saturates at the last 4 injections. These types of interactions are an indication of a 1:2 molar ratio binding.

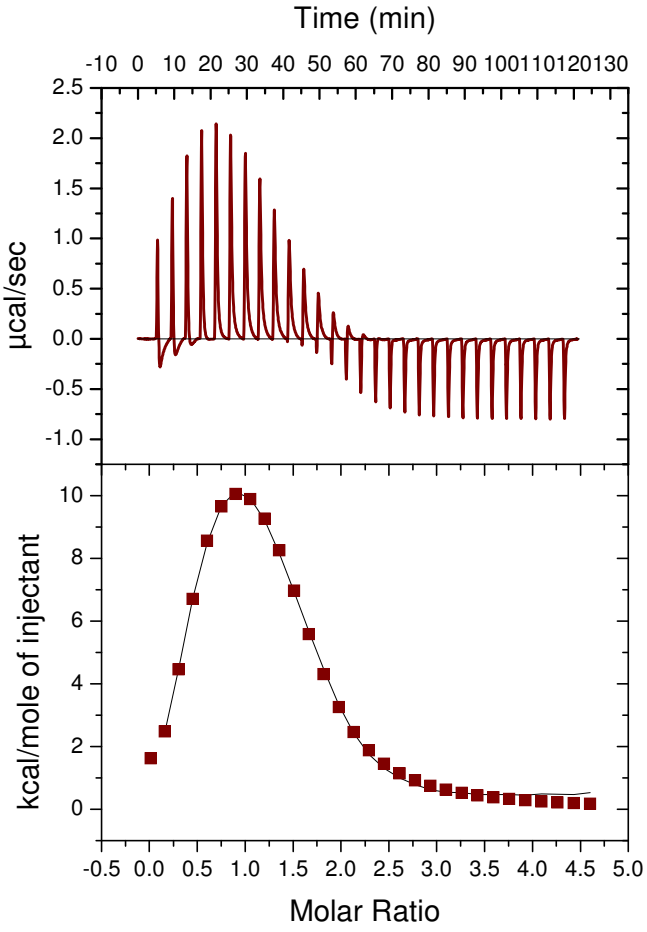

Figure 6. Appendix 2. ITC Titration curve for Talin H domain and PIP2(C6).

The ITC titration between Talin H domain and PIP2(C6) is shown in figure 6. The data did fit into a 2 site binding interaction model indicating a 1:2 molar ratio binding event. This is consistent with figure 5, F2F3 and Talin PIP2(C6) interaction of a 1:2 molar ration interaction.

Our data of two site binding sites for PIP2 on F2F3 is consistent with: a recently published paper and ongoing studies, where the two binding sites for PIP are on F2 and F3 sub-domains respectively (Saltel et al., 2009).

NMR experiment: Talin F2F3 domain and PIP2(C8) interaction

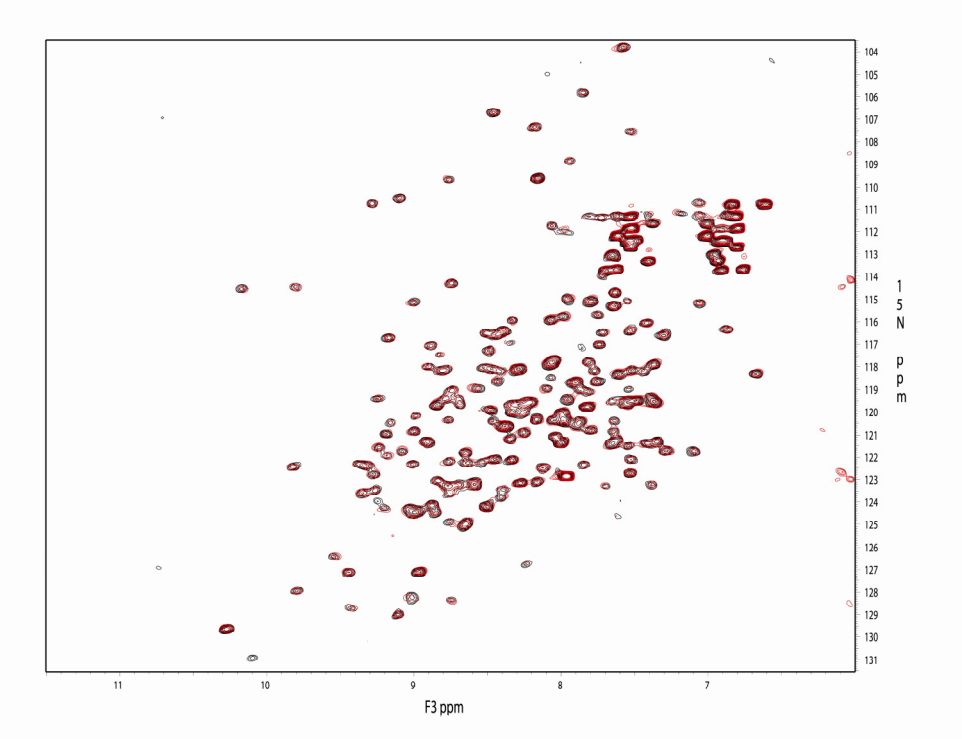

Figure 7. Appendix 2. Overlay of ^{1}H-^{15}N HSQC spectra of Talin F2F3 and PIP2C8) titration. Black- HSQC Talin F2F3 free, red – Talin F2F3 and PIP2 at 1:1 molar ratio.

The interaction between Talin F2F3 and PIP2(C8) is shown in figure 7. The protein precipitates after 1:1 molar ratio of F2F3 and PIP2(C8). The chemical shifts are very small compared to Talin F3 itself.